EFFICACY AND SAFETY OF DOCOSAHEXAENOIC ACID ACYLATED PHLORIDZIN FOR TREATING TRIPLE NEGATIVE BREAST CANCER

by

T R G Wasundara Fernando

Submitted in partial fulfilment of the requirements for
the degree of Master of Science

at

Dalhousie University

Halifax, Nova Scotia

August 2014

Dedication

I was raised and I didn't just grow-up...

This work is dedicated to my Amma and Thaththa with love and respect.

"Our greatest weakness lies in giving up. The most certain way to succeed is always to try just one more time."

Thomas A. Edison

TABLE OF CONTENTS

LIST OF TABLES

LIST OF FIGURES

ABSTRACT

Phloridzin (PZ), a polyphenol compound found in apple, exerts glucose transporter inhibitory and estrogen-like effects. Therapeutic applications of PZ are limited due to its poor bioavailability. In this study, anitiproliferative efficacy of docosahexaenoic acid (DHA) acylated PZ (PZ-DHA) was investigated using a triple negative breast cancer cell line (MDA-MB-231). PZ-DHA, but not PZ, caused the death of MDA-MB-231 *in vitro* which was both time- and dose-dependent. PZ-DHA-induced apoptosis was indicated by DNA fragmentation and activation of caspase 3/7. However, reactive oxygen species production was not required for PZ-DHA-mediated cell death. PZ-DHA showed low cytotoxicity toward human mammary epithelial cells. Moreover, *in vivo* tumor suppresser effect of PZ-DHA was observed when MDA-MB-231 cells xenografted non-obese diabetic severe combined immune-deficient (NOD-SCID) mice were subjected to intratumoral injections of PZ-DHA. Anticancer efficacy observed in cell cultures and mice warrant further investigations of PZ-DHA as a potential treatment for breast cancer.

Key words: Triple negative breast cancer, tumor suppression, NOD-SCID, phloridzin, docosahexaenoic acid, PZ-DHA

LIST OF ABBREVIATIONS AND SYMBOLS USED

× g	Gravity
7-AAD	7-Aminoactinomycin
ABTS	2,2'-azino-bis(3-ethylbenzothiazoline-6-sulphonic acid
AKT	Protein Kinase B
ANOVA	Analysis of Variance
AOX	Azoxymethane
AP	Activator Protein
ATCC	American Type Culture Collection
ATM	Ataxia Telangiectasia Mutated
BAD	Bcl-2-Associated Death Promoter
Bax	Bcl-2-associated X protein
Bcl-2	B-cell lymphoma 2
Bcl-xL	B-cell lymphoma-extra large
BRCA1	Breast Cancer Gene 1
BRCA2	Breast Cancer Gene 2
BSA	Bovine Serum Albumin
$CaCl_2$	Calcium chloride
Caspase	Cysteine-dependent aspartate-directed protease
CDH1	Cadherin 1
Cdk1	Cyclin-dependent kinase-1
Cdk2	Cyclin-dependent kinase-2
Cdk4	Cyclin-dependent kinase-4
cDMEM	Complete Dulbecco's Modified Eagle's Medium
$CH_3COO^-Na^+$	Sodium acetate
CHEK2	Checkpoint Kinase 2
CO_2	Carbon dioxide
CR	Cytokine Receptor
DCIS	Ductal Carcinoma In Situ
DHA	Docosahexaenoic acid
DMBA	7,12-dimethyl benz[a]anthracene
DMEM	Dulbecco's Modified Eagle's Medium
DMH	1,2-dimethylhydrazine
DMSO	Dimethylsulfoxide
DNA	Deoxyribonucleic Acid
DOC	Docetaxel
DOX	Doxorubicin
DSS	Dextran sodium sulfate
EGCG	Epigallocatechin gallate
EGF	Epidermal Growth Factor

ELK1	ETS domain-containing protein
ER	Estrogen Receptor
ERK	Extracellular Signal Regulated Kinase
E-selectin	Endothelial Leukocyte Adhesion Molecule-1
FBS	Fetal Bovine Serum
FOXO	Forkhead box O3
G_0	Gap 0
G_1	Gap 1
G2	Gap 2
GRB2	Growth factor Receptor-Bound protein 2
GSE	Grape Seed Extracts
H_2O_2	Hydrogen peroxide
HBSS	Hank's Balanced Salt Solution
HBV	Hepatitis B Virus
HCV	Hepatitis C Virus
HEPES	N-2- hydroxyethylpiperazine-N'-2-ethanesulfonic acid
HER2	Human Epidermal Growth Factor Receptor 2
HIF-1α	Hypoxia-Inducible Factor-1α
HPV	Human Papilloma Virus
HRE	Hypoxia Response Element
HRP	Horseradish peroxidase
HRT	Hormone Replacement Therapy
ICAM-1	Intercellular Adhesion Molecule-1
IEA	Intermediate Electron Acceptor
JAK	Janus Kinase
Ki- 67	Antigen Ki-67 associated with cell proliferation
LCIS	Lobular Carcinoma In Situ
LPH	Lactase Phlorizin Hydrolase
M	Mitosis
MAPK	Mitogen-Activated Protein Kinase
MAPKp42	Mitogen-Activated Protein Kinase Protein 42
MAPKp44	Mitogen-Activated Protein Kinase Protein 44
MEK	MAPK/ERK Kinase
MEpiCM	Mammary Epithelial Cell Medium
MKP-1	Mitogen-Activated Protein Kinase Phosphatase-1
MMP	Matrix Metalloproteinase
mTOR	Mammalian Target Of Rapamycin
MTS	3-(4,5-dimethylthiazol-2-yl)-5-(3-carboxymethoxyphenyl)-2-(4-sulfophenyl)-2H-tetrazolium, inner salt
MTT	3-(4, 5-dimethyl-2-thiazolyl)-2, 5-diphenyl-2H-tetrazolium bromide

NAC	N-acetylcystein
NaCl	Sodium chloride
NaOH	Sodium hydroxide
Na_3VO_4	Sodium orthovanadate
NF-κB	Nuclear Factor KappaB
NMR	Nuclear Magnetic Resonance
NOD-SCID	Non-Obese Diabetic Severe Combined Immunodeficiency
NSCLC	Non-small-cell lung cancer
OH-BBN	N-butyl-N-(4-hydroxybutyl)-nitrosamine
PBS	Phosphate Buffered Saline
PFA	Paraformaldehyde
PGR	Progesterone Receptor
PHD	Prolyl Hydroxylase Enzyme
PI	Propidium iodide
PI-3K	Phosphoinositide 3-Kinase
PIP2	Phosphatidylinositol (4,5)-bisphosphate
PIP3	Phosphatidylinositol(3,4,5)-trisphosphate
PMS	Phenazine methosulfate
PPA	Phenylpropionic
Pr	Proline
PT	Phloretin
PTEN	Phosphatase and Tensin Homolog
PUFA	Polyunsaturated Fatty Acid
pVHL	Von Hippel–Lindau protein
PZ	Phloridzin
PZ-DHA	Phloridzin docosahexaenoate
RAF	RAF proto-oncogene serine/threonine-protein kinase
RAS	Rat Sarcoma
RLU	Relative luminescence units
ROS	Reactive Oxygen Species
RTK	Receptor Tyrosine Kinase
SEM	Standard Error Mean
siRNA	Small Interfering Ribonucleic Acid
SHR	Spontaneously Hypertensive Rat
SOD	Superoxide dismutase
SOS	Son of Sevenless
STAT	Signal Transducers and Activators of Transcription
STK11	Serine/Threonine Kinase 11
STS	Staurosporine
TdT	Deoxynucleotidyl transferase

TGF-α	Transforming Growth Factor alpha
TNF	Tumor Necrosis Factor
TNFα	Tumor Necrosis Factor α
TP53	Tumor Protein p53
TPA	12-O-tetradecanoyl phorbol-13-acetate
Trypsin-EDTA	Trypsin- Ethylenediaminetetraacetic acid
TUNEL	Terminal deoxynucleotidyl transferase dUTP nick end labeling
Ub	Ubiquitin
UCLA	University Committee on Laboratory Animals
v/v	Volume by volume
VCAM-1	Vascular Cell Adhesion Molecule-1
VEGF	Vascular Endothelial Growth Factor
VHL	Von Hippel–Lindau Tumor Suppressor
w/v	Weight by volume

ACKNOWLEDGEMENT

It is with heartfelt gratitude that I acknowledge the support, help and advice of my supervisor, Dr. H. P. Vasantha Rupasinghe, not only for giving me the opportunity to pursue my graduate studies at Dalhousie University, but also for cheerfully encouraging me whenever I lost my confidence and guaranteeing that I gained the best training in every aspects to successfully complete this exciting research project. Your enthusiasm, immense knowledge, patience, interest on exploring new sites of research and excellent supervision have deeply influenced myself to improve my scientific and analytical thinking and thank you for further strengthening my research in a fruitful collaboration with Faculty of Medicine. It gives me great pleasure in acknowledging the support and help of my supervisory committee member, Dr. David W. Hoskin, Department of Pathology, Faculty of Medicine, Dalhousie University. I do consider it as an honor working in your lab under your supervision and I am ever grateful for all your guidance. I would like to express my utmost gratitude for my supervisory committee member, Dr. Bernhard Benkel, Department of Animal and Plant Sciences, Faculty of Agriculture, Dalhousie University. Your great ideas have always had a big impact on improving my critical thinking.

I owe my deepest gratitude to Dr. Sandhya Nair, Dr. Melanie Coombs, Dr. Carolyn Doucette and Dr. Anna Greenshields. This thesis would not have been possible if it was not for your support and valuable advices. A special thank goes to Dr. Melanie Coombs for proof-reading my thesis document and I was blessed to have support from you all when it was a "hard" time for me to try a whole new protocol or an experiment for the very first time.

I cannot find words to express my grateful emotions to my awesome colleagues in Dr. Rupasinghe's lab. You all were with me to share my smiles and tears and thank you for amazing team work on creating a wonderful environment in the lab to work together. I would like to express my gratitude to my wonderful colleagues in Dr. Hoskin's lab as well for helping me to complete a significant part of my research and for making my visits to Halifax unforgettable. I share the credit of my work with everybody who helped me in many different ways; specially, Purnima Narayanan for training me on mice handling and anaesthesia, Patricia Colp for histology training, Mary Anne Trevors for flow cytometer

training and Stephen Whitefield for fluorescence and bright field microscopy trainings. I would like to take this as an opportunity to thank Faye Bradley for taking a great care of me like a mother and for giving me a wonderful family experience during my stay in Canada and a big thank goes to all my friends and Louise Primeau for their support and care. I also would like to extend my sincere thanks to the funding agencies, NSERC Discovery grant and Atlantic Canada Opportunity Agency (ACOA) for supporting my research work and all the staff in Dalhousie University, specially Departments of Environmental Sciences, Pathology and Carlton Animal Care Facility.

Last, but definitely not least, my loving family: Amma, Thaththa, sister-Narmada and two brothers-Deeghayu and Kapil... Though I am miles and miles away from you all physically, I was always held tight to the core of your hearts and you never let me feel alone. I thank you for being my side, hugging me every day with caring words, giving me the courage every moment to face all the difficulties, believing me on my capabilities, wishing me the success in every step I am taking and holding my hand to walk this long journey with me. Clearly, this thesis would have remained a dream had it not been for your unconditioned eternal love, warm care, emotional support and true smiles, which I will never be able to find elsewhere on this Earth. My family is my greatest inspiration and you all just made my days for two years… Though the debt for all these cannot be paid back, let me say these two words with my whole heart, THANK YOU!

CHAPTER 1 : INTRODUCTION

1.1 Cancer

Cancer is a population of abnormal cells which divide without control, with the ability to invade other tissues and is a leading cause of death, worldwide. Under normal circumstances, cell survival, proliferation and differentiation are kept under control, but in cancer, these cellular events continue to take place beyond its control. (Katzung, 2006). Among the most common types of cancers (lung, liver, stomach, colorectal, breast), lung cancer has continued to be the most common cancer diagnosed in men and breast cancer is the most common cancer diagnosed in women (Globocan, 2012). An estimated 8.2 million deaths were accounted with cancer across the world in 2012 and 14.1 million cases were diagnosed during the same year (Globocan, 2012). Lung cancer, breast cancer, colorectal cancer and stomach cancer accounted for two-fifths of the total cases of cancers diagnosed worldwide (Cancer Research UK, 2014). According to Canadian cancer statistics, issued by the Canadian Cancer Society, it is estimated that 97,700 Canadian men and 93,600 Canadian women will be diagnosed with cancer in 2014. During 2014, 40,000 men and 36,600 women are expected to die due to cancers in Canada (Canadian Cancer Statistics, 2014). The lowest number of incidences and mortality rate is recorded in British Columbia. Both incidence and mortality rates are higher in Atlantic Canada and Quebec (Canadian Cancer Statistics, 2014). Breast cancer occurs mostly in women, but men can also get it (Giordano, 2005). Further, it is estimated nearly 200 Canadian men will be diagnosed with breast cancer annually, with 60 fatalities (Breast Cancer Foundation, 2013). Every year, 182,000 women are diagnosed with breast cancer, and 43,300 die from the disease. More than 30% of cancers are caused by modifiable behavioural and environmental risk factors,

including tobacco and alcohol use, dietary factors, insufficient regular consumption of fruits and vegetables, obesity, physical inactivity, chronic infections from *Helicobacter pylori*, hepatitis B virus (HBV), hepatitis C virus (HCV) and some types of human papilloma virus (HPV), environmental and occupational risks including exposure to ionizing and non-ionizing radiation (de Martel et al., 2012).

1.2 Triple Negative Breast Cancer

It was estimated that over 508,000 women died in 2011 due to breast cancer worldwide (WHO, 2013). Triple negative breast cancer (TNBC) represents nearly 15% of all invasive breast cancers and TNBC cells do not express estrogen receptor (ER), progesterone receptor (PGR) and human epidermal growth factor receptor 2 (HER2) (Ovcaricek et al., 2011). Therefore, treatment of TNBC is challenging since neither hormone therapy nor HER2 target therapy is effective. Among all the types of breast cancers, TNBC and HER2-enriched breast cancers are reported to have poor prognosis when compared to hormone receptor positive breast cancers (Al-Ejeh et al., 2014).

1.3 Pathophysiology of Breast Adenocarcinoma

A malignant tumor that starts in the cells of the breast is referred to as a breast cancer and it is closely associated with the characteristic ability to invade the surrounding tissue (metastasis) (American Cancer Society, 2012). Breast cancer results from genetic and environmental factors, which leads to the accumulation of mutations in essential genes. Inherited and sporadic are the main two types of breast cancer which are categorized based upon the criterion of presence or absence of breast cancer family history (Nathanson et al., 2001). A breast cancer could be either in situ or invasive (Agnantis et al., 2004). The two types differ in the ability of invading adjacent breast stroma beyond the epithelial basement

membrane (Agnantis et al., 2004). In situ breast cancer is non-invasive and confined only to either mammary ducts (Ductal Carcinoma In Situ (DCIS)) or mammary lobules (Lobular Carcinoma In Situ (LCIS)) (Cancer Australia, 2012). In contrast, invasive breast cancer spreads into the surrounding breast tissue. Origin of the invasive cancer could also be either ductal or lobular. Invasive breast cancer is confined to the breast tissue and lymph nodes in the armpit at early stage and it may have spread outside the breast tissue in secondary breast cancer (Cancer Australia, 2012). However, DCIS is associated with increased risk of development into invasive breast cancer.

1.4 Breast Adenocarcinoma Risk Factors

A risk factor (genetic, hormonal or environmental) can be defined as anything that contributes toward development of a breast cancer (Martin, 2000). The risk of developing breast cancer increases with age (Sweeney et al., 2004). Incidence of breast cancer is higher at older age and the rate doubles every ten years until menopause (Mcpherson et al., 2000). Benign breast disease, a family history of breast cancer, exposure to radiation, hormone replacement therapy (HRT), and reproductive factors such as early age at menarche, late age menopause, nulliparity and an older age at the time of the first full-term pregnancy are associated with an increased risk of breast cancer (Agnantis et al., 2004; Dolle et al., 2009; Mcpherson et al., 2000). The risk of developing breast cancer is higher in women whose close blood relatives are afflicted by the same disease (American Cancer Society, 2012). Having a first degree relative with breast cancer doubles the risk and the risk is about three-fold higher if two first degree relatives have the disease. However, 5-10% of breast cancer cases are considered to be hereditary directly from parents (American Cancer Society, 2012). Inherited mutations in Breast Cancer Gene 1 (BRCA1) and Breast Cancer Gene 2

(BRCA2) are the most commonly found causes of hereditary breast cancer since these are high penetrance genes (Agnantis et al., 2004; Warner et al., 2001). Having inherited a mutated copy of either gene increases the risk of developing breast cancer (Milne and Antoniou, 2011). Defects and mutations in genes such as Ataxia telangiectasia mutated (ATM) (Stankovic et al., 1998), tumor protein p53 (TP53) (Malkin et al., 1990), which carries instructions for synthesizing a cancer suppressor proteins p53, checkpoint kinase 2 (CHEK2) (Weischer et al., 2007), Phosphatase and tensin homolog (PTEN) (Nelen et al., 1996), cadherin 1 (CDH1) (Lei et al., 2002) and serine/threonine kinase 11 (STK11) (Boardman et al., 1998; Schumacher et al., 2005) are also associated with an elevated risk of developing breast cancer.

1.5 Breast Cancer Subtypes and Genetics Involved

The classification system of breast cancer is based on the expression of receptors, genes and proteins such as estrogen receptor (ER), progesterone receptor (PGR), human epidermal growth factor receptor 2 (HER2) and antigen Ki-67 (Eroles et al., 2012; Goldhirsch et al., 2011). This classification divides breast cancers into six different subtypes namely, luminal A (ER or PR positive, HER2 negative, Ki-67<14%) (Voduc et al., 2010), luminal B, HER2-enriched, basal-like, normal breast and claudin-low (Eroles et al., 2012; Polyak, 2011). Complexity of breast cancer is well-reflected by the heterogeneity in clinical parameters (tumor size, involvement of lymph nodes and stage) and also by expression or suppression of biomarkers (e.g.: ER, PGR and HER2) (Eroles et al., 2012). Inherited gene mutations (changes in DNA) increase the risk of developing breast cancers in some individuals. Specially, mutations in cancer suppressor genes such as BRCA1 and BRCA2 prevent suppression of abnormal growth and cancer is more likely to develop

(Imyanitov and Hanson, 2004). These mutations can be inherited from parents. Breast cancer is staged to describe the extent of the cancer in the body based on the criterion whether the cancer is invasive or non-invasive. Staging of breast cancer is a process of recognizing how widespread a cancer is when it is diagnosed. This is also important in determining the treatment, as similar stages are treated in a similar way (Hammer et al., 2008). Non-invasive in situ breast cancers are staged as “Stage 0”. Invasive breast cancers are staged from “Stage I” to “Stage IV”, based upon the spread of cancer tissue to adjacent and distal tissues (Hammer et al., 2008).

Table 01: Biological model classification system of breast cancer (Adapted from Eroles et al., 2012)

Molecular subtype	Frequency (%)	ER/PR/HER2	Characteristic Genes	Tp53 Mutation	Prognosis
Basal like	10-20	ER-/PR-/HER2-	KRT5, CDH3, ID4, FABP7, KRT17, TRIM29, LAMC2	High	Bad
HER2 enriched	10-15	ER-/PR-/HER2+	ERBB2, GRB7	High	Bad
Normal breast-like	5-10	ER-/+HER2-	PTN, CD36, FABP4, AQP7, ITGA7	Low	Intermediate
Luminal A	50-60	ER+/PR+/HER2-	ESR1, GATA3, KRT8, KRT18, XBP1, FOXA1, TFF3, CCND1, LIV1	Low	Excellent
Luminal B	10-20	ER+/PR+/HER2+	ESR1, GATA3, KRT8, KRT18, XBP1, FOXA1, TFF3, SQLE, LAPTM4B	Intermediate	Intermediate/Bad
Claudin-low	12-14	ER-/PR-/HER2-	CD44, SNAI3	High	Bad

1.6 Cell Death by apoptosis and necrosis

The term “apoptosis” was suggested by Kerr et al. (1972) to describe the mechanism of controlled cell deletion, while, the phenomenon of “program cell death” was first discussed by Lockshin and Williams in 1964-5 (Lockshin, 1969; Lockshin and Williams, 1964, 1965). In contrast, necrosis is the cell death that results from direct cell injury, hence it usually begins at the cell surface. Apoptosis is also termed as programmed cell death and it explains a series of morphological and biochemical changes taking place in a cell (Collins et al., 1997). These morphological changes include the changes mainly in cell surface and nuclear morphology. Cell shrinkage, membrane blebbing, chromatin condensation (pyknosis), DNA fragmentation and formation of apoptotic bodies due to the loss of cell membrane integrity can be considered as the most prominent morphological changes that occur during apoptosis (Baba, 2009; Collins et al., 1997; Elmore, 2007; Krysko et al., 2008). These morphological hallmarks and biochemical changes are often used to characterize apoptosis. No distinct morphological or biochemical parameters are available to identify necrosis; hence, the absence of apoptotic biomarkers (negative biomarkers) such as activation of caspase family enzymes, DNA fragmentation and cytochrome c release are used to characterize necrosis (Baba, 2009; Collins et al., 1997; Elmore, 2007). Morphological changes such as cell shrinkage and membrane blebbing can be identified under the light microscopy. However, transmission electron microscopy is considered as the “gold standard” for the detection of cell morphology changes to distinguish apoptosis from necrosis. Translocation of phosphatidylserine residues, an anionic phospholipid from the inner leaflet to the outer leaflet of the cell membrane is a key cell membrane morphology change frequently utilized to detect apoptosis (Lee et al., 2013). This

translocation is detected by the flow cytometric analysis of cells strained with Annexin-V, a Ca^{2+}-dependent phospholipid-binding protein that binds to phosphatidylserine (negatively charged phospholipids) and therefore is considered as a useful marker of early-stage apoptotic cell death (Denecker et al., 2000). Apoptosis is driven by the extrinsic pathway (initiated by an extracellular death ligand binding to cell surface death receptor) and intrinsic pathway (intracellular activation due to intracellular stresses) (Figure 1.1). Induction of apoptosis is also characterized by detecting the activation of components involved in the extrinsic and intrinsic pathways of apoptosis. Caspase activation is identified by the cleavage of luminogenic or fluorogenic substrates or Western blot analysis of activated caspase family proteins (Krysko et al., 2008). Expression of Bcl-2 and Bax, followed by determination of Bax/Bcl-2 ratio (Raisova et al., 2001), and cytochrome release is also detected on Western blot analysis to distinguish apoptosis from necrosis. Another major hallmark of apoptosis, oligonucleosomal DNA fragmentation is detected by either gel electrophoresis or TUNEL staining (Collins et al., 1997; Labat-Moleur et al., 1998; Nagata, 2000).

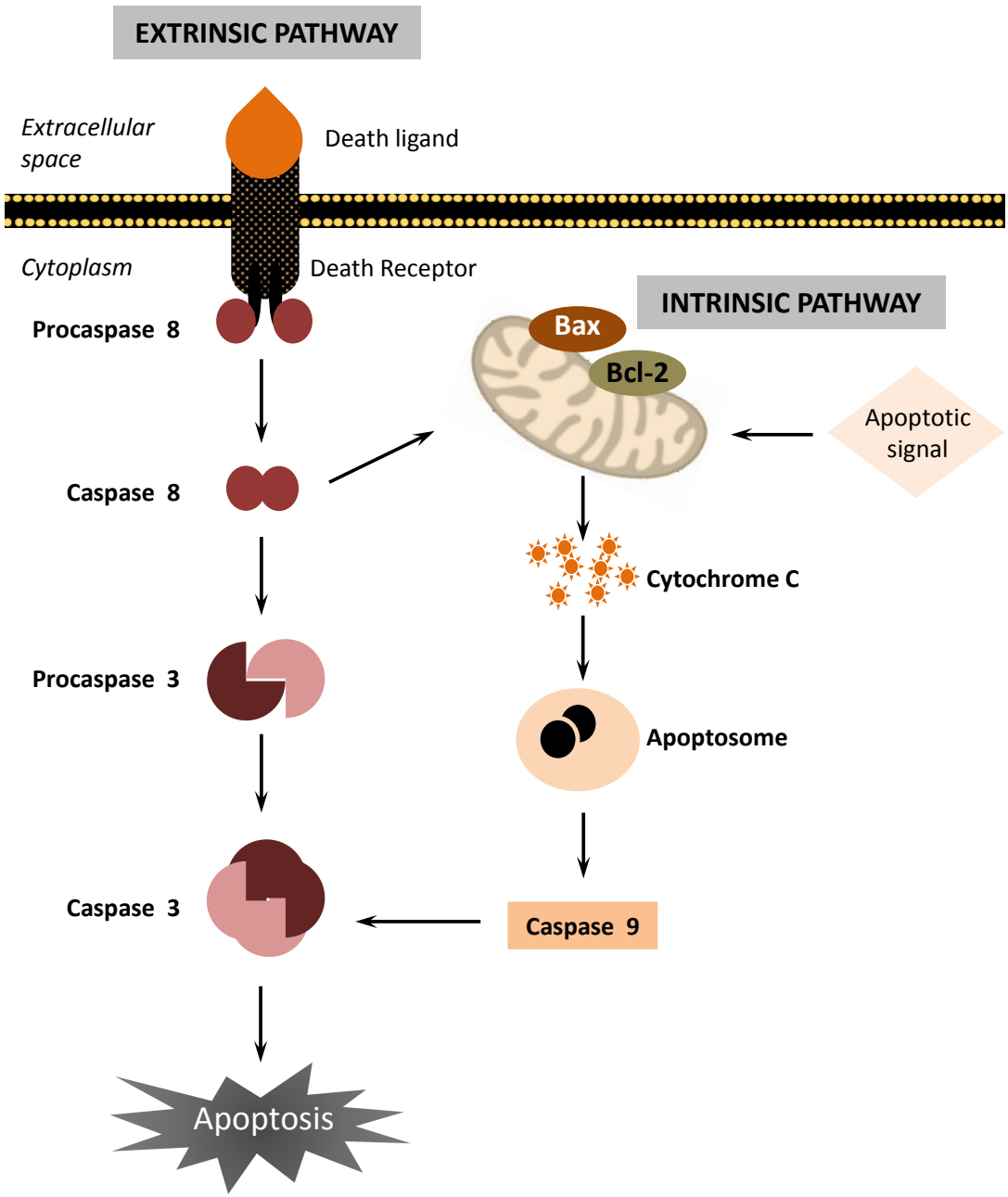

Figure 1.1: Extrinsic and intrinsic pathways of apoptosis

Bcl-2: B-Cell Lymphoma 2; **Bax:** BCL2-associated X protein

1.7 Phytochemicals as Cancer Inhibitors

Phytochemicals (Figure 1.2), plant secondary metabolites found abundantly in higher plants, are known to possess health benefits. Phytochemicals are considered as nutritious molecules with disease-fighting capabilities, but are not essential for life. Due to the increasing rate of mortality associated with cancer and the adverse or toxic side effects of cancer chemotherapy and radiation therapy, the discovery of new anticancer agents derived from nature, especially plants, receives a distinct interest (Bhanot et al., 2011; Fernando and Rupasinghe, 2013; Nirmala et al., 2011; Rupasinghe et al., 2012). Phytochemicals represent a vast majority of chemical groups such as alkaloids, flavonoids, tannins, terpenes and terpenoids, saponins and glycosides (Figure 01). Screening of medicinal plants as a source of anticancer agents was started in the 1950s, with the discovery and development of vinca alkaloids, vinblastine and vincristine and the isolation of the cytotoxic podophyllotoxins (Cragg and Newman, 2005). Vinca alkaloids were isolated from *Catharanthus roseus* (L.) (Apocynaceae) and were considered as the first ever natural anticancer agents to proceed into clinical use to treat cancer (Shoeb, 2006) . Podophyllotoxin was isolated from *Podophyllum hexandrum* (L.) (Berberidaceae) (Williams, 2001). Later, isolation of taxol from the bark of the *Taxus brevifolia* (L.), camptothecin from *Camptotheca acuminate* (L.) (Cornaceae) and homoharringtonine from *Cephalotaxus harringtonia* (L.), (Taxaceae) (Shoeb, 2006) marked important milestones in the discovery of natural phytochemicals as anticancer agents.

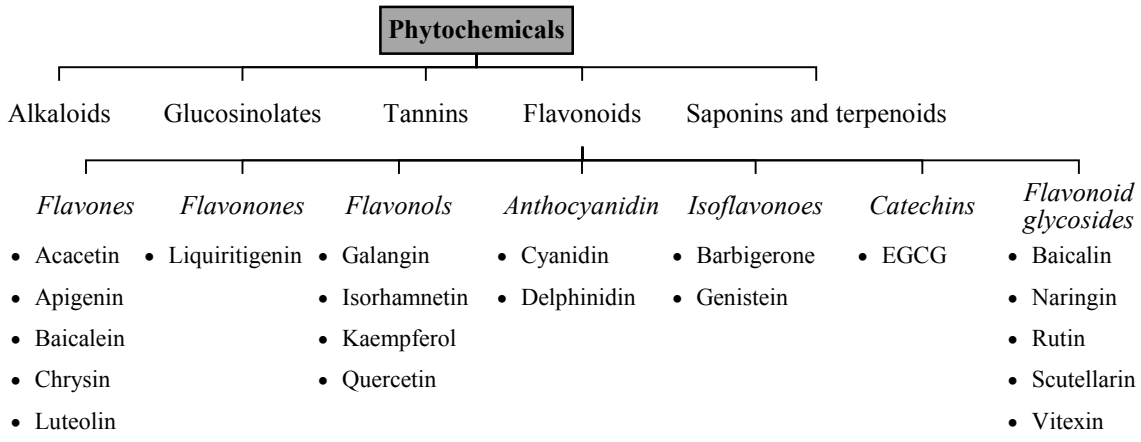

Figure 1.2: Major flavonoid sub-groups showing disease-fighting properties

1.8 Anticancer Properties of Flavonoids

1.8.1 Flavonoids

Flavonoids are polyphenolic compounds found in nature which generally consist of two aromatic rings, connected through a three-carbon bridge (C6-C3-C6 system) (Ehrenkranz et al., 2005) that may be part of a six-membered heterocyclic pyran ring (Figure 1.3) (Merken and Beecher, 2000). Flavonoids consist of a large group of compounds including flavones, flavonones, flavonols, anthocyanidins, isoflavones, catechins and flavonoid glycosides. Dietary flavonoids (abundantly found in fruits, vegetables, tea and wine) are known to play an important role in the prevention of cancer (Ren et al., 2003; Yao et al., 2011).

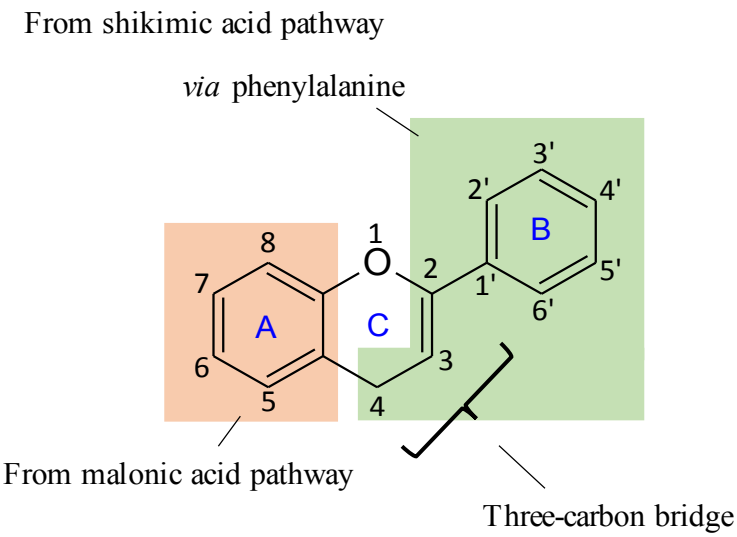

Figure 1.3: Basic skeleton of flavonoids

1.8.2 *In Vitro* Anticancer Properties of Flavonoids

Among many biological activities shown by plant flavonoids, antimicrobial, antioxidant, anti-inflammatory and anticancer properties are the most promising in terms of impacting human health. A successful anticancer drug is supposed to kill cancer cells selectively, causing minimum adverse side effects to the normal healthy cells at low physiological concentrations. Flavonoids are expected to fulfill this requirement successfully because of their natural source origin. Flavonoids are emerging as anticancer agents with the ability to act at multiple sites of cell signal pathways. Therefore, flavonoids may be successfully used to prevent and treat cancers (Fernando and Rupasinghe, 2013; Rupasinghe et al., 2012). These compounds exhibit their antiproliferative properties on different cell lines and mostly the activity is dose- and time-dependent. They exert their anticancer properties by affecting reactive oxygen species (ROS) production and signal transduction pathways governing cell proliferation and growth, apoptosis, and angiogenesis. Flavonoids affect metastasis and carcinogenesis at different levels as well (Figure 1.4) (Yao et al., 2011).

Flavonoids induce both intracellular and extracellular ROS production. For example, Quercetin, a flavonol reduces intracellular glutathione concentration and increases intracellular ROS production to a level to cause death of cancer cells (Gibellini et al., 2010). The treatment of human ovarian cancer cells (HeLa) with quercetin increases intracellular ROS production, caspase activation and B-cell lymphoma 2 (Bcl-2) expression (Bishayee et al., 2013). Quercetin-induced intracellular ROS production causes apoptosis in human hepatocellular carcinoma (HepG2) cells as well (Chang et al., 2006). In human lung cancer cells (H23, H2009, H460, and A549) luteolin (a flavone) blocks Tumor Necrosis Factor (TNF)-activated Nuclear Factor-kappaB (NF-κB) pathway, resulting ROS accumulation-mediated apoptosis (Ju et al., 2007). Pre-treatment of human prostate cancer (22Rv1) and isogenic prostate cells (PC-3 ($p53^{-/-}$) and PC-3 ($p53^{+/+}$)) with antioxidant (N-acetylcystein (NAC)) and p53 inhibitor (pifithrin-α) reverses apigenin-induced ROS production and p53 accumulation in mitochondria respectively (Shukla and Gupta, 2008). Similarly, pretreatment with caspase inhibitors (Z-VAD-FMK and DEVD-CHO) reverses apigenin-induced reduction of cellular levels of B-cell lymphoma-extra-large (Bcl-xL) and B-cell lymphoma 2 (Bcl-2) and increase in Bcl-2-associated X protein (Bax) of 22Rv1 cells. This suggests apigenin-induced cell death is ROS production-, p53- and caspase activation-dependent (Shukla and Gupta, 2008). Acacetin, an *O*-methylated flavone induces caspase activation, ROS generation and reduces Bcl-2 expression in breast cancer cells (MCF-7) (Shim et al., 2007). However, pre-incubation of cells with NAC or caspase 8 inhibitor (Z-IETD-FMK) reverses ROS production and caspase activation reducing mitochondrial membrane potential loss, respectively (Shim et al., 2007). This indicates the involvement of ROS production and caspase activation in acacetin-induced MCF-7 cell death as well.

Epigallocatechin gallate (EGCG), a type of catechin selectively inhibits the growth of transformed fibroblasts (NIHpATMras) while having no growth inhibitory effects on the normal fibroblasts. Further, it inhibits tyrosine kinase and mitogen-activated protein kinase (MAPK) activities without suppressing the normal cells (Wang and Bachrach, 2002). EGCG also shows antiproliferative properties in human pancreatic cancer cells (AsPC-1 and BxPC-3) (Vu et al., 2010) and human breast cancer cells (MCF-7) (Ono et al., 2014). Myricetin, a natural flavonol, inhibits the growth of human bladder cancer cells (T24) causing cell cycle arrest at gap 2 (G2) / mitosis (M) and down regulates cyclin B1 level (Sun et al., 2012). Plant extracts containing flavonoids have also shown anticancer properties in *in vitro* cell cultures. For example, a mixture of flavones isolated from *Scutellaria barbata* D. (Lamiaceae) (Barbed skullcap) reduces the expression of vascular endothelial growth factor (VEGF) in a dose-dependent manner both in human hepatocellular carcinoma (MHCC97-H) and human umbilical vein endothelial cells (HUVECs) (Dai et al., 2013). Grape seed extracts (GSE) are widely used as dietary supplements and consist of at least 85% w/w procyanidins (Wen et al., 2008). GSE inhibits VEGF-induced phosphorylation of both forms of mitogen-activated protein kinase (MAPK) proteins (MAPKp42 and MAPKp44) in HUVECs (Wen et al., 2008). A warm water extract of cranberry presscake (material remaining after pressing cranberries to collect its juice) inhibits proliferation of human androgen-dependent prostate (LNCaP), skin (SK-MEL-5), colon (HT-29), lung (DMS114), brain (U87), estrogen-independent breast (MDA-MB-435, MCF-7) and androgen-independent prostate (DU145) cancer cells (Ferguson et al., 2004). It also blocks cell cycle progression of MDA-MB-435 in a dose-dependent manner (Ferguson et al., 2004). Aqueous leaf extract (ALE) of *Nelumbo*

nucifera L. contains gallic acid, rutin, and quercetin as main flavonoid constituents. *N. nucifera* L. ALE inhibits human breast cancer cell proliferation (MCF-7) arresting cell cycle progression at gap 0 (G_0) / gap 1 (G_1) phase (Yang et al., 2011a). Apple is one of the primary sources of flavonoids in North American diet. A flavonoid enriched fraction (AF4) of apple peel induces cell cycle arrest, Deoxyribonucleic acid (DNA) topoisomerase II inhibition and apoptosis in human liver cancer cells (HepG2) (Sudan and Rupasinghe, 2014 (in press)). An apple pomace ethanol extract rich with flavonoids shows a dose-dependent reduction in cell number at 72 hr post treatment in human colon cancer cells (HCT116) (Morton et al., 2013). Further, flavonoids play a crucial role in inducing synergistic effect *in vitro* in combination with other cytotoxic drugs as well (Achanta, 2012; Aksamitiene, 2012; Xu et al., 2011).

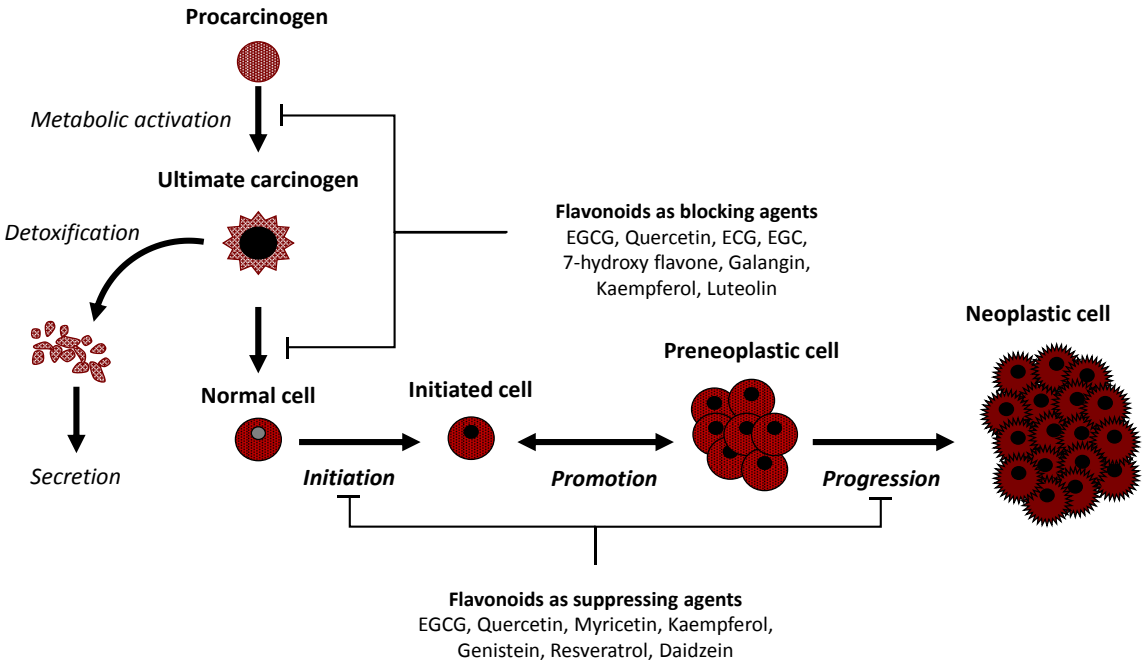

Figure 1.4: Flavonoids inhibit carcinogenesis at cellular level

(Regenerated from figures adapted from (Kale et al., 2008; Surh, 1999))

Carcinogenesis is a collection of series of processes taking place when a normal healthy cell becomes a cancer cell. Carcinogenesis can be divided into main three stages namely, tumor initiation, tumor promotion and tumor progression.

EGCG: Epigallocatechin gallate; **ECG:** (-)-Epicatechin gallate; **EGC:** (-)-Epigallocatechin.

1.8.3 *In Vivo* Tumor Suppressor Activity of Flavonoids

In vivo tumor suppressor activities of naturally-occurring flavonoids have been studied in different animal models. Tumor suppressor activities of flavonoids in experimental animal models include inhibition of cell growth, protein kinase activities, matrix metalloproteinase (MMP) secretion, tumor cell invasion, adhesion and spreading (Kandaswami et al., 2005). These suppressor activities eventually lead to induction of apoptosis and prevention of

angiogenesis and metastasis (Kandaswami et al., 2005). MDA-MB-435 human breast tumor growth is inhibited when tumor bearing mice are fed with cranberry presscake (Guthrie, 2000). Oral administration of cranberry concentrate reduces the growth of N-butyl-N-(4-hydroxybutyl)-nitrosamine- (OH-BBN) induced urinary bladder tumors in female Fisher-344 rats (Prasain et al., 2008). However, the reduction in tumor growth and the decrease in the number of urinary bladder papillomas in the cranberry concentrate-treated rats is not statistically significant (Prasain et al., 2008). Dietary supplementation of quercetin significantly suppresses growth of orthotopically transplanted MIA PaCa-2 human pancreatic cells in nude mice (Angst et al., 2014). Oral administration of EGCG inhibits the growth of orthotopically implanted human pancreatic cancer cells (PANC-1) in the pancreas of Balb C nude mice (Shankar et al., 2013). Growth of subcutaneously transplanted human non-small-cell lung cancer (NSCLC) (A549) cells in $Nrf2^{-/-}$ mice is reduced significantly when luteolin is orally administered either in the presence or absence of cisplatin (Chian et al., 2014). Human prostate (PC-3) tumor bearing BALB/cA male nude mice show significant reduction in tumor volume and weight when tumors are treated with luteolin (Fang et al., 2007a; Pratheeshkumar et al., 2012a) and quercetin (Pratheeshkumar et al., 2012b) intraperitoneally. Intraperitoneal administration of luteonin inhibits the growth of subcutaneously implanted Lewis lung carcinoma (LLC) cells in C57BL/6 mice (Kim et al., 2007) as well. Melanoma is the most common skin cancer in North America. Galangin, a flavonol, shows inhibitory effects on metastasis of human melanoma cells (B16F10) *in vitro* and *in vivo* (Zhang et al., 2013). Galangin shows antimetastatic properties *in vivo* in a mouse model of metastasis (Zhang et al., 2013). Intraperitoneal administration of fisetin (a flavonol) to LLC bearing C57BL/6J female mice

decreases the tumor size by 50% and reduces vascularization as well (Touil et al., 2011). Some flavonoids have shown antiangiogenic and antimetastatic properties in *in vivo* models as well. Oral administration of xanthohumol, a flavonoid from *Humulus lupulus* L. (Cannabaceae) inhibits angiogenesis induced by kaposi's sarcoma cells (KS-IMM) implanted in nude mice in a dose-dependent manner (Albini et al., 2006). Xanthohumol also shows antiangiogenic properties *in vivo* in C57/b16N male mice (Albini et al., 2006). *In vivo* antiproliferative properties of flavonoids as well as extracts rich with flavonoids have been reported. However, despite of the extensive *in vitro* evaluations being carried out to investigate the antiproliferative properties of flavonoids, not many have been preceeded to the level of clinical trials due to the lack of promising *in vivo* data. Therefore, there is a need for further *in vivo* investigations to validate the *in vitro* antiproliferative properties of flavonoids.

1.8.4 Mechanisms of Action of Flavonoids-induced Anticancer Activity

Flavonoids are a large group of plant secondary metabolites and their well-recognized effectiveness as antiproliferative agents is exerted through regulation of a number of cell signaling pathways (Figure 1.5). Phosphoinositide 3-Kinase (PI-3K)/Protein Kinase B (AKT)/mammalian target of rapamycin (mTOR) (PI-3K/AKT/mTOR), rat sarcoma (RAS)/Mitogen-activated protein kinase (MAPK) (RAS/MAPK), Janus kinase (JAK)/ signal transducers and activators of transcription (STAT) (JAK/STAT) and AKT/hypoxia-inducible factor-1α (HIF-1α) (AKT/HIF-1α) are common cell signaling pathways that are subject to flavonoid-induced suppression/activation. AKT plays a significant role in regulating apoptosis, cell growth and proliferation, protein synthesis and angiogenesis. Apigenin, baicalein, baicalin and fisetin inhibit PI-3K/AKT/mTOR pathway in various

human cancer cell lines and also at different sites. Apigenin, a flavone, is involved in the suppression of AKT signaling of human ovarian cancer cells (OVCAR-3 and A2780/CP70) and thereby inhibits vascular endothelial growth factor (VEGF) at its transcriptional level (Fang et al., 2005, 2007b; Patel et al., 2007). Treatment DU-145 human prostate cancer cells with chrysin, a natural flavone, reduces the stability of HIF-1α by promoting its ubiquitination and prolyl hydroxylation (Fu et al., 2007). In addition, fisetin (a flavonol) (Adhami et al., 2012) and baicalin (a flavone) (Zhang et al., 2014a) suppress the PI-3K/AKT/mTOR pathway. Galangin, serves as a flavonol affecting multiple points of cell signaling cascades such as RAS/MAPK and JAK/STAT. In addition galangin (Ansó et al., 2010) and quercetin (Ansó et al., 2010; Triantafyllou et al., 2007) prevent stabilization and phosphorylation of HIF-1α; thus, block activation of HIF-1α targeted genes, regulating cell proliferation and angiogenesis. Quercetin (Muthian and Bright, 2004; Senggunprai et al., 2014), EGCG (Senggunprai et al., 2014) and icaritin (a flavonol glycoside) (Li et al., 2013) inhibit activation of STAT-induced cell proliferation and angiogenesis. Acacetin inhibits tyrosine phosphorylation of STAT1 and 3 and blocks nuclear translocation of phosphorylated STAT3 in human umbilical vein endothelial cells (HUVEC) (Bhat et al., 2013). As a result of this STAT suppression and nuclear translocation of phosphorylated STAT, STAT-induced VEGF activation is reduced (Bhat et al., 2013).

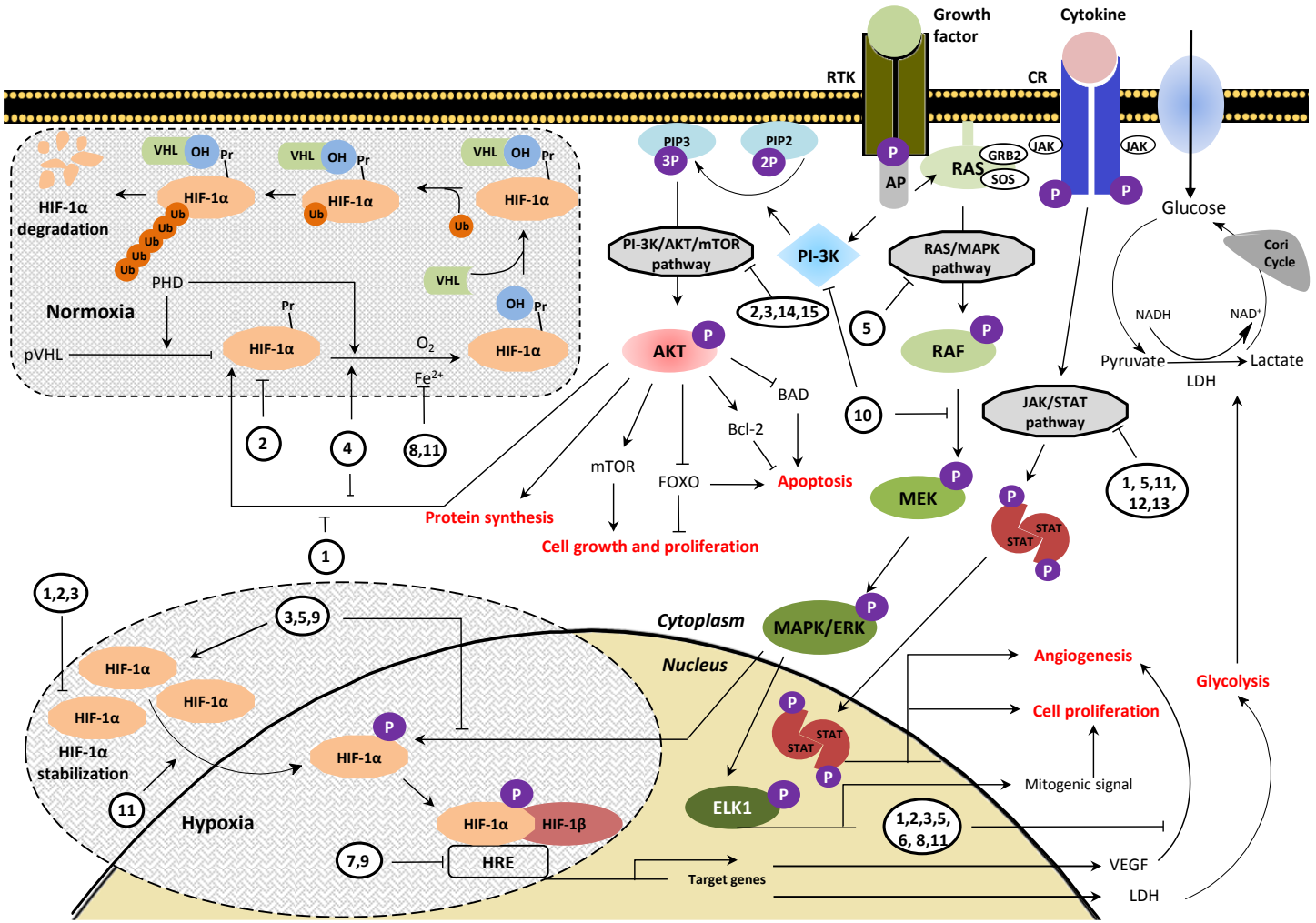

Figure 1.5: Flavonoids inhibit PI-3K/AKT/mTOR, RAS/MAPK, JAK/STAT and HIF-1α pathways in a hypothetical cancer cell

1: Acacetin; **2:** Apigenin; **3:** Baicalein; **4:** Chrysin; **5:** Galangin; **6:** Hesperetin; **7:** Isorhamnetin; **8:** Kaempferol; **9:** Luteolin; **10:** Myricetin; **11:** Quercetin; **12:** Epigallocatechin gallate; **13:** Icaritin; **14:** Fisetin; **15:** Baicalin;

AKT: Protein Kinase B; **AP:** Activator Protein; **BAD:** Bcl-2-Associated Death Promoter; **Bcl-2:** B-Cell Lymphoma 2; **CR:** Cytokine Receptor; **ELK1:** ETS domain-containing protein; **ERK:** Extracellular Signal Regulated Kinase; **FOXO:** Forkhead box O3; **GRB2:** Growth factor Receptor-Bound protein 2; **HIF-1α:** Hypoxia-Inducible Factor 1-α; **HRE:** Hypoxia Response Element; **JAK:** Janus kinase; **MAPK:** Mitogen Activated Protein Kinase; **MEK:** MAPK/ERK Kinase; **mTOR:** Mammalian Target of Rapamycin; **PHD:** Prolyl Hydroxylase Enzyme; **PI-3K:**Phosphatidylinositol-3-kinase; **PIP2:** Phosphatidylinositol (4,5)-bisphosphate; **PIP3:** Phosphatidylinositol(3,4,5)-trisphosphate; **Pr:** Proline; **pVHL:** Von Hippel–Lindau protein; **RAS:** a family of related proteins "Rat sarcoma"; **RTK:** Receptor Tyrosine Kinase; **SOS:** Son Of Sevenless; **STAT:** Signal Transducer and Activator of Transcription; **Ub:** Ubiquitin; **VHL:** Von Hippel–Lindau Tumor Suppressor.

1.8.5 Acylation of Flavonoids

Flavonoids exert protective properties against many chronic diseases such as cancers, neurodegenerative disorders, cardiovascular diseases and diabetes. However, low cellular uptake and reduced stability are major drawbacks of naturally occurring flavonoid glycosides, which restrict their successful applications in treating diseases. This will eventually lead to poor bioavailability. Therefore, many attempts have been made to improve the bioavailability of flavonoids while protecting or improving their biological properties. The modifications made to achieve high systemic bioavailability include incorporation into microemulsions to enhance the intestinal absorbance (Shen et al., 2011; Shikov and Pozharitskaya, 2008), methylation of flavonoids to increase the hepatic

metabolic stability and intestinal absorption (Walle et al., 2007) and enzymatic modification to increase cellular uptake (Nielsen et al., 2006; Ziaullah et al., 2013). The most commonly used enzymatic modification of flavonoids is acylation with saturated or mono/poly-unsaturated fatty acids catalyzed by immobilized lipase from *Candida antarctica* (Mellou et al., 2006; De Oliveira et al., 2009; Stevenson et al., 2006; Ziaullah et al., 2013). Generally, the regioselective acylation of flavonoids is carried out in non-toxic organic solvents (e.g.: 2-methyl-2-butanol, 2-methyl-2-propanol and acetone) (Mellou et al., 2006; De Oliveira et al., 2009; Stevenson et al., 2006; Ziaullah et al., 2013). The synthesis is followed by the chromatographic purification and ^{1}H and ^{13}C nuclear magnetic resonance (NMR) analyses. NMR analysis confirms the single-targeted product synthesis (Ardhaoui et al., 2004a; Mellou et al., 2005; Stevenson et al., 2006; Ziaullah et al., 2013). The acylation of flavonoid glycosides such as naringin (naringenin-7-*O*-rhamnoglucoside) and isoquercetin (quercetin-3-*O*-glucopyranoside) is done using carboxylic acids (palmitic, cinnamic and phenylpropionic (PPA) acids and hydroxylated derivatives of PPA) as acyl donors. This results in major mono-acylated products but also with minor mono-acylated products (Stevenson et al., 2006). However, esterification of apple and blueberry extracts using lipase B shows specificity for acylation of glycosides with a primary aliphatic hydroxyl group on the sugar moiety (Ardhaoui et al., 2004a; Stevenson et al., 2006; Ziaullah et al., 2013). This feature is found in flavonoids such as phloridzin (phloretin-2-glucoside) (PZ) and anthocyanidin glucosides and galactosides (Ardhaoui et al., 2004a; Stevenson et al., 2006). Both conversion yield and initial rate measure the rate of an acylation reaction. The rate of an acylation reaction depends on various factors such as the water content in the medium, length and degree of unsaturation

of the acylating donor carbon chain (Ardhaoui et al., 2004a, 2004b). The conversion yield maintains high when aliphatic acids having high carbon chain length are used as acylation donors to esterify the glycosides, rutin (also known as quercetin-3-*O*-rutinoside) and esculin (Ardhaoui et al., 2004b). However, the efficiency of isoquercitrin acylation decreases with the increase of length of the carbon chain of the acyl donor (Salem et al., 2010). Acylated flavonoids have shown a significant improvement in biological effects as well. Acylated derivatives of a monosaccharidic flavonoid chrysoeriol-7-*O*-β-D-(3''-E-p-coumaroyl)- glucopyranoside as well as of a disaccharidic flavonoid chrysoeriol-7- [6'''-*O*-acetyl-β-D-allosyl- (1→2) -β-D-glucopyranoside], isolated from *Stachys swainsonii* ssp. *argolica* (Lamiaceae) and *St. swainsonii* ssp. *swainsonii* (Lamiaceae) respectively, show enhanced antimicrobial and antioxidant activity towards both LDL and serum model *in vitro* (Mellou et al., 2005). Oleic, linoleic and γ-linolenic acid acylated rutin decreases VEGF secretion significantly in K562 (human chronic myelogenous leukemia) cells (Mellou et al., 2006). Fatty acid esters of isoquercitrin results in higher xanthine oxidase inhibition activities and antiproliferative effects on Caco-2 (human colorectal adenocarcinoma) cells than isoquercitrin. In addition, the lipophilicity of the derivative esters exhibits positive correlation with the inhibition capacity of xanthine oxidase and superoxide radical scavenging activity (Salem et al., 2010).

1.9 Phloretin and Phloridzin

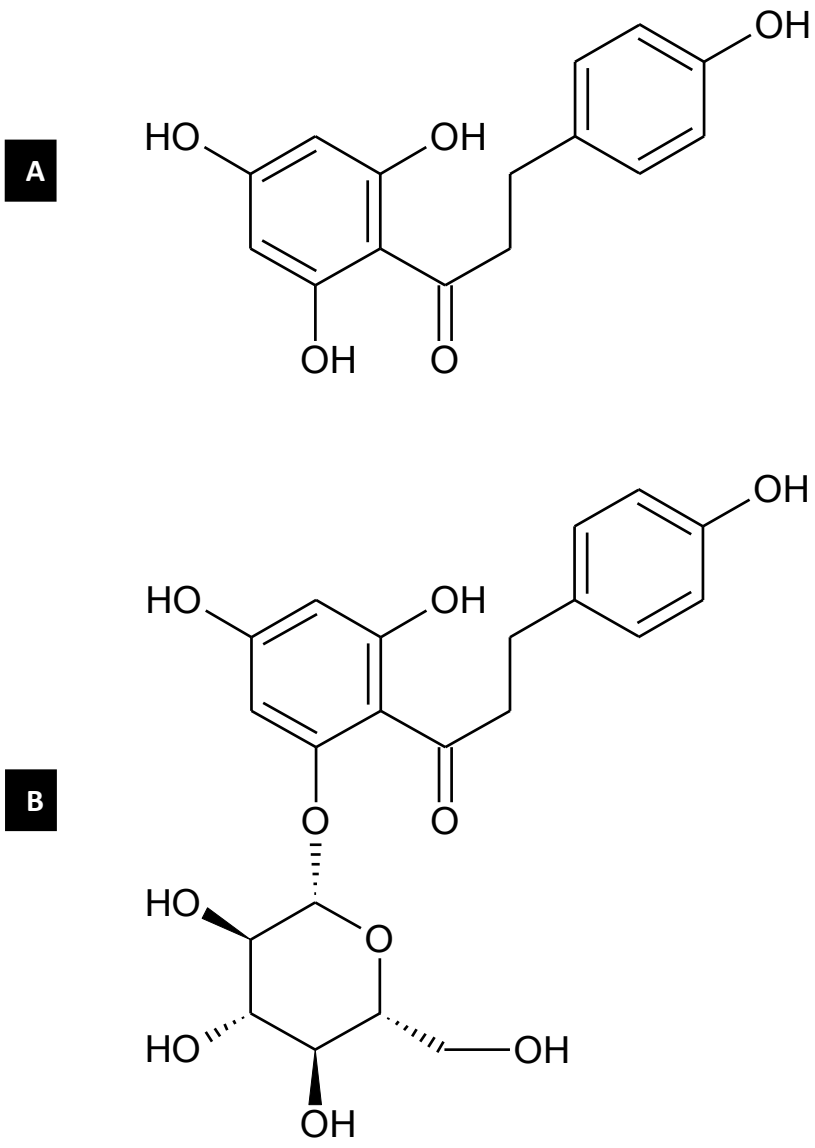

Figure 1.6: Structure of A) Phloretin and B) Phloridzin

Phloretin: 3-(4-hydroxyphenyl)-1-(2,4,6-trihydroxyphenyl)propan-1-one; (Molecular Formula: $C_{15}H_{14}O_5$ and Formula Weight: 274.27 g/mol); Phloridzin: 1-[2,4-dihydroxy-6-[(2S,3R,4R,5S,6R)-3,4,5-trihydroxy-6-(hydroxymethyl)tetrahydropyran-2-yl]oxy-phenyl] -3-(4-hydroxyphenyl)propan-1-one (Molecular Formula = $C_{21}H_{24}O_{10}$ and Formula Weight = 436.41 g/mol)

1.9.1 Biological Properties of Phloretin and Phloridzin

Phloretin (PT) (3-(4-hydroxyphenyl)-1-(2,4,6-trihydroxypropiophenone)), (Figure 1.6-A) is a naturally occurring dihydrochalcone compound (a type of flavonoid in the polyphenol family) abundantly found in leaves, bark and seed of *Malus domestica* L. (Rosaceae) and seeds of *Prunus mandshurica* L. (Rosaceae) Phloretin-induced antioxidant properties and the inhibition of lipid peroxidation have been shown in the peroxynitrite scavenging assay and lipid peroxidation assay, respectively (Rezk et al., 2002). The pharmacophore of PT, which is required for its antioxidant activity is 2, 6-dihydroxyacetophenone (Rezk et al., 2002). Antioxidant activity of PT has also been shown in the DPPH free radical-scavenging capacity and the 2,2'-azino-bis(3-ethylbenzothiazoline-6-sulphonic acid (ABTS) free radical-scavenging capacity (Zuo et al., 2011). Favorable effects of PT in the management of cardiovascular diseases have been shown in human umbilical vein endothelial cells (HUVECs). PT prevents TNFα-stimulated up-regulation of the cytokine-induced expression of intercellular adhesion molecule-1 (ICAM-1), vascular cell adhesion molecule-1 (VCAM-1) and endothelial leukocyte adhesion molecule-1 (E-selectin) (Stangl et al., 2005). PT inhibits TNFα-stimulated adhesion of monocytic THP-1 cells to HUVECs and human aortic endothelial cells with no effect on TNFα-stimulated activation of nuclear factor κB (NF-κB) (Stangl et al., 2005). PT suppresses adenosine diphosphate (ADP)-stimulated platelet aggregation as well (Stangl et al., 2005). Both PT (a GLUT-2 inhibitor) and PZ (1-[2,4-dihydroxy-6-[(2S,3R,4R,5S,6R)-3,4,5-trihydroxy-6-(hydroxymethyl) tetrahydropyran-2-yl]oxy-phenyl]-3-(4-hydroxyphenyl)propan-1-one) (Figure 1.6-B) (SGLT1 inhibitor) suppress the glucose uptake of intestinal cell lines, Caco-2, RIE-1, and IEC-6 (Zheng et al., 2012). PT inhibits the growth of both Gram positive (*Staphylococcus*

aureus, *Listeria monocytogenes* and methicillin-resistant *Staphylococcus aureus*) and Gram negative bacteria (*Salmonella typhimurium*). Glycosylated derivatives show diminished antimicrobial activity in comparison to PT, suggesting that glycosyl moiety reduces the antimicrobial efficacy of PT (Barreca et al., 2014). PT inhibits the growth of Gram positive and Gram negative bacteria by inhibiting the phosphorus uptake by bacterial cells. Though PT is effective against both Gram negative and positive bacteria, the inhibitory effects are shown to be more promising toward Gram positive bacteria than Gram negative bacteria (MacDonald and Bishop, 1952).

1.9.2 Anticancer Properties of Phloretin and Phloridzin

Anticancer properties of PT and PZ are reported less frequently. PT suppresses protein kinase C activity and cause apoptosis of B16 melanoma 4A5 cells as shown by DNA fragmentation (Kobori et al., 1997). Reversal of PT-induced apoptosis of B16 melanoma 4A5 cells by addition of extracellular glucose suggests the involvement of PT in inhibition of glucose transmembrane transport (Kobori et al., 1997). Significant *in vivo* antiproliferative efficacy of PT and PZ has been shown on Fischer 344 male rats subcutaneous transplanted with FBC cells (methylcholanthrene induced stage 3 transitional cell bladder carcinoma). This model is known as Fischer bladder carcinoma *in vivo* tumor model. PT and PZ also inhibit mammary adenocarcinoma (also known as mammary adenocarcinoma *in vivo* tumor model) subcutaneously transplanted into Fischer 344 female rats (Nelson and Falk, 1993a). PT and PZ block glucose transport (measured using 2-deoxy-D-glucose uptake by brain, liver, spleen and tumor tissue) into viable tumor cells both *in vitro* and *in vivo* (Nelson and Falk, 1993b).

1.10 Docosahexaenoic Acid

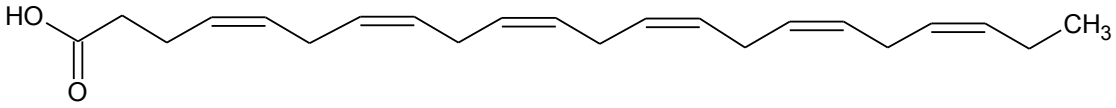

Figure 1.7: Structure of Docosahexaenoic acid

Docosahexaenoic acid: (4Z,7Z,10Z,13Z,16Z,19Z)-docosa-4,7,10,13,16,19-hexaenoic acid (Molecular Formula = $C_{22}H_{32}O_2$ and Formula Weight = 328.57 g/mol).

1.10.1 Biological Properties of Docosahexaenoic Acid

Docosahexaenoic acid (22:6 n-3 DHA), ((4Z,7Z,10Z,13Z,16Z,19Z)-docosa-4,7,10,13,16,19-hexaenoic acid) (Figure 1.7) is an omega-3 polyunsaturated fatty acid (ω-3 PUFAs), abundantly found in fish oil. It is considered as an essential PUFA required for the normal function (McCann and Ames, 2005) of adult brain and growth and functional development of infant brain (Morse, 2012). Hence, DHA helps to prevent neurodegenerative diseases through maintaining the proper functionality of brain (Cunnane et al., 2009; Hashimoto et al., 2002; Horrocks and Yeo, 1999). Favorable protective activities of DHA on reducing the incidence risk of Alzheimer's disease have been shown in a human clinical trial (Connor and Connor, 2007). This emphasizes the link of fish oil and ω-3 PUFAs (DHA is one of the major constituents) consumption with reduced Alzheimer's disease incidence risk (Connor and Connor, 2007; Morris et al., 2003). DHA has shown a wide variety of biological properties proven *in vitro* as well as *in vivo*. Antinociceptive properties of orally administered DHA on the thermal (tail flick test) and chemical nociception (writhing test and formalin test) models indicate dose-dependent

antinociceptive capacity in male ddY mice (Nakamoto et al., 2010). Showing cardiovascular protective properties, DHA reduces the development of hypertension in spontaneously hypertensive rats (SHR) *in vivo* (McLennan et al., 1996). In a double-blind, placebo-controlled human clinical trial DHA significantly reduces 24-hour, daytime and nighttime heart rates and daytime ambulatory blood pressure relative to the placebo group (Mori et al., 1999). It also reduces ambulatory heart rate and blood pressure in mildly hyperlipidemic men (Mori et al., 1999).

1.10.2 Anticancer Properties of Docosahexaenoic Acid

DHA is a well-tested PUFA for its antiproliferative properties on different cancer cell lines *in vitro* and *in vivo*. DHA induces apoptosis and cell death of MDA-MB-231 breast adenocarcinoma cells detected by mitochondrial membrane potential loss, caspase activation and DNA fragmentation (Schley et al., 2005). DHA treatment also reduces AKT phosphorylation and NF-κB DNA binding activity of MDA-MB-231 cells suggesting DHA-induced decrease in signal transduction of AKT/NF-κB pathway (Schley et al., 2005). Dose-dependent antiproliferative properties of DHA on human metastatic hepatocellular carcinoma cells (MHCC97L) indicates the effectiveness of DHA in treating metastatic liver cancer and this cytotoxicity is associated with the suppression of cyclin A/ cyclin-dependent kinases (Cdk2) protein and cell cycle arrest at S phase (Lee et al., 2010) as well. DHA-induced cellular death of human hepatocellular carcinoma cells (Bel-7402) is associated with less suppression of Bcl-2 and Bim messenger ribonucleic acid (mRNA) levels, and caspase-3 and Bax activation (Sun et al., 2013). Pretreatment of human B-cell lymphoma cells (DHL-4) with vitamin E prevents DHA-induced death exhibiting the involvement of lipid peroxidation in cell death of DHL-4 (Ding et al., 2004). DHA down

regulates the expression of key antioxidant enzyme, superoxide dismutase (SOD) as well indicating the sensitivity of DHL-4 to DHA-mediated SOD regulation (Ding et al., 2004). DHA inhibits the proliferation of mouse mammary cancer cells (FM3A), by arresting the cell cycle at G_1 and suppressing cell cycle-associated proteins such as cyclin E phosphorylation, Cdk2 activity (Khan et al., 2006). DHA induces the cell growth inhibition of human lung adenocarcinoma (Mv1Lu mink, A549) and human lung squamous carcinoma cells (BEN) (Serini et al., 2008). This involves DHA-induced specificity toward inhibition of phosphatase activity and Mitogen-Activated Protein Kinase Phosphatase-1 (MKP-1) (Serini et al., 2008). Treatment of Mv1Lu mink and A549 cells with a phosphatase inhibitor, Sodium orthovanadate (Na_3VO_4), and by silencing the MKP-1 gene with the specific Small Interfering RNA (siRNA), indicates these activities are important for cancer cell growth (Serini et al., 2008).

These *in vitro* antiproliferative capabilities of DHA have been demonstrated on animal models as well. Oral administration of DHA suppresses the growth of MDA-MB-231 cells transplanted into thoracic mammary fat pad of female nude mice (Connolly et al., 1999). Incorporation of DHA in a rodent fat diet containing linoleic acid enhances the total tumor suppressor activity showing significant inhibition in proliferation of metastatic breast cancer cells in athymic nude mice (Connolly et al., 1999; Rose et al., 1995). Furthermore, reduced expression of the Ki-67 associated proliferation marker and Terminal deoxynucleotidyl transferase dUTP nick end labeling (TUNEL) staining of DNA fragmentation *in vivo* suggests DHA-induced antiproliferative and apoptosis, respectively (Rose and Connolly, 1993). Feeding of Balb/c mice bearing mouse mammary carcinoma cell (4T1) tumors shows significant *in vivo* reduction in tumor growth due to inhibition of

cell proliferation and induction of apoptosis (Xue et al., 2014). *In vivo* tumor suppressor activity of DHA has been shown on estrogen-dependent cells as well. Athymic nude mice bearing MCF-7 human breast cancer cells, fed with rodent diet containing fish oil shows significant reduction in tumor volume (Kang et al., 2010). Oral administration of high fat diet containing DHA reduces the growth of human colon carcinoma cells (COLO 205), carrying wild type p53, transplanted subcutaneously in athymic mice (Kato et al., 2007).

1.11 Research Hypothesis

Structurally modified phloridzin docosahexaenoate (PZ-DHA), a fatty acid ester derivative of PZ, exhibits enhanced antiproliferative properties *in vitro* and breast tumor suppressor activity *in vivo*, possibly due to increased ability of PZ-DHA to penetrate the plasma membrane than its precursor PZ.

1.12 Objectives and Research Approach

The overall objective of this research was to determine the *in vitro* and *in vivo* cytotoxic and antiproliferative properties of PT, PZ, DHA and PZ-DHA using human triple negative breast adenocarcinoma cells (MDA-MB-231), human mammary epithelial cells (HMEpiCs) and non-obese diabetic severe combined immunodeficient (NOD-SCID) mice model xenografted with MDA-MB-231 cells.

Fruits, vegetables, tea and wine are well known sources rich with dietary flavonoids having tremendous disease-fighting abilities including prevention of cancers, so have been studied for their health benefits widely (Kandaswami et al., 2005; Ren et al., 2003; Yao et al., 2011). Flavonoids, being a large group of plant secondary metabolites have shown anticancer properties on a range of *in vitro* cell culture systems and also in animal models.

Interestingly, flavonoids exert their antiproliferative activity by manipulating many crucial sites of cell signaling cascades such as suppression of PI-3K/AKT/mTOR (Fang et al., 2005; Hwang et al., 2008; Mirzoeva et al., 2008; Adhami et al., 2012; Pratheeshkumar et al., 2012b), AKT/HIF (He et al., 2013; Liu et al., 2011), MAPK (Triantafyllou et al., 2007) and JAK/STAT (Li et al., 2013; Muthian and Bright, 2004; Senggunprai et al., 2014) leading to inhibition of protein synthesis, cell growth and proliferation, angiogenesis, metastasis and induction of apoptosis. However, poor bioavailability and diminished stability of flavonoids restrict its use in the treatment of many ailments and various approaches have been practiced to overcome these limitations. (Nielsen et al., 2006; Shen et al., 2011; Shikov and Pozharitskaya, 2008; Walle et al., 2007). Enzymatic modification of flavonoids, especially lipase catalyzed esterification of flavonoids with fatty acids (saturated and unsaturated), is a novel approach to increase membrane permeability and eventually their biological activities (Chebil et al., 2006; Mellou et al., 2005, 2006; Viskupicova et al., 2010; Zhao et al., 2011). In the current study, the antiproliferative properties of PZ-DHA (Figure 1.8) which was synthesized in an attempt to increase lipophilicity and cellular uptake of PZ was investigated. Furthermore, this activity was evaluated with comparison to its parent compounds, PZ and DHA, using MDA-MB-231, a triple negative breast cancer cell line and HMEpiC, human mammary epithelial cells. PZ-DHA is reported for its antioxidant properties and tyrosinase inhibition activity (Ziaullah et al., 2013), and my research team has previously shown its promising antiproliferative properties on HepG2 and THP-1 cells (data not published yet). To the best of my knowledge, the antiproliferative efficacy of PZ-DHA on triple negative breast cancer cells has not yet been recorded. Therefore, a research gap, which is not fully understood due to

the lack of resources on the cytotoxic efficacy of a novel PZ fatty acid ester on killing triple negative breast cancer cells, is expected to be filled through the findings of current study. Dose- and time-dependent cytotoxic properties of PT, PZ, DHA and PZ-DHA were measured in 3-(4,5-dimethylthiazol-2-yl)-5-(3-carboxymethoxyphenyl)-2-(4-sulfophenyl)-2H-tetrazolium, inner salt (MTS) and acid phosphatase assays with doxorubicin (DOX) and docetaxel (DOC) in place as positive controls. Assays to evaluate the involvement of PZ-DHA-induced ROS in cell death, apoptosis and cell cycle arrest were also carried out. *In vitro* findings were confirmed in a NOD-SCID mice model xenografted with MDA-MB-231 breast cancer cells.

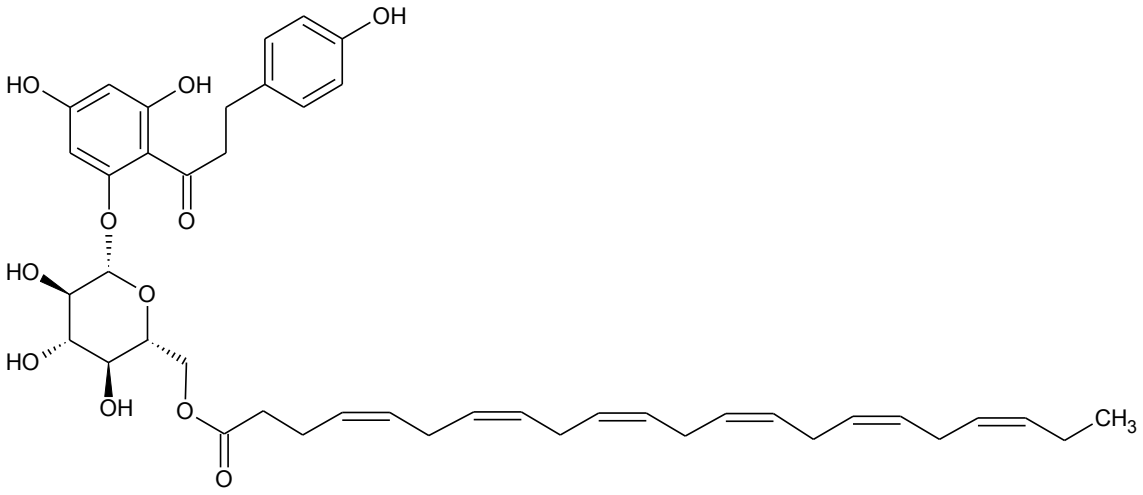

Figure 1.8: Chemical structures of phloridzin docosahexaenoate

(Molecular Formula = $C_{43}H_{54}O_{11}$ and Formula Weight = 746.88 g/mol)

CHAPTER 2 : MATERIALS AND METHODS

2.1 Chemicals and Reagents

Trypsin-EDTA (Trypsin- Ethylenediaminetetraacetic acid) (0.25% trypsin/0.53 mM EDTA in HBSS (Hank's Balanced Salt Solution) without calcium and magnesium for *in vitro* work, phosphate buffered saline (PBS) with Ca^{2+} and Mg^{2+}, phosphate buffered saline (PBS) without Ca^{2+} and Mg^{2+} and dimethylsulfoxide (DMSO) were purchased from ATCC (American Type Culture Collection) through Cedarlane labs (Burlington, ON). Sterile irrigation water was from Baxter (Mississauga, ON, Canada) and methanol and ethanol were purchased from BDH chemicals, VWR International (Mississauga, ON, Canada). Magnesium chloride and paraformaldehyde was from Bioshop® Canada Inc. (Burlington, ON, Canada). Staurosporine and docetaxel were purchased from Biovision Incorporated, Milpitas, CA, USA) and Cayman Chemicals (Ann Arbor, MI, USA) respectively. Fetal bovine serum (FBS), N-2- hydroxyethylpiperazine-N'-2-ethanesulfonic acid (HEPES), L-glutamine, penicillin-streptomycin (Pen-strep), trypsin (0.25% with EDTA (1×)) for *in vivo* work, TryPLE express were from Gibco® by Life Technologies Inc. (Burlington, ON, Canada). Docosahexaenoic acid was purchased from Nuchek (Elysian, MN, USA) and both 5-[3-(carboxymethoxy) phenyl]-3-(4,5-dimethyl-2-thiazolyl)-2-(4-sulfophenyl)-2H-tetrazolium inner salt (MTS) and caspase-Glo® 3/7 assay kit were from Promega (Madison, WI, USA). Annexin-V-FLUOS and propidium iodide (PI) were purchased from Roche Diagnostics (Laval, QC, Canada) and saline was from Hospira Healthcare Corporation (Montreal, QC, Canada). Serum-free, HEPES and bicarbonate buffered mammary epithelial cell medium, mammary epithelial cell growth supplement,

penicillin/streptomycin solution and poly-L-lysine was purchased from ScienCell (Carlsbad, CA, USA). Doxorubicin, phloretin, phloridzin, phenazine methosulfate (PMS), Dulbecco's Modified Eagle's Medium (DMEM), phenol red-free Dulbecco's Modified Eagle's Medium (DMEM), phosphatase substrate, Triton X-100, sodium acetate ($CH_3COO^-Na^+$), sodium hydroxide (NaOH), sodium chloride (NaCl), calcium chloride ($CaCl_2$) and hydrogen peroxide (H_2O_2) were all ordered from Sigma-Aldrich (Oakville, ON, Canada).

2.2 Animals

Ethical approval for animal use was obtained from the Dalhousie University Committee on Laboratory Animals (UCLA) (Protocol number: 13-077). Six to eight weeks old female non-obese diabetic severe combined immunodeficient (NOD-SCID) mice were purchased from Charles River Canada (Lasalle, QC, Canada). Animals were housed under sterile conditions in the Carleton Animal Care Facility, Tupper Building of Dalhousie University and fed on a sterilized rodent diet and water was supplied *ad libitum*.

2.3 Stock Solutions

Unless otherwise stated all the stock solutions for *in vitro* assays were stored at – 80 ◦C in 50 µL aliquots. Stock solutions of PT, PZ, DHA and PZ-DHA (40 mM) were prepared in sterile DMSO. Stock solutions (8.33 mM, 40 mM and 107.17 µM) of DOX, DOC and staurosporine (STS) were prepared respectively and stored in – 80 ◦C in 50 µL aliquots. The highest concentration of working solution prepared was 200 µM except for STS and it was 1 µM. DMSO was used as the vehicle control for all the test compounds. All the test compounds were prepared in complete DMEM immediately before use and a serial

dilution method was used to prepare the working solution series. In the same way vehicle controls were also diluted to compare the working test compound solutions with their respective vehicle controls. All the stocks of test compounds for *in vivo* work were made in sterile DMSO at 200 mM concentration and stored at – 80 ◦C. Working concentration of 1.33 mM of test compounds was achieved by an appropriate dilution of stocks in sterile saline. DMSO (0.6% v/v) in sterile saline was used as the control.

2.4 MDA-MB-231 Cell Culture System

MDA-MB-231 is adherent, epithelial like cell line derived from the metastatic site (pleural effusion) of human breast (mammary gland) tissue of 51 year old female Caucasian (Cailleau et al., 1978) (MDA-MB-231: ATCC catalogue number HTB 26, Manassas, VA, USA). It is an estrogen independent cell line which serves as a useful *in vitro* model for human breast adenocarcinoma studies and express epidermal growth factor (EGF) and transforming growth factor alpha (TGF-α) (Bates et al., 1988, 1990; Ciardiello et al., 1991)

2.5 HMEpiC Cell Culture System

Human mammary epithelial cells (HMEpiC) are isolated from normal human breast tissue (HMEpiC: ScienCell catalogue number 7610, Carlsbad, CA, USA) and described by immunofluorescence staining of antibodies specific to cytokeratine 14, 18 and 19.

2.6 Cell Culture Conditions

MDA-MB-231 and HMEpiC are generous gifts from Dr. David W. Hoskin, Department of Pathology, Faculty of Medicine, Dalhousie University. The base medium for MDA-MB-231 cell line is Dulbecco's Modified Eagle's Medium (Cat no. D5796: Sigma-Aldrich

Canada Ltd., Oakville, ON) was supplemented with 10% heat-inactivated (56 °C for 30 min) fetal bovine serum (Cat no. 12483: Life Technologies Inc. Burlington, ON), 5 mM N-2- hydroxyethylpiperazine-N'-2-ethanesulfonic acid (7.4 pH: Cat no. 15630-080: Life Technologies Inc. Burlington, ON), 2 mM L-glutamine (Cat no. 25030-081: Life Technologies Inc. Burlington, ON), 100 U/mL penicillin, and 100 µg/mL streptomycin (Cat no. 15140-122: Life Technologies Inc. Burlington, ON). DMEM was supplied with 4500 mg glucose/L, sodium bicarbonate, L-glutamine and cells were maintained at 37 °C in a humidified incubator (VWR International, Mississauga, ON) supplied with 5 % CO_2. T-75 tissue culture flasks (Falcon™ Fisher Scientific, Ottawa, ON) with 10-12 mL of media were used for regular culturing. Sub-culturing was performed in 1:1, 1:2, 1:3, 1:4 or 1:5 ratio (cell cultures were maintained at a cell density between 5×10^4 - 5×10^5 cells/cm^2) every 3 to 4 days or at 70-90% confluency. For splitting, the culture medium was removed. The adhered cell monolayers were lift up using 3 mL of 0.25% (w/v) Trypsin - 0.53 mM EDTA (from Life Technologies Inc. Burlington, ON) solution as the dissociation solution. Trypsinization was done for 3-5 min and was followed by addition of 7 mL of complete DMEM to inactive the dissociation solution. Cells were aspirated by gently pipetting and the cell suspension was aliquot suitably into new culture vessels. For cryopreservation, complete growth medium supplemented with 5% v/v DMSO and 5% heat inactivated FBS were used and cells were stored in liquid nitrogen. HMEpiC were grown in serum-free, HEPES and bicarbonate buffered mammary epithelial cell medium (MEpiCM, Cat no. 7611: ScienCell, Carlsbad, CA, USA) supplemented with 5 mL of mammary epithelial cell growth supplement (MEpiCGS, Cat no. 7652: ScienCell, Carlsbad, CA, USA) and 5 mL of penicillin/streptomycin solution (P/S, Cat. No. 0503: ScienCell, Carlsbad, CA, USA).

Cells were maintained at 37 °C in a humidified incubator supplied with 5 % CO_2. Tissue culture flasks (T-75) with 9-10 mL of media were used for regular culturing. Sub-culturing was performed in 1:1 ratio every 4 days at 90% confluency. Medium was changed 2 days after splitting. Ten milliliter of sterile double distilled water and 15 µL of poly-L-lysine stock solution (10 mg/mL, Cat No. 0413: ScienCell, Carlsbad, CA, USA) was directly added to a T-75 flask to prepare poly-L-lysine-coated culture flask (2 µg/cm^2, T-75 flask). The flask was incubated in 5% CO_2 incubator at 37 °C for 3 hr. At the end of incubation, poly-L-lysine coated culture flask was rinsed with 10 mL of sterile double distilled water twice. For splitting, complete MEpiCM, 1 × sterile PBS, and trypsin EDTA was warmed in a 37 °C water bath. The adhered cell monolayers were rinsed with 5 mL warm PBS and lift up using 3 mL of 0.25% (w/v) Trypsin - 0.53 mM EDTA solution in 3 mL PBS. Trypsinization was done for 3-5 min in a 37 °C incubator and detached cells were transferred to a 50 mL tube containing 5 mL FBS. Cells were spun down at 500 ×g for 5 min and washed with 5 mL warm MEpiCM and cell pellet was resuspended in 5 mL warm MEpiCM. Cell suspension (200 µL) was seeded into poly-L-lysine coated T-75 containing 9 mL complete growth medium.

Unless otherwise stated, 96-well and 6-well plates were seeded with 5×10^3 and 5×10^4 cells/well, respectively. All the centrifugations were performed at 500 gravity (g) for 5 min, except for acid phosphatase assay. Tryphan blue (0.1% v/v) in 1 × PBS was used to test cell viability. Cells were stained with trypan blue and dead cells turned blue when viewed under the microscope. Live cells extruded the dye as their cell membrane integrity was not damaged. Cells used for all the *in vitro* and *in vivo* assays were 95-100% viable on trypan blue staining.

2.7 MTS Assay

The cytotoxic activity of the test compounds was measured using MTS assay, which is a non-radioactive colorimetric assay used to measure the cell viability and cytotoxicity (Hoskins et al., 2012). Mitochondrial succinate dehydrogenase and NADH-dependent oxidoreductases catalyze the intracellular reduction of water insoluble 3-(4, 5-dimethyl-2-thiazolyl)-2, 5-diphenyl-2H-tetrazolium bromide (MTT) to water insoluble formazan product (Berridge et al., 2005; Lau et al., 2004). Reduction of second generation tetrazolium, 5-[3-(carboxymethoxy)phenyl] -3-(4,5-dimethyl-2-thiazolyl) -2-(4-sulfophenyl)-2H-tetrazolium inner salt (MTS), a weakly acidic inner salt closely related to MTT into its water soluble formazan is indicated by the conversion of yellow color into brown. This reduction is also associated with the requirement to employ an intermediate electron acceptor (IEA) (phenazine methosulfate: PMS) to facilitate the cellular reduction of MTS. Increased negative charge on MTS reduces cell permeability and therefore the reduction takes place extracellularly or at the level of cell membrane (Figure 2.1) (Berridge et al., 2005). Therefore, the principle of this assay was to measure the reduction of MTS to a water soluble formazan and then quantifying the absorbance at 490 nm using a spectrophotometer or micro plate reader.

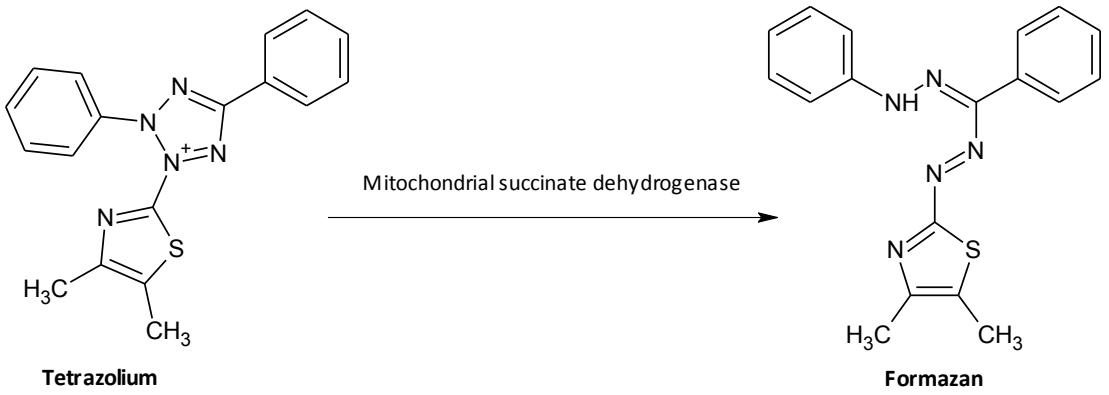

Figure 2.1: Succinate dehydrogenase catalyzed conversion of tetrazolium (MTS) into aqueous formazan in MTS assay

The assay was performed using commercially available MTS assay kit (Promega, Madison, WI, USA). MDA-MB-231 cells (100 µL) were seeded in 96-well flat-bottom cell culture plates at a density of 5×10^3 cells per well and were incubated overnight to facilitate cell adhesion. Adhered cells were treated with PT, PZ, DHA, PZ-DHA, DOX and DOC (10, 50, 100, 150 and 200 µmol/L) and incubated for 3, 6, 12, 18 and 24 hr at 37 ˚C. Vehicle controls were used for all the treatment concentrations separately and untreated control (cells treated with cDMEM without any treatment) was also used. Treatment blank (cDMEM with treatment) and vehicle control (cDMEM with vehicle) were used to compensate the background absorbance. After the incubation of cells with treatments, 20 µL of combined MTS/PMS reagent (final concentrations of 333 µg/mL MTS and 25 µM PMS (Sigma Aldrich, Oakville, ON)) was added to all the experimental wells in the plate and incubated for 3 hr at 37 ˚C. To determine the percentage inhibition of metabolic activity, the absorbance of the colored product was measured at 490 nm using a micro-plate reader (BMG-LABTECH) (Ortenberg, Germany). Percentage relative metabolic activity was calculated as shown in the following equation, where A_T: absorbance of test

compound treated cells; A_{TB}: absorbance of treatment blanks; A_C: absorbance of vehicle treated cells; A_{CB}: absorbance of vehicle blanks.

$$\% \text{ Relative metabolic activity} = \frac{(A_T - A_{TB})}{(A_C - A_{CB})} \times 100$$

2.8 Acid Phosphatase Assay

Acid phosphatase assay measures the metabolic activity of live cells in terms of cytosolic acid phosphatase activity by hydrolyzing the phosphatase substrate, p-nitrophenyl phosphatase at acidic pH levels (Yang et al., 1996). The hydrolyzed product, p-nitrophenol produces the yellow-colored end product, p-nitrophenolate under alkaline conditions which could be read at 405 nm in a microplate reader and the absorbance is directly proportional to viable cell count. In alkaline pH, the acid phosphatase activity is ceased marking the end point of reaction (Figure 2.2).

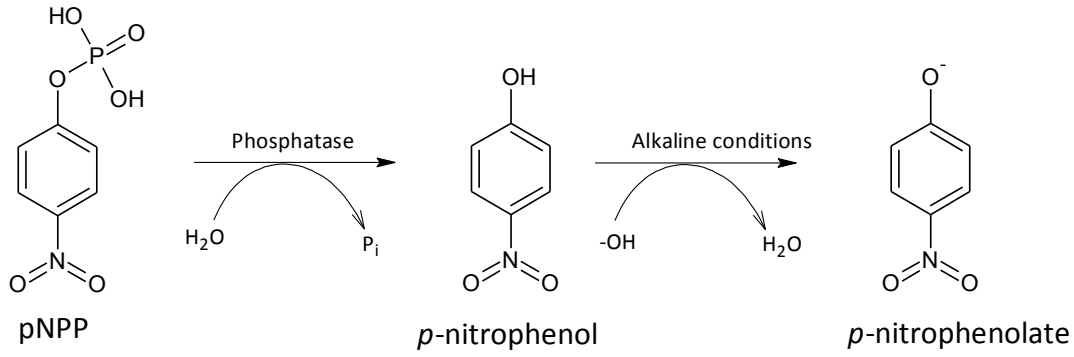

Figure 2.2: Acid phosphatase catalyzed conversion of pNPP into p-nitrophenol and end point conversion of p-nitrophenol into p-nitrophenolate under alkaline conditions in acid phosphatase assay

Acid phosphatase assay was performed as described in Yang et al., (1996) with minor modifications. MDA-MB-231 cells (in 100 µL cDMEM) were seeded in 96-well flat-bottom cell culture plates at a density of 5×10^3 cells per well and were incubated overnight to promote cell adhesion. Adhered cells were treated with PT, PZ, DHA, PZ-DHA, DOX and DOC (10, 50, 100, 150 and 200 µmol/L) and incubated for 3, 6, 12, 18 and 24 hr at 37 ˚C. Vehicle controls were used for all the treatment concentrations separately and untreated control (cells treated with cDMEM without any treatment) was also included. At the end of the incubation period the plates were centrifuged at 405 × g for 10 min and supernatant was discarded. Cell monolayers were then washed with 200 µL 1 × sterile PBS. Assay buffer (100 µL) (0.1 M sodium acetate; pH 5.5, 0.1% v/v Triton X-100 and 4 mg/mL phosphatase substrate) was added to each well and incubated for 2 hr at 37 ˚C. Ten microliter of 1N NaOH was added to each well to cease the reaction and to develop the color of the end product. The absorbance of the colored product was measured at 405 nm using a micro-plate reader (BMG-LABTECH) (Ortenberg, Germany) and percentage relative phosphatase activity was calculated as given in the following equation where A_T: absorbance of test compound treated cells; A_C: absorbance of vehicle treated cells; A_B: absorbance of blanks. Blank (100 µL of assay buffer with 10 µL of 1N NaOH) was used to compensate the background absorbance.

$$\% \text{ Relative phosphatase activity } = \frac{(A_T - A_B)}{(A_C - A_B)} \times 100$$

2.9 Amplex Red Assay

The Amplex Red assay was carried out in a cell-free environment with H_2O_2 as the positive control and with comparison to 100 µM of EGCG in phenol red-free cDMEM. This assay

was performed to assess whether test compounds (PT, PZ, DHA and PZ-DHA) reacted with sodium bicarbonate in cell culture medium to produce hydrogen peroxide (H_2O_2). In the presence of horseradish peroxidase (HRP) Amplex red (10-acetyl-3, 7-dihydroxyphenoxazine) is oxidized by H_2O_2 to an intensely red fluorescent product, resorufin (Figure 2.3) (Reszka et al., 2005). The color of this oxidized product can be measured using a spectrophotometer and the absorbance readings measured at 570 nm are directly proportional to the amount of H_2O_2 produced.

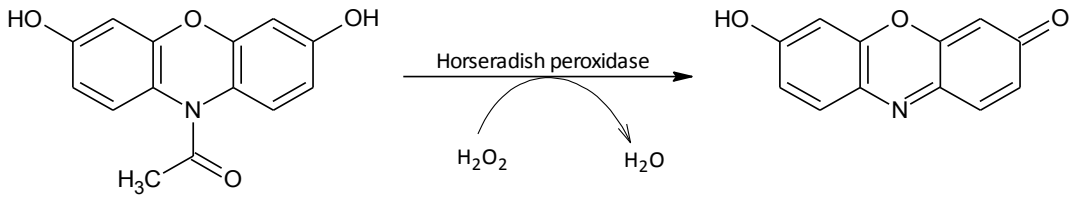

Figure 2.3: Horseradish peroxidase catalyzed conversion of Amplex red into resorufin in Amplex red assay

Amplex Red assay was performed in a 96-well flat-bottom plate in quadruplicates and the final concentration of PT, PZ, DHA, PZ-DHA and positive control was kept at 100 µmol/L. Standard curve of H_2O_2 was generated using a standard series (0.1, 0.056, 0.032, 0.018, 0.01 and 0.006 mM) of H_2O_2. In the dark, 100 µL/well of master mix (at a final concentration of 25 µM Amplex red and 0.005 U/mL HRP in phenol red-free cDMEM) was added on top of the treatments and incubated for 2 and 24 hr at 37 °C. Absorbance was measured at 570 nm on an Expert 96-well microplate reader (Admiral Place, Guelph, ON) at 2 and 24 hr post-treatment.

2.10 7-AAD Staining

7-AAD (7-Aminoactinomycin) assay was carried out to confirm the reduction in metabolic activity measured in MTS and acid phosphatase assays was due to the death of cells and not false positive results given by cell growth inhibition. 7-AAD discriminate dead cells from viable cells by intercalating between cytosine and guanine bases of DNA of dead cells that allow 7-AAD uptake (Philpott et al., 1996; Schmid et al., 1992).

For 7-AAD staining, MDA-MB-231 cells were plated at a density of 1×10^5 cells per well in 6-well plates. The cells were incubated overnight at 37 ˚C to support cell adhesion. Adhered cells were treated with 50 and 100 μmol/L of PT, PZ, DHA, PZ-DHA, vehicle or medium and incubated for 24 hr at 37 ˚C. At the end of incubation period, cells were harvested using TrypLE Express and combined with its respective media. Cells were centrifuged at 500 × g and resuspended in 1 × PBS. Cells were incubated with 5 μL of 7-AAD viability staining solution (eBioscience Inc. San Diego, CA, USA) at room temperature. Flow cytometric analysis was performed using a FACS Calibur instrument (BD Bioscience, Mississauga, ON) on detector, FL3. Cells (1×10^4) were counted per sample and both live and dead cells were included in counts.

2.11 Annexin V and Propidium Iodide Staining

The Annexin-V-FLUOS/propidium iodide (PI) assay was used to determine whether test compounds induced cell death by apoptosis and/or necrosis. The assay was modified to incorporate an extra incubation step with NAC to determine the involvement of ROS in cell death. During apoptosis, phosphatidylserine residues, an anionic phospholipid shift from the inner leaflet to the outer leaflet of the cell membrane marking the loss of cell

membrane integrity (Lee et al., 2013). In normal healthy cells these residues are found in the inner leaflet of cell membrane and during apoptosis it is translocated to the outer leaflet as a result of decreased aminophospholipid translocase activity and activation of a calcium-dependent scramblase (Fadok et al., 1998; Lee et al., 2013; Vermes et al., 1995). Annexin-V-FLUOS is a calcium-dependent phospholipid-binding protein, with high affinity for phosphatidylserine, and cell surface expression of phosphatidylserine is encountered as an important part of the apoptotic membrane dynamics (Fadok et al., 1998; Kenis et al., 2004; Vermes et al., 1995). During necrosis/late apoptosis, the fluorochrome PI, a DNA intercalating agent enters the cells when the cell membrane becomes permeable (Nicoletti et al., 1991; Riccardi and Nicoletti, 2006; Vitale et al., 1993).

MDA-MB-231 cells were plated at a density of 1×10^5 cells per well in 6-well plates. The cells were incubated overnight at 37 ˚C to promote cell adhesion. Adhered cells were treated with 100 μmol/L of PT, PZ, DHA, PZ-DHA, vehicle or medium either in the presence or absence of NAC and incubated for 6 hr at 37 ˚C. At the end of incubation period cells harvested using TrypLE express were combined with its respective media. Cells were centrifuged at 500 × g and rinsed with 1 × PBS and incubated with Annexin-V-FLUOS/PI prepared according to the manufacturer's instructions (Roche Diagnostics, Laval, QC) and PI (1 μg/mL) in staining buffer (10 mM HEPES, 10 mM NaCl, and 5 mM $CaCl_2$) for 15 min at room temperature. Flow cytometric analysis was performed using a FACSCalibur instrument (BD Bioscience, Mississauga, ON) on detectors, FL1 and FL2. Cells (1×10^4) were counted per sample and both live and dead cells were included in counts.

2.12 Luminescent Assay of Caspase-3/7 Activation

Activation of caspase 3 and 7 enzymes were tested using caspase-Glo® 3/7 assay kit (Promega, Madison, WI, USA). Caspase (cysteine-dependent aspartate-directed protease) (Nicholson and Thornberry, 1997) enzymes are the central components of apoptosis and caspase 3 is the most frequently activated protease in mammalian cell apoptosis (Porter and Jänicke, 1999). Since caspase 7 is comparable to caspase 3 in *in vitro* substrate preference (toward substrate Ac-DEVD-pNA) this assay measures activation of both caspase 3 and 7 (Talanian et al., 1997) (Figure 2.4).

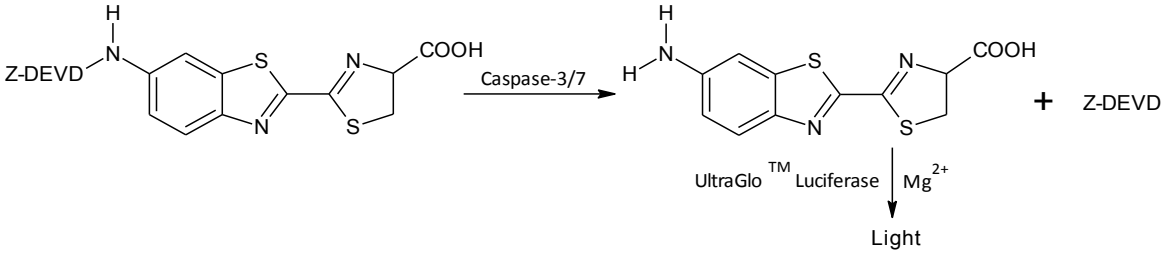

Figure 2.4: Caspase-3/7 cleavage of the luminogenic substrate

The assay was performed in triplicate according to the manufacturer's instructions. MDA-MB-231 cells (in 100 µL cDMEM) were seeded in 96-well, flat-bottom white-walled cell culture plates at a density of 5×10^3 cells per well and were incubated overnight to activate cell adhesion. Adhered cells were treated with 100 µmol/L of PT, PZ, DHA or PZ-DHA and incubated for 6 and 12 hr at 37 ˚C. Doxorubicin, docetaxel (100 µmol/L) and staurosporine (1 µmol/L) were used as positive controls. Vehicle controls and medium controls were also included in triplicates. At the end of the incubation period, contents of Caspase-Glo® 3/7 buffer vial was transferred into Caspase-Glo® 3/7 substrate and mixed by swirling. The 96-well plates incubated at 37 ˚C were equilibrated to room temperature

before adding Caspase-Glo® 3/7 assay buffer mixture. Assay mixture (100 µL) was added to each well taking extreme care to avoid cross contamination and incubated for 2 hr at 37 ˚C. Luminescence (RLU: Relative luminescence units) was measured on a microplate reader (BMG-LABTECH) (Ortenberg, Germany) using a blank (cDMEM with DMSO and assay buffer mixture in the absence of cells) to compensate for the background luminescence.

2.13 TUNEL Staining of DNA Fragmentation

Apoptosis is characterized by a series of morphological and biochemical changes taking place in a cell and DNA fragmentation is considered a hallmark. TUNEL staining was carried out using commercially available In *Situ* Cell Death Detection Kit, POD (Roche Applied Science, Laval, QC, Canada) according to the manufacturer's instructions. The assay consisted of mainly two stages. In the first stage, double stranded DNA fragments were labeled with terminal deoxynucleotidyl transferase (TdT) and in the second stage stained cells were detected under fluorescent microscope [AxioPlan 11MOT AxioCam HRc, Carl Zeiss Canada Ltd] (Thornwood, NY, USA) in the range of 515-565 nm (green fluorescence).

MDA-MB-231 cells were seeded in 6-well plates containing sterile cover slips, at a density of 4×10^5 cells per well and incubated overnight at 37 ◦C to induce cell adhesion. Adhered cells were incubated with 100 µmol/L of PT, PZ, DHA, PZ-DHA, vehicle or medium and incubated for 12 hours at 37 ˚C. of DOX, DOC (100 µmol/L) and 1 µmol/L staurosporine were used as the positive control to induce DNA fragmentation. $MgCl_2$ (2 mM) in 1 × PBS was used as the washing buffer in all the steps. At the end of incubation cells attached on

cover slips were washed with washing buffer and fixed in freshly prepared 4% w/v paraformaldehyde (PFA) in 1 × PBS for 1 hr at room temperature. Cells were rinsed with washing buffer and incubated in blocking solution (freshly prepared 3% v/v H_2O_2 in methanol) at room temperature for 10 min. Then, cells were rinsed with washing buffer and incubated in permeabilization solution (0.1% v/v Triton X-100 in 1 × PBS) for 8 min at -20 ◦C. Cells were again thoroughly washed with washing buffer and area around the sample was dried for staining. The TUNEL reaction mixture (50 µL) (50 µL, enzyme solution and 450 µL label solution) was placed carefully and spread homogeneously on the sample. Cells were incubated for 1 hr at 37 ◦C in humidified atmosphere in the dark. At the end of incubation, cells were washed with washing buffer, dried and mounted on a glass slide for viewing under the fluorescence microscope at the excitation wavelength in the range of 450-500 nm and detected in the range of 515-565 nm.

2.14 Cell Cycle Analysis

Cell cycle analysis was performed to determine the effect of PZ-DHA on arresting cell cycle. DNA binding dyes used in cell cycle analysis proportionately stain DNA present in cells (Hang and Fox, 2004). This stoichiometric staining of cellular DNA distinguishes cells in different phases of cell cycle according to a fluorescent signal given in the histogram of cell number on FL2-A of flow cytometer analysis. Cells in G_2/M phase give the highest fluorescent signal as they carry two copies of DNA and cells in G_0/G_1 phase give approximately a half of the fluorescent signal as given in G_2/M. S phase cells lie in a valley between G_0/G_1 and G_2/M peaks since they have varying amounts of DNA (Hang and Fox, 2004) (Figure 2.5).

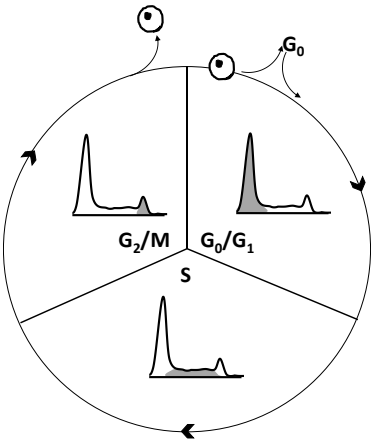

Figure 2.5: Progression of a cell through cell cycle

(Regenerated from figure adapted from (Rabinovitch, 1994))

MDA-MB-231 cells were synchronized into G_0 phase of cell cycle by incubating cells in FBS-free cDMEM for 24 hr in 75 cm^2 tissue culture flask. Synchronized cells were plated at a density of 1×10^4 cells per well in 6-well plates. The cells were incubated overnight 37◦C to stimulate cell adhesion. Adhered cells were treated with 40 μM PZ-DHA, vehicle or medium and incubated for 48 hr at 37 ˚C for 60% cell viability that was expected. At the end of incubation period, cells harvested using TrypLE Express (Gibco® by Life Technologies Inc. (Burlington, ON, Canada)) were combined with its respective media. Cells were centrifuged at 500 × g and rinsed with ice-cold 1 × PBS and resuspended in ice-cold 1 × PBS. While vortexing, ice-cold 70% ethanol was flowed slowly, drop-by-drop and incubated for at least 24 hr at -20 ˚C for fixing. Fixed cells were washed with 1 × PBS and resuspended in cell cycle solution containing PI [0.1% v/v Triton X-100; 2 μL/mL DNA-free Rnase A (Qiagen Inc., Mississauga, ON); 20 μL/mL 1 mg/mL PI in 1 × PBS] and incubated for 30 min at room temperature. Flow cytometric analysis was performed

using a FACSCalibur instrument (BD Bioscience, Mississauga, ON) on FL2A and FL2W. Cells (1×10^4) were counted per sample and counts were gated on the live cell population.

2.15 MDA-MB-231 cell xenografted NOD-SCID mice model

Six to eight weeks old NOD-SCID mice were acclimatized for 1 week. MDA-MB-231 cells for injection were mouse-pathogen tested and freshly thawed from liquid nitrogen. They were grown in T-75 and only cells in 3-4 flasks were harvested at a time. To maintain cells at maximum viability, cells were maintained at ice cold temperature throughout the procedure preparing them for injection. Injections were prepared in 1 mL syringes (BD PrecisionGlideTM, Franklin Lakes, NJ, USA) and not more than 4 injections were prepared at a time. Cells (5×10^5) were subcutaneously injected into right hind flank in 100 µL plain DMEM (without supplements) using 26G needles (BD PrecisionGlideTM, Franklin Lakes, NJ, USA) and body weights were recorded. Two weeks after xenografting, tumor sizes and body weights were started to record every other day till the last day (day 15) of the experiment. Tumor volume was calculated according to the equation, ((L×P^2))⁄2 where, L: longest tumor diameter and P: diameter perpendicular to the longest diameter. Once the tumor volume reached 100 mm^3 in size (recorded as day one), mice were randomly assigned into three treatment groups and vehicle control group and intratumoral injections were started to achieve estimated 200 µM drug concentration in the tumor. Altogether, five intratumoral injections of each test compound (PT: 0.27 mg/kg; DHA: 0.327 mg/kg and PZ-DHA: 0.75 mg/kg) or vehicle control (0.6 % v/v DMSO in saline) were given every other day (day 1, 3, 5, 7 and 9) for nine days. Mice were monitored for one more week (day 11, 13 and 15) and their tumor sizes and body weights were recorded. Tumor bearing mice were euthanized by isofluorane inhalation followed by CO_2 inhalation at day-15 (at the end

of experimental period) or earlier if they show any signs of tumor ulceration or distress. Euthanized mice were photographed and the tumors were excised. Excised tumors were weighed, photographed and fixed in 10% v/v acetate buffered formalin (0.2 L, 37% formaldehyde, 1.8 L, distilled water and 46.1 g sodium acetate.$3H_2O$) (Fisher Scientific, ON, Canada).

2.16 Mycoplasma test

Mycoplasma test was performed a day before subcutaneous injection of cells using MycoAlert® Mycoplasma detection kit (Lonza, Rockland, ME, USA), with use of positive and negative controls. Test was performed in sterile 1.5 mL eppendorf tubes. Fifty microliters of culture medium was incubated with 50 µL of reagent for 5 min at room temperature and read on luminator and recorded the reading as "A". The reaction mixture was incubated with 50 µL of substrate again for 5 min at room temperature and recorded the second reading, "B" on laminator. Ratio of B⁄A>1.2 considered to indicate mycoplasma contamination.

2.17 Histological analysis of excised tumors

Fixation solution was replaced with 70% ethanol after 48-72 hr and embedded in paraffin. Paraffin embedded tumors were cut into 5 µm thick sections using microtome (Leica Rm 2255, Leica Biosystems, ON, Canada) and mounted on glass slides for staining. Slides were dried overnight and stained with haemotoxylin and eosin. Stained slides were mounted (Cytoseal™ XYL, Richard-Alan Scientific, Thermo Scientific, Walldorf, Germany) and photographed under bright field microscope [AxioPlan 11MOT AxioCam HRc, Carl Zeiss Canada Ltd] at × 100 magnification.

2.18 Statistical Analysis

All the data were analyzed statistically using Minitab 16 or Instat softwares at 5%, 1% or 0.1% significance level. Results were expressed as mean ± SEM of three independent experiments conducted in quadruplicate. Differences among means were analysed using one way ANOVA using Tukey's test as the multiple means comparison method. Differences were considered statistically significant at $P < 0.05$ in all *in vitro* assays and at $P < 0.05$, 0.01 or 0.001 in *in vivo* assays.

CHAPTER 3 : PT, DHA AND PZ-DHA BUT NOT PZ INHIBIT PROLIFERATION OF MDA-MB-231 BREAST CANCER CELLS *IN VITRO* AND *IN VIVO* IN NOD-SCID MICE

3.1 PT, DOX and DOC Inhibit Metabolic Activity of MDA-MB-231 Cells in both Time- and Dose-Dependent Manner

Metabolism is a key feature of live cells, hence the effect of PT, PZ, DHA and PZ-DHA on metabolic activity of MDA-MB-231 cells was measured in MTS assays, in which the live cell population is characterized by detecting formazan produced by the reduction of a tetrazolium salt which indicates the involvement of cellular enzymes of live cells. As measured by the MTS assay, PT, DHA and PZ-DHA but not PZ showed a time- and dose-dependent inhibition of metabolic activity (Figure 3.1 and 3.3). PT-induced metabolic activity inhibition was both time- and dose-dependent. Dose dependency was observed for PT through 3-24 hr (Figure 3.1). DOX and DOC were used as positive controls and both the positive control showed time- and dose-dependency.

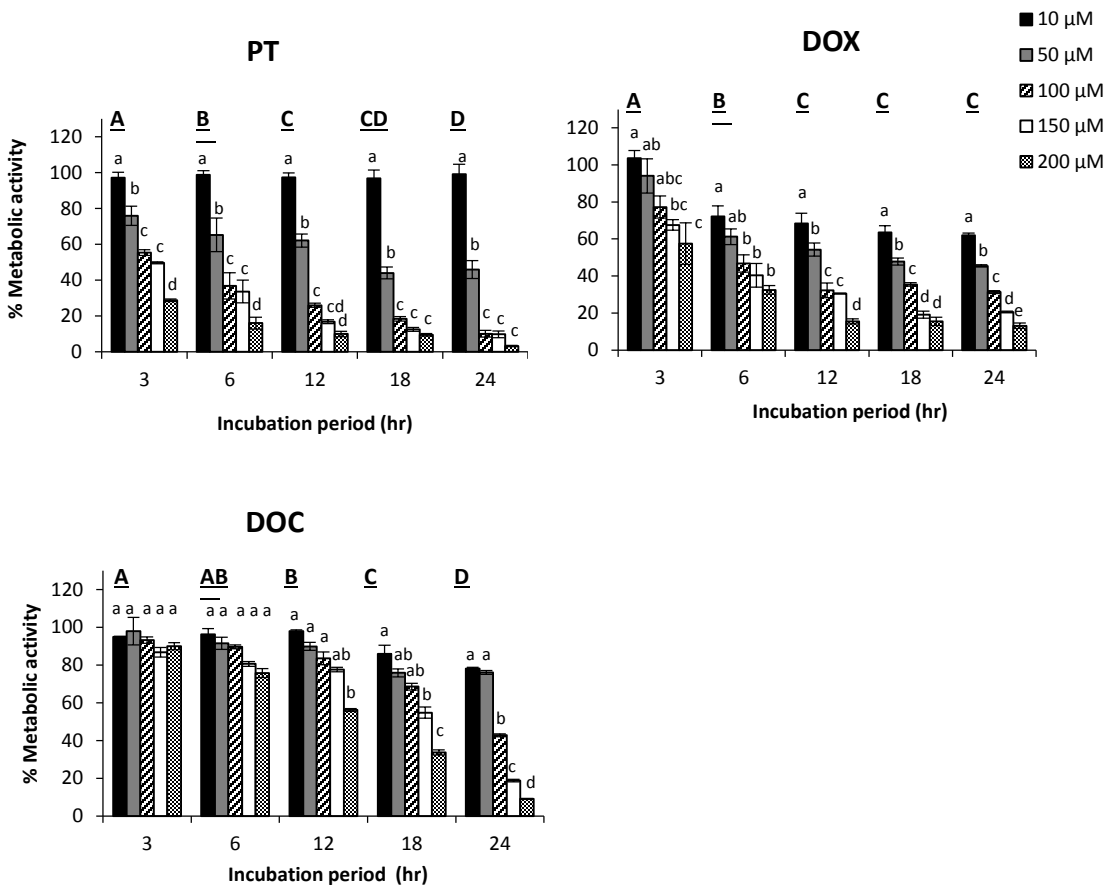

Figure 3.1: Dose- and time-dependent reduction in metabolic activity of PT, DOX and DOC on MDA-MB-231 triple negative breast cancer cells

The reduction in metabolic activity induced by PT, DOX and DOC was evaluated using MTS assay. MDA-MB-231 cells were seeded at 5×10^3 cells/well density in flat-bottom 96 well plated and incubated over night for cell adhesion. Cells were then treated with 10, 50, 100, 150 and 200 µM concentrations of test compounds and the enzyme activity was determined at the end of incubation at 37 ˚C for 3, 6, 12, 18 and 24 hr. Data expressed above as mean ± SEM (n=12) are averaged results of three independent experiments conducted in quadruplicates. Differences among means were compared using Tukey's test. Values with different letters (A-D: Time-dependency, a-e: Dose-dependency) are significantly different at $\alpha = 0.05$ ($P<0.05$).

3.2 DOX and DOC but not PT Inhibit Cytosolic Acid Phosphatase Activity of MDA-MB-231 Cells in both Time- and Dose- Dependent Manner

Cytosolic acid phosphatase activity of MDA-MB-231 cells was inhibited by all the test compounds as in MTS assay except for PT and PZ. Both PT and PZ did not inhibit phosphatase activity significantly (Figure 3.2 and 3.4). However, the inhibitory effects of DHA and PZ-DHA on the phosphatase activity were more prominent than their effect on metabolic activity measured in MTS assay. Dose-dependent phosphatase activity inhibition showed by DHA was started at a relatively early time point (12 hr) (Figure 3.4). PZ-DHA showed a unique consistency in inhibiting phosphatase activity in a time- and dose-dependent manner throughout the experimental period (Figure 3.4).

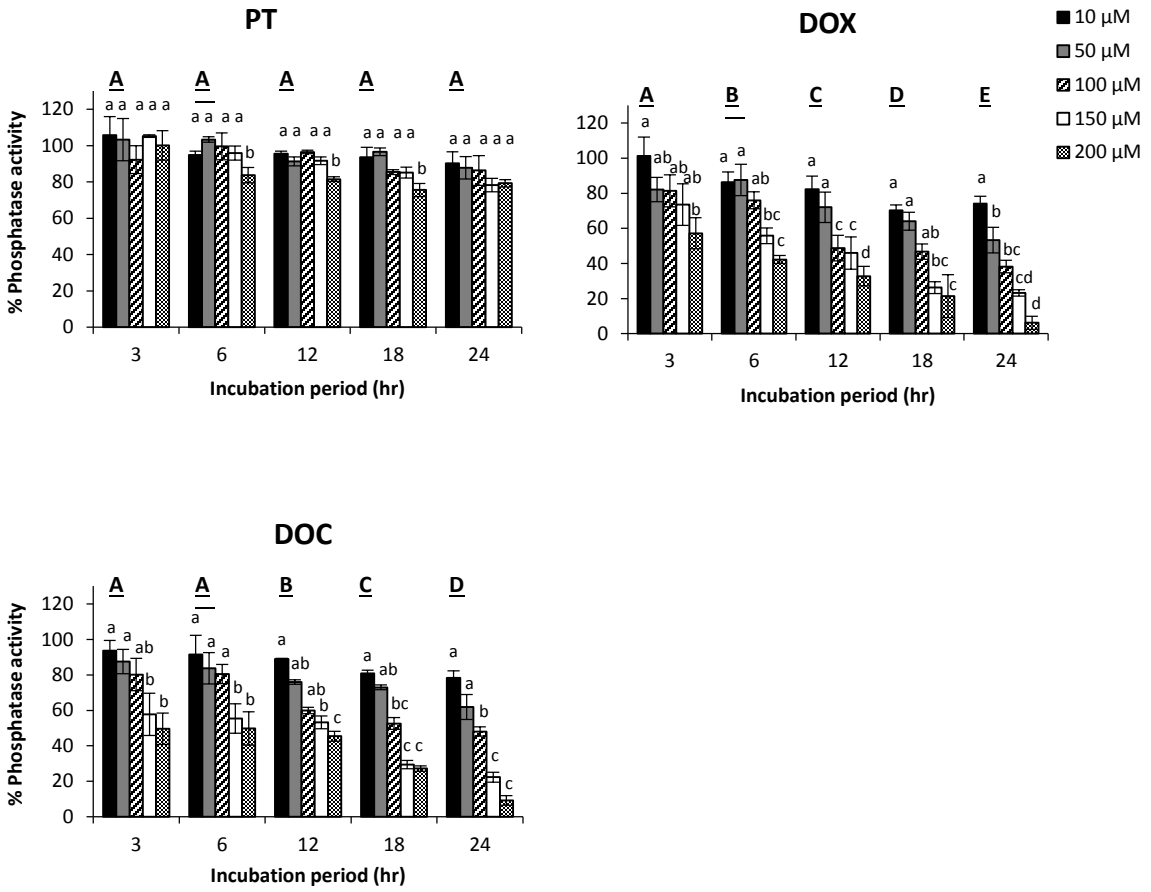

Figure 3.2: Dose- and time-dependent phosphatase activity inhibition by PT, DOX, and DOC on MDA-MB-231 triple negative breast cancer cells

Inhibitory effects of PT, DOX and DOC on cytosolic phosphatase activity were evaluated using acid phosphatase assay. MDA-MB-231 cells were seeded at 5×10^3 cells/well density in flat-bottom 96 well plated and incubated over night for cell adhesion. Cells were then treated with 10, 50, 100, 150 and 200 µM concentrations of test compounds and phosphatase activity inhibition was determined at the end of incubation at 37 ˚C for 3, 6, 12, 18 and 24 hr. Data expressed above as mean ± SEM (n=12) are averaged results of three independent experiments conducted in quadruplicates. Differences among means were compared using Tukey's test. Values with different letters (A-D: Time-dependency, a-e: Dose-dependency) are significantly different at $\alpha = 0.05$ ($P<0.05$).

3.3 PZ-DHA Significantly Inhibits Metabolic Activity of MDA-MB-231 Cells in Comparison to Parent Compounds, PZ and DHA

PZ did not show inhibition of the metabolism of MDA-MB-231 cells (Figure 3.3). DHA started showing dose-dependent activity at 12 hr (Figure 3.3). The ester, PZ-DHA showed dose dependency starting at an early time point of treatment (3 hr). At and above 50 μM concentration of PZ-DHA, effect of time-dependency was observed through 3-24 hr treatment duration. It was interesting to evaluate the PZ-DHA-induced metabolic inhibition shown in MTS assay in comparison to its parent compounds PZ and DHA. Significant reduction in metabolic activity was showed almost at an early stage (3 hr) (Figure 3.3-A) and also at relatively low concentrations (50 μM) (Figure 3.3-D and E) of PZ-DHA.

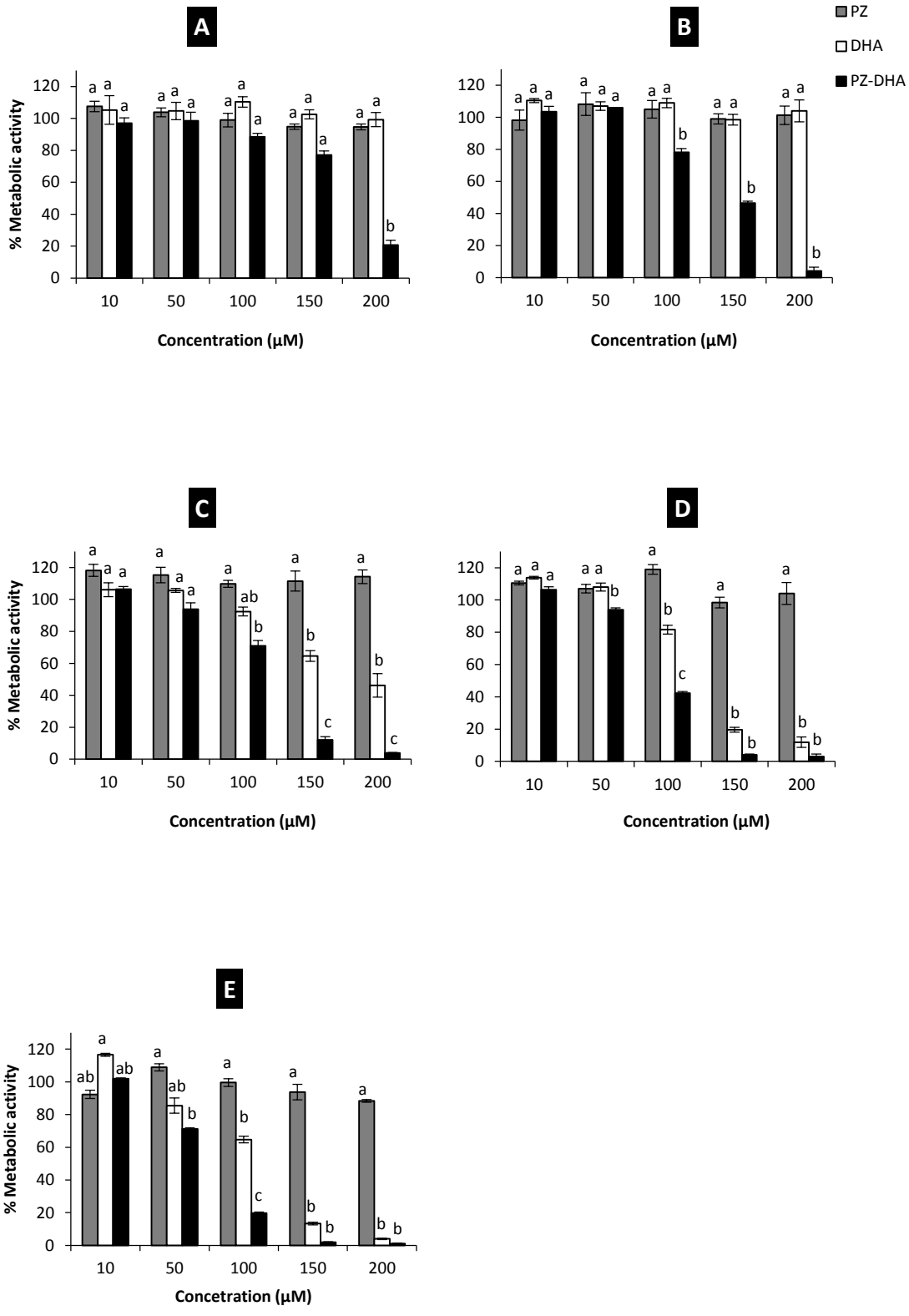
A
B
C
D
E
PZ
DHA
PZ-DHA
% Metabolic activity
Concentration (µM)
Concetration (µM)
10
50
100
150
200
0
20
40
60
80
100
120

Figure 3.3: Significant metabolic inhibition of MDA-MB-231 cells by PZ-DHA at early hours of treatment and low concentrations in comparison to parent compounds

Inhibition of metabolic activity of MDA-MB-231 cells by PZ-DHA was compared to its parent compounds at **A)** 3, **B)** 6, **C)** 12, **D)** 18 and **E)** 24 hr of treatment at 10, 50, 100, 150 and 200 μM concentrations. Data expressed above as mean ± SEM (n=12) are averaged results of three independent experiments conducted in quadruplicates. Differences among means were compared using Tukey's test. Values with different letters for each concentration level are significantly different at $\alpha = 0.05$ ($P<0.05$).

3.4 PZ-DHA Significantly Inhibits Phosphatase Activity of MDA-MB-231 Cells in Comparison to Parent Compounds, PZ and DHA

Effect of PZ-DHA on cytosolic acid phosphatase activity was measured in parallel to PZ and DHA in a time- and dose-dependent manner. PZ-DHA-induced metabolic inhibition demonstrated by acid phosphatase assay was compared to its parent compounds PZ and DHA at all five time points using five concentrations. Significant reduction in metabolic activity was showed almost at an early stage (3 hr) (Figure 3.4-A) and also at low concentrations (10 μM) (Figure 3.4-D and E) of PZ-DHA.

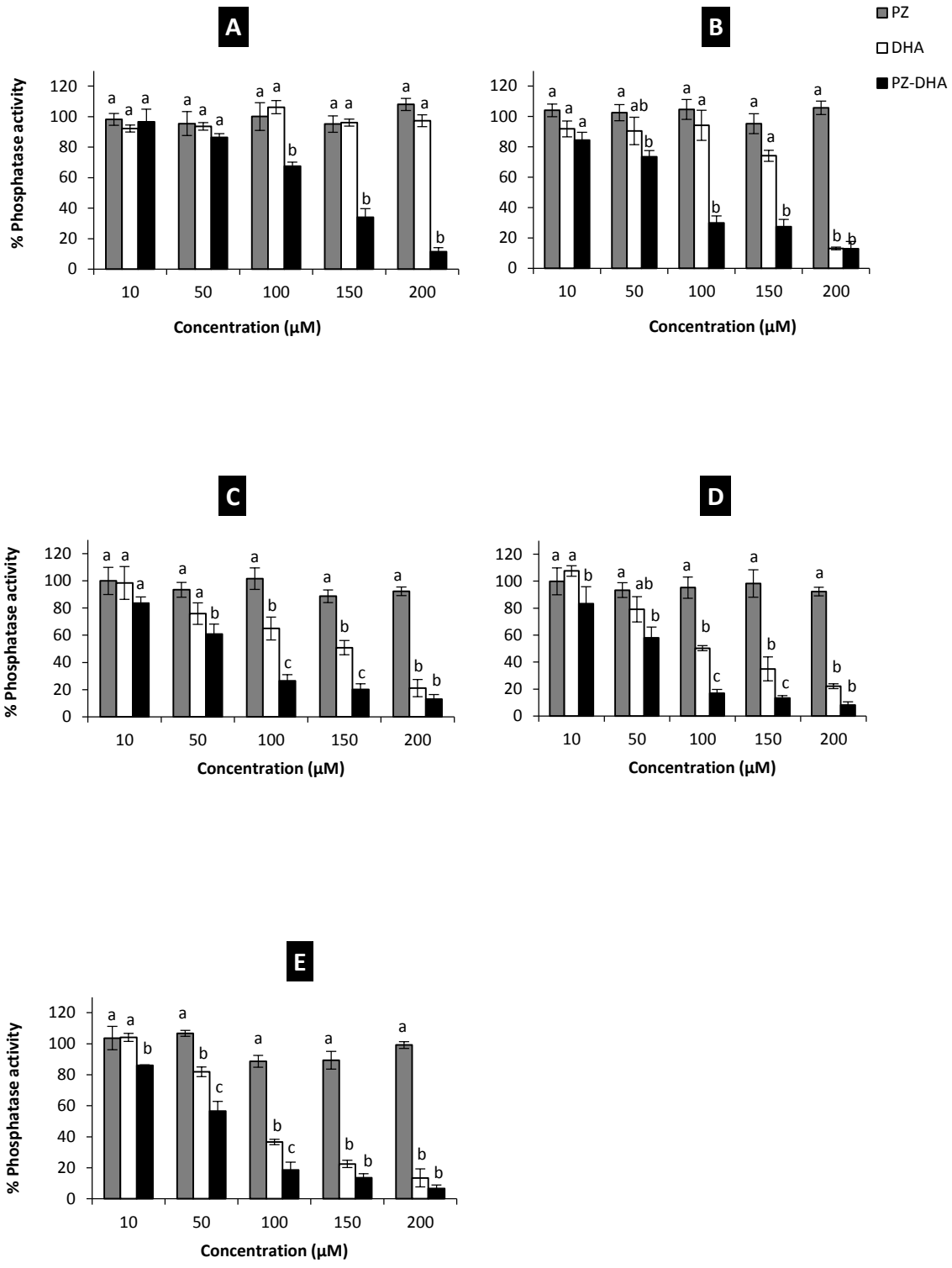
A
B
C
D
E
PZ
DHA
PZ-DHA
% Phosphatase activity
Concentration (µM)
10
50
100
150
200
0
20
40
60
80
100
120

Figure 3.4: Significant phosphatase enzyme inhibition of MDA-MB-231 cells by PZ-DHA at early hours of treatment and low concentrations in comparison to parent compounds

Inhibition of phosphatase enzyme activity of MDA-MB-231 cells by PZ-DHA was compared to its parent compounds at **A)** 3, **B)** 6, **C)** 12, **D)** 18 and **E)** 24 hr of treatment at 10, 50, 100, 150 and 200 μM concentrations of test compounds. Data expressed above as mean ± SEM (n=12) are averaged results of three independent experiments conducted in quadruplicates. Differences among means were compared using Tukey's test. Values with different letters for each concentration level are significantly different at $\alpha = 0.05$ ($P<0.05$).

3.5 PT, DHA and PZ-DHA but not PZ Cause Morphological Changes in MDA-MB-231 Cells

Apoptosis is associated with a series of biochemical and morphological (membrane blebbing, formation of apoptotic bodies) changes taking place in a dying cell. Cells undergoing morphological changes were observed at × 400 magnifications on a phase contrast microscope and the cells were photographed. Cell morphology of MDA-MB-231 cells started to change within 3 hr of PZ-DHA treatment. Cells underwent gradual morphological changes over the experimental period (Figure 3.5).

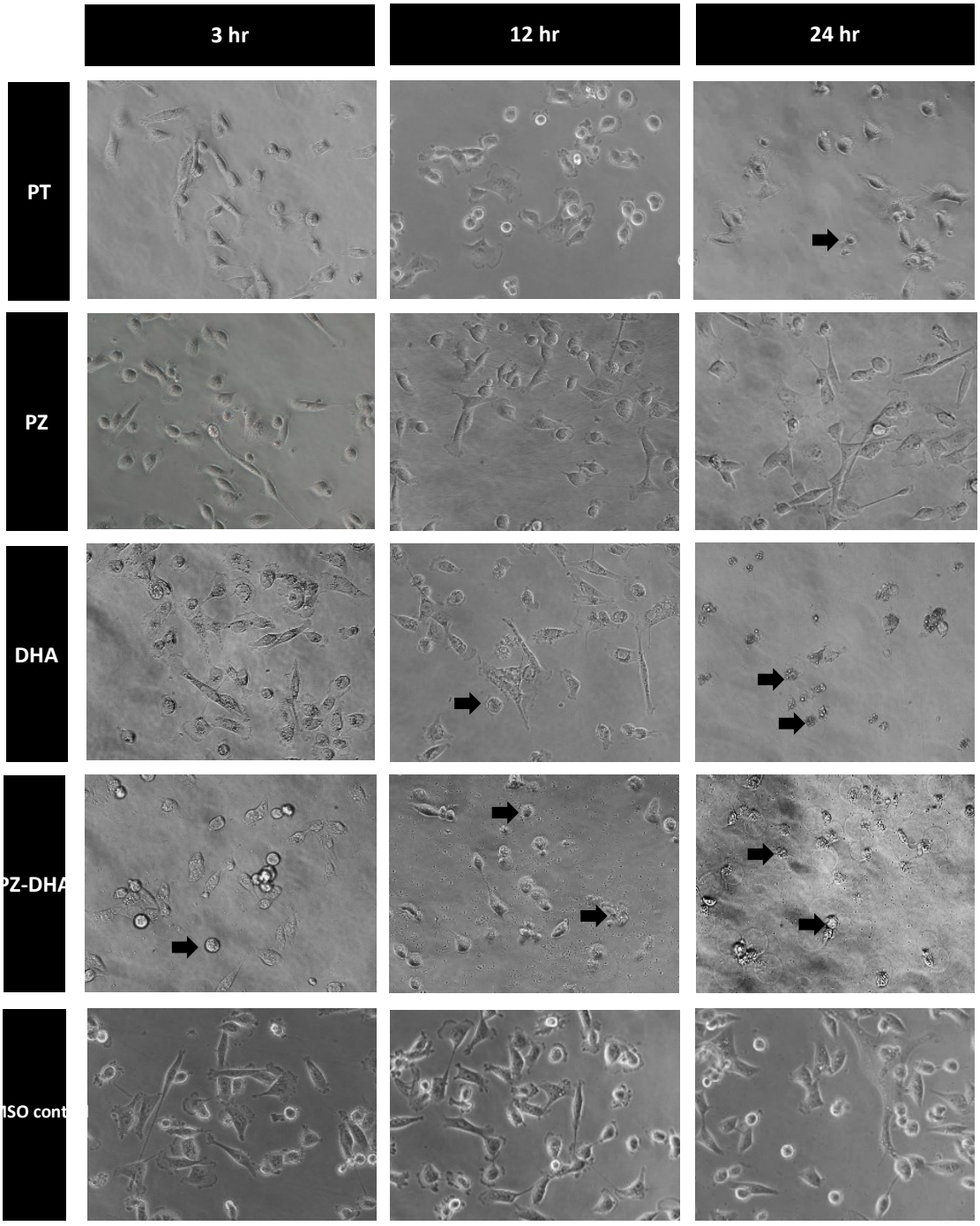
3 hr
12 hr
24 hr
PT
PZ
DHA
PZ-DHA
DMSO cont

Figure 3.5: Morphological changes caused by test compounds at 100 µM concentration on MDA-MB-231 triple negative breast cancer cells

MDA-MB-231 cells were treated with 100 µM of PT, PZ, DHA, PZ-DHA and vehicle controls and incubated for 3, 6, 12, 18 and 24 hr. Cells were photographed using Nikon eclipse TS 100 phase contrast microscope equipped with Infinity 1 camera at × 400 magnification. Representative photographs shown above are taken at 3, 12 and 24 hr of treatment of three independent experiments conducted in quadruplicates. Arrows indicate cells that have under gone morphological changes.

3.6 PT, DHA and PZ-DHA Induced Cytotoxicity cause MDA-MB-231 Cell Death not Cell Growth Inhibition

Sometimes, cell viability studies are not able to distinguish between cell growth inhibition and cell death. Therefore, inhibition of metabolic (shown by MTS assay) and phosphatase (shown by acid phosphatase assay) activities, and morphological changes observed under phase contrast microscope were required to be confirmed by detecting cell death on an appropriate assay. 7-AAD, a DNA-intercalating agent was used to confirm the cell death caused by test compounds. Loss of cell membrane integrity at the late apoptosis/necrosis could be measured by 7-AAD, which could penetrate into the cells: once membrane becomes permeable. Upon 7-AAD staining, cell death (Figure 3.6) was detected on FL3 after incubating cells at 50 μM and 100 μM concentrations of the test compounds for 24 hr. The percentage of dead cells noticed in PT, DHA, PZ-DHA but not PZ treated cultures was notably different from both vehicle and medium treated cells. However, PT-, DHA- and PZ-DHA- induced cell death observed at 100 μM and 50 μM were comparable.

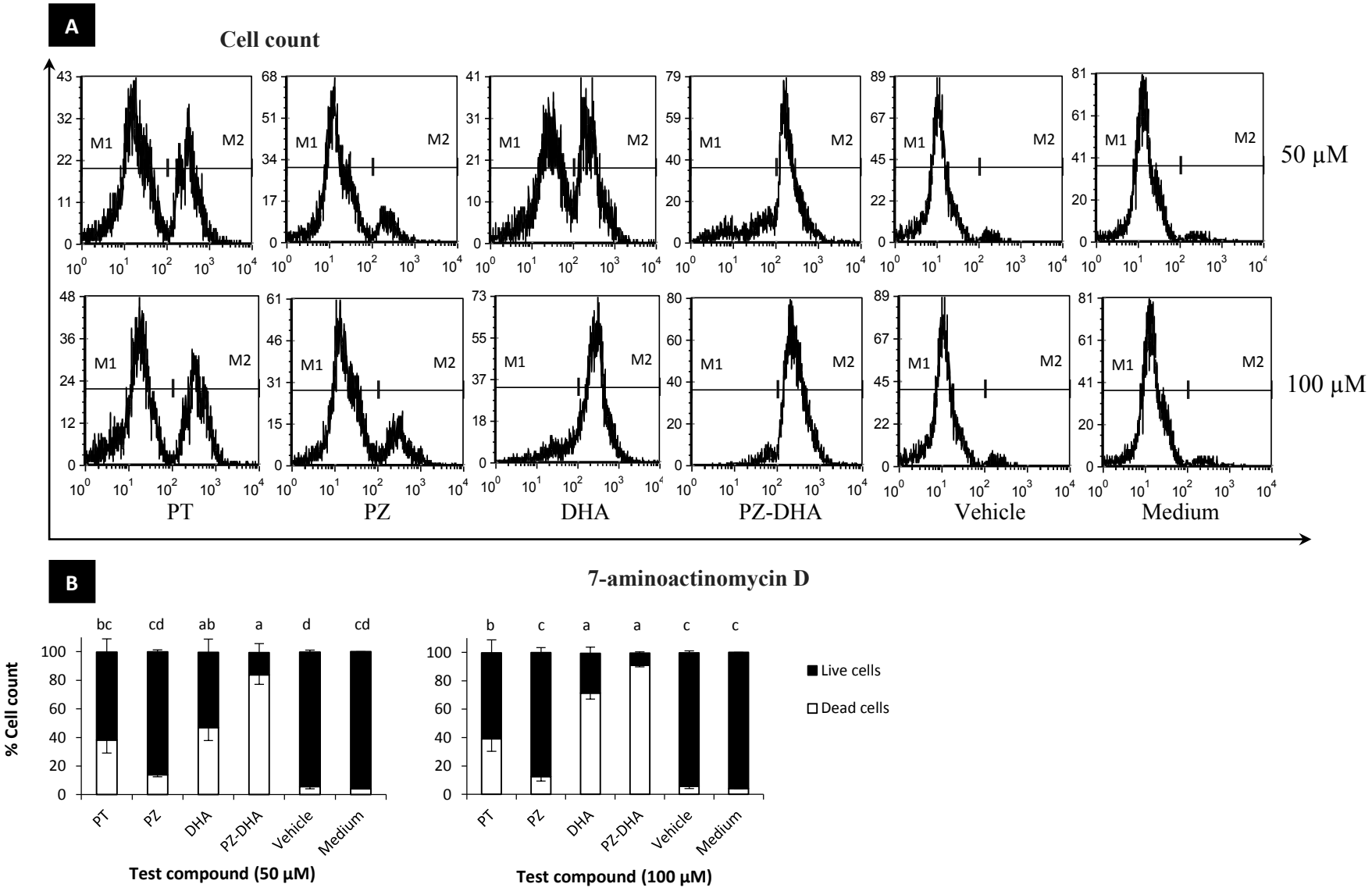
A
Cell count
M1
M2
50 µM
100 µM
PT
PZ
DHA
PZ-DHA
Vehicle
Medium
B
7-aminoactinomycin D
% Cell count
bc cd ab a d cd
b c a a c c
Live cells
Dead cells
PT
PZ
DHA
PZ-DHA
Vehicle
Medium
Test compound (50 µM)
Test compound (100 µM)

Figure 3.6: PT, DHA and PZ-DHA caused cell death detected in 7-AAD staining

MDA-MB-231 cells were treated with 50 and 100 μM of PT, PZ, DHA, PZ-DHA, vehicle controls and medium and stained with 7-AAD at 24 hr post treatment. Stained cells were read on detector, FL3. Representative pictures of histograms of **A)** 50 μM and 100 μM treated cells (M1; Marker 1: Live cells and M2; Marker 2: Dead cells) and **B)** mean ± SEM of % cell counts of 50 μM and 100 μM treated cells from three independent experiments are shown. Percent cell death with different letters are significantly different at $\alpha = 0.05$ ($P<0.05$).

3.7 PT, DHA and PZ-DHA Induced Death of MDA-MB-231 Cells does not Require Reactive Oxygen Species Production

Extensive morphological changes observed under phase contrast microscope and promising results given in 7-AAD staining confirmed PT, DHA and PZ-DHA-induced cell death. Then the possible mechanisms involved in the test compound induced cell death needed to be evaluated. Artifacts of oxidative stress due to extracellular H_2O_2 production in cell culture medium can give false positive results. Chemicals including some flavonoids trigger this phenomenon (Odiatou et al., 2013). Therefore, the involvement of ROS and the contribution of HCO_3^- containing medium toward the production of H_2O_2 was conducted (Mohanty et al., 1997; Wagner et al., 2005), and the negative results demonstrated by the Amplex red assay indicated that PT, PZ, DHA and PZ-DHA (Figure 3.7-A) are not involved in H_2O_2 production in the absence of MDA-MB-231 cells. The standard curve (Figure 3.7-B) was generated using a log-fold diluted H_2O_2 concentration series. EGCG, the positive control, showed significant H_2O_2 production at $P < 0.05$ significance level. Involvement of ROS in PT, DHA and PZ-DHA-induced cell death was investigated by incorporating NAC in Annexin-V-FLUOS/PI staining. NAC is an antioxidant that scavenges the ROS produced in the cells which could be involved in the induction of cell apoptosis (Kang et al., 2010). The cell death caused by the test compounds was measured by Annexin-V-FLUOS/PI staining at 6 hr of post treatment. Apoptosis and late apoptosis/necrosis was detected by analyzing cells at FL1 and FL2 for Annexin-V-FLUOS and PI, respectively. Incorporation of NAC in the culture medium did not alter the cytotoxicity induced by the test compounds (Figure 3.8). Hence, NAC failed to protect breast cancer cells from cell death induced by the test compounds. When the anticipated

background indicated by DMSO vehicle control treated cells is considered, late apoptosis/necrosis noticed in PZ-treated cells was minimal, while all the other test compounds showed more substantial cell death on Annexin-V-FLUOS/PI staining.

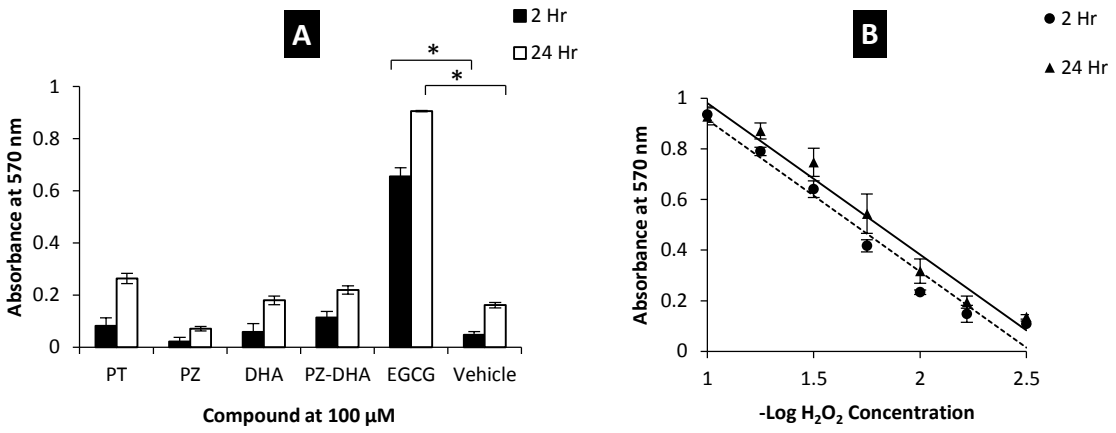

Figure 3.7: None of the test compounds caused substantial H_2O_2 production in cell culture medium in the absence of breast cancer cells

PT, PZ, DHA, PZ-DHA and EGCG-induced H_2O_2 production at 100 µM concentration in a HCO_3^- containing cell culture medium was measured in Amplex red assay. H_2O_2 generation induced by **A)** test compounds prepared in phenol red free DMEM and **B)** standard curve of H_2O_2 was measured by incubating compounds/H_2O_2 standards with Amplex red master mix in dark at 37 °C for 2 and 24 hr. The product was detected at 570 nm on a microplate reader. Data shown are the mean of 3 independent experiments ± SEM. Values considered significant at * $p < 0.05$.

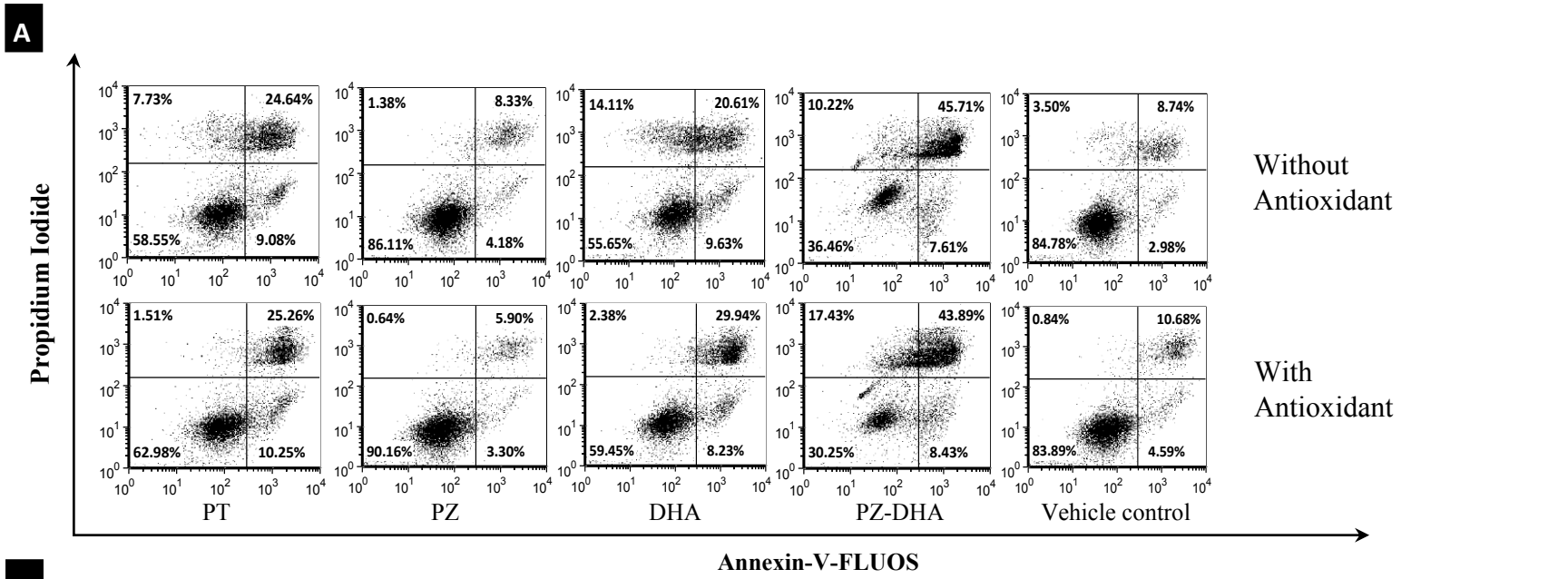
A
Propidium Iodide
7.73%
24.64%
58.55%
9.08%
1.38%
8.33%
86.11%
4.18%
14.11%
20.61%
55.65%
9.63%
10.22%
45.71%
36.46%
7.61%
3.50%
8.74%
84.78%
2.98%
1.51%
25.26%
62.98%
10.25%
0.64%
5.90%
90.16%
3.30%
2.38%
29.94%
59.45%
8.23%
17.43%
43.89%
30.25%
8.43%
0.84%
10.68%
83.89%
4.59%
PT
PZ
DHA
PZ-DHA
Vehicle control
Annexin-V-FLUOS
Without Antioxidant
With Antioxidant

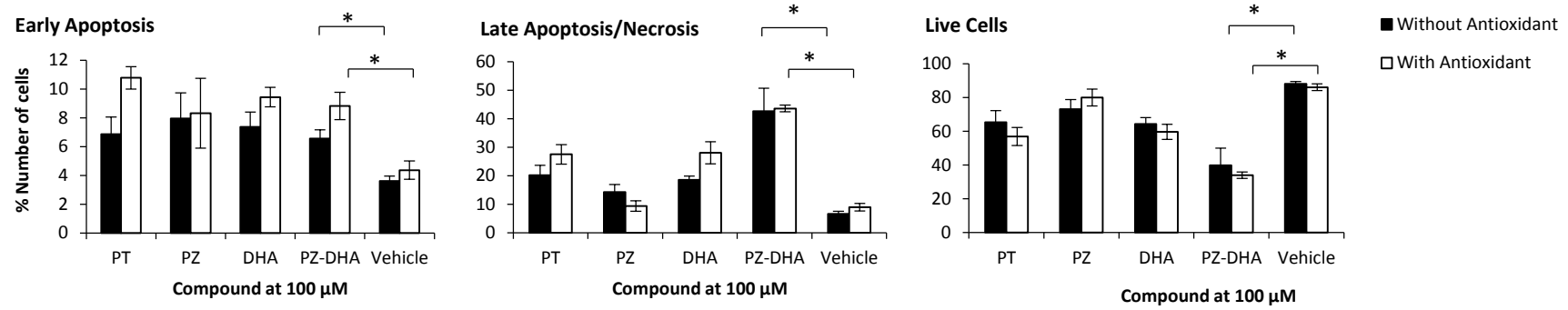
B
Early Apoptosis
% Number of cells
Compound at 100 µM
Late Apoptosis/Necrosis
Live Cells
PT
PZ
DHA
PZ-DHA
Vehicle
*
Without Antioxidant
With Antioxidant

Figure 3.8: N-Acetylcysteine fails to protect MDA-MB-231 breast cancer cells from apoptosis/necrosis induced by PT, DHA and PZ-DHA

MDA-MB-231 cells were treated with test compounds or vehicle control at 100 μM concentration either in the presence or absence of 10 mM N-Acetylcystein. All the samples were stained with Annexin-V-FLUOS/PI at 6 hr post treatment and analyzed by Flow Cytometry. **A)** Representative dot plots were extracted from three independent experiments incubated without antioxidant and with antioxidant. Data shown in **B)** are the mean percentages of cells in early apoptosis, late apoptosis/necrosis and live cells of 3 independent experiments ± SEM. NAC (10 mM) was used as the antioxidant. Values considered significant at * $p < 0.05$.

3.8 PZ-DHA Activates Caspase 3/7-dependent Apoptosis of MDA-MB-231 Cells

Activation of caspase 3/7 was shown by measuring caspase 3/7 cleavage of a luminogenic substrate, Ac-DEVD-pNA. Since this substrate is cleaved by both caspase 3 and 7 in *in vitro* environment, the activation did not distinguish between caspase 3 and 7. At 6 hr of post treatment except for STS, none of the other positive controls or test compounds demonstrated significant caspase 3/7 activation with compared to the vehicle control. With extended exposure of cells to the test compounds or positive controls (12 hr), PZ, DHA and PZ-DHA indicated a significant activation of caspase 3/7 compared to the control. PZ-induced caspase 3/7 activation was comparable to as that of doxorubicin and docetaxel, and PZ-DHA induced activation measured was statistically equivalent to staurosporine. The highest caspase 3/7 activation was observed with DHA and this was also statistically equivalent to staurosporine, but not to PZ-DHA (Figure 3.9).

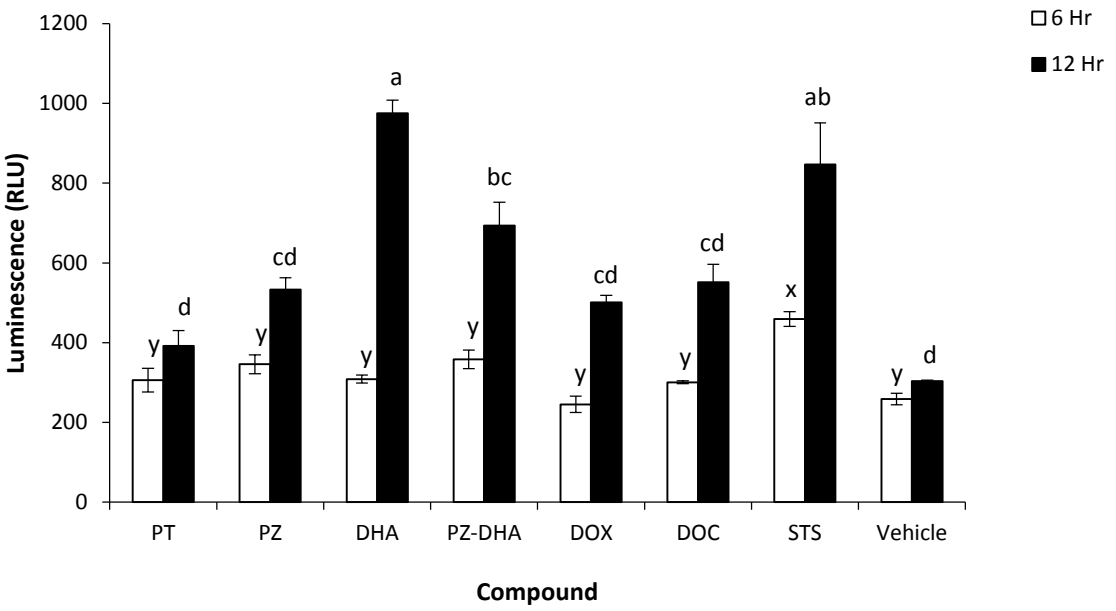

Figure 3.9: DHA and PZ-DHA activates caspase 3/7

MDA-MB-231 cells were treated with test compounds at 100 μM concentration at 37 °C for 6 and 12 hr. Caspase-Glo® 3/7 assay buffer mixture (100 μL) was added to each well and incubated for 2 hr at 37 ˚C. Luminescence was measured on a micro plate reader. Data illustrated are the mean luminescence measured in three independent experiments ± SEM. Differences among means were compared using Tukey's test. Values with different letters for each incubation period are significantly different at $\alpha = 0.05$ ($P<0.05$).

3.9 PZ-DHA Causes DNA Fragmentation in MDA-MB-231 cells

PZ-DHA-induced apoptosis detected in the caspase 3/7 activation assay was confirmed by TUNEL staining of MDA-MB-231 cells at 12 hr post treatment. DNA strand fragments labeled by terminal TdT, which catalyzes polymerization of labeled nucleotides to free 3'-OH ends, was detected in fluorescent microscopy in the range of 515-565 nm excitation. Very few labeled DNA fragments were seen in PT-treated cells, however, PZ-DHA-treated cells showed extensive labeling of DNA fragments (Figure 3.10-D). In contrast, DHA-treated cells did not show any TUNEL stained DNA fragments even though caspase 3/7 activation was detected. Similarly, PZ-treated cells also did not show positive results on TUNEL staining (Figure 3.10).

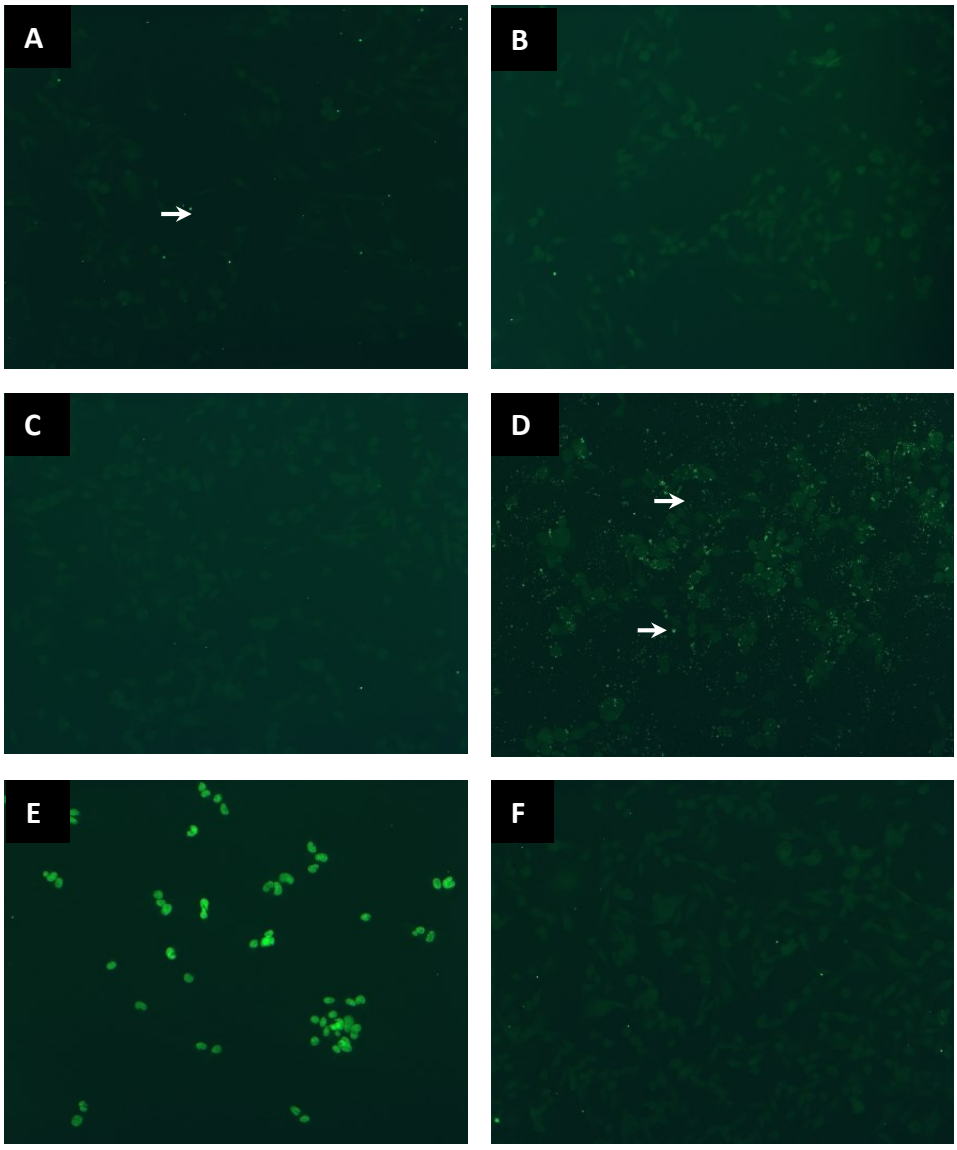

Figure 3.10: PZ-DHA cause extensive DNA fragmentation within 12 hours

MDA-MB-231 cells treated with test compounds at 100 μM concentration were incubated for 24 hr at 37 ˚C. The cells were then fixed and incubated with TUNEL reaction mixture in dark for 1 hr at 37 ˚C. Representative pictures of cells treated with **A)** PT, **B)** PZ **C)** DHA, **D)** PZ-DHA, **E)** DOX and **F)** DMSO vehicle control of two independent experiments are shown. Arrows indicate possible TUNEL staining of fragmented DNA.

3.10 PZ-DHA does not Affect Cell Cycle

Involvement of PZ-DHA in the regulation of the cell cycle was also tested to identify possible PZ-DHA-induced cell cycle arrest at specific phase(s). MDA-MB-231 cells exposed to PZ-DHA at 40 μM concentration for 48 hr and stained with PI were analyzed in flow cytometer at FL2. PZ-DHA did not induce cell cycle arrest at any of the phases as shown by the histogram of cell count vs FL2-A (Figure 3.11).

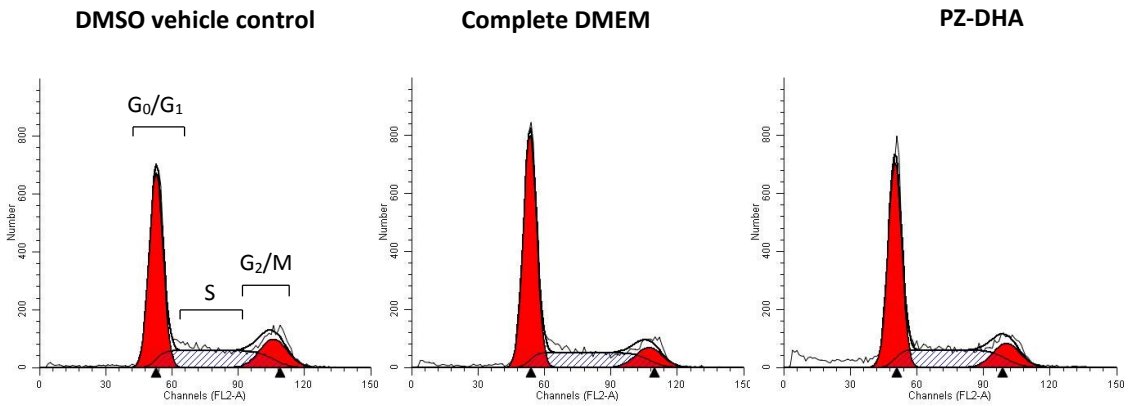

Figure 3.11: PZ-DHA does not cause cell cycle arrest

Synchronized MDA-MB-231 cells were treated with DMSO vehicle control, complete DMEM or PZ-DHA at 40 μM concentration and incubated for 48 hr. Then cells were harvested and fixed. Fixed cells were stained with PI and analyzed by Flow Cytometry on FL2. Data shown are representative histograms of cells treated with DMSO vehicle control, complete DMEM or PZ-DHA.

3.11 PZ-DHA Selectively Inhibits MDA-MB-231 Cell Growth

Selectivity of antiproliferative properties of PZ-DHA on MDA-MB-231 triple negative breast cancer cells with minimum inhibitory effects on normal healthy epithelial cells was shown in MTS assay in terms of reduction of percentage metabolic activity. One hundred and 200 μM concentrations killed both MDA-MB-231 cells and HMEpiCs equally, but interestingly, PZ-DHA-induced cytotoxicity was selective toward MDA-MB-231 breast cancer cells at 50 μM concentration causing almost no toxicity to HMEpiCs (Figure 3.12).

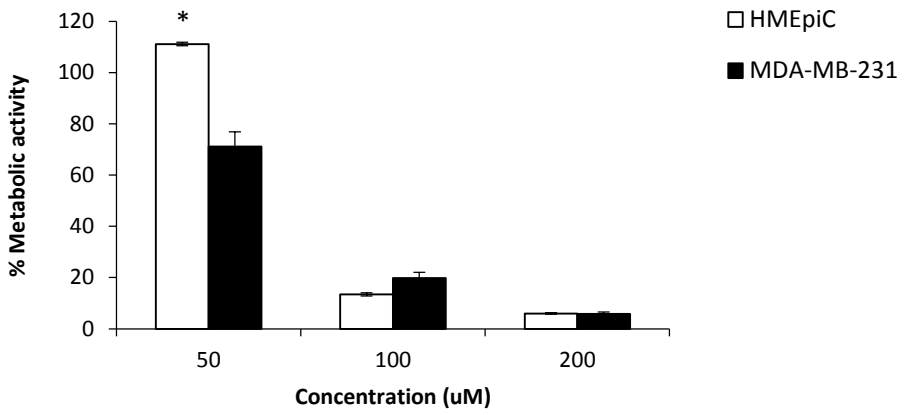

Figure 3.12: Low PZ-DHA concentration selectively inhibits MDA-MB-231 triple negative breast cancer cells

Selectivity of PZ-DHA-induced cytotoxicity was evaluated using MTS assay. MDA-MB-231 cells and HMEpiC were seeded at 5×10^3 cells/well density in flat-bottom 96 well plated and incubated over night for cell adhesion. Cells were then treated with 50, 100 and 200 μM concentrations of test compounds and the metabolic activity inhibition was determined at the end of incubation at 37 ˚C for 24 hr. Data expressed above as mean ± SEM (n=12) are averaged results of three independent experiments conducted in quadruplicates. Values considered significant at * $p < 0.05$.

3.12 DHA, PZ-DHA and to a lesser extent PT suppress tumor growth in NOD-SCID mice xenografted with MDA-MB-231 cells

In vivo tumor suppression was shown in NOD-SCID mice xenografted with MDA-MB-231 cells to the right hind flank. After five intratumoral injections mice were monitored for 1 more wk and at the end of the experimental period tumor volumes were recorded as vehicle: 392.2651± 27.58, PT: 263.69± 21.32, DHA: 213.19 ± 12.11 and PZ-DHA: 195.58± 11.91 mm^3 (Figure 3.13-A). All test compound-treated tumors showed statistically significant reductions in the tumor volumes. (PT: $p<0.01$, DHA and PZ-DHA: $p<0.001$). Weights of excised tumors were noted at the day 15 as vehicle: 238.8±18.6, PT: 170.4±20.5, DHA: 153.9±19.8 and PZ-DHA: 144.5±10.9 mg (Figure 3.13-C). Though PT-induced *in vivo* tumor suppression was significant at $p < 0.01$ in terms of tumor volume, the difference in tumor weight was not statistically significant compared to the vehicle control. Mice were euthanized and their tumors were photographed and representative pictures of (Figure 3.13-B) mice and (Figure 3.13-D) tumors are shown.

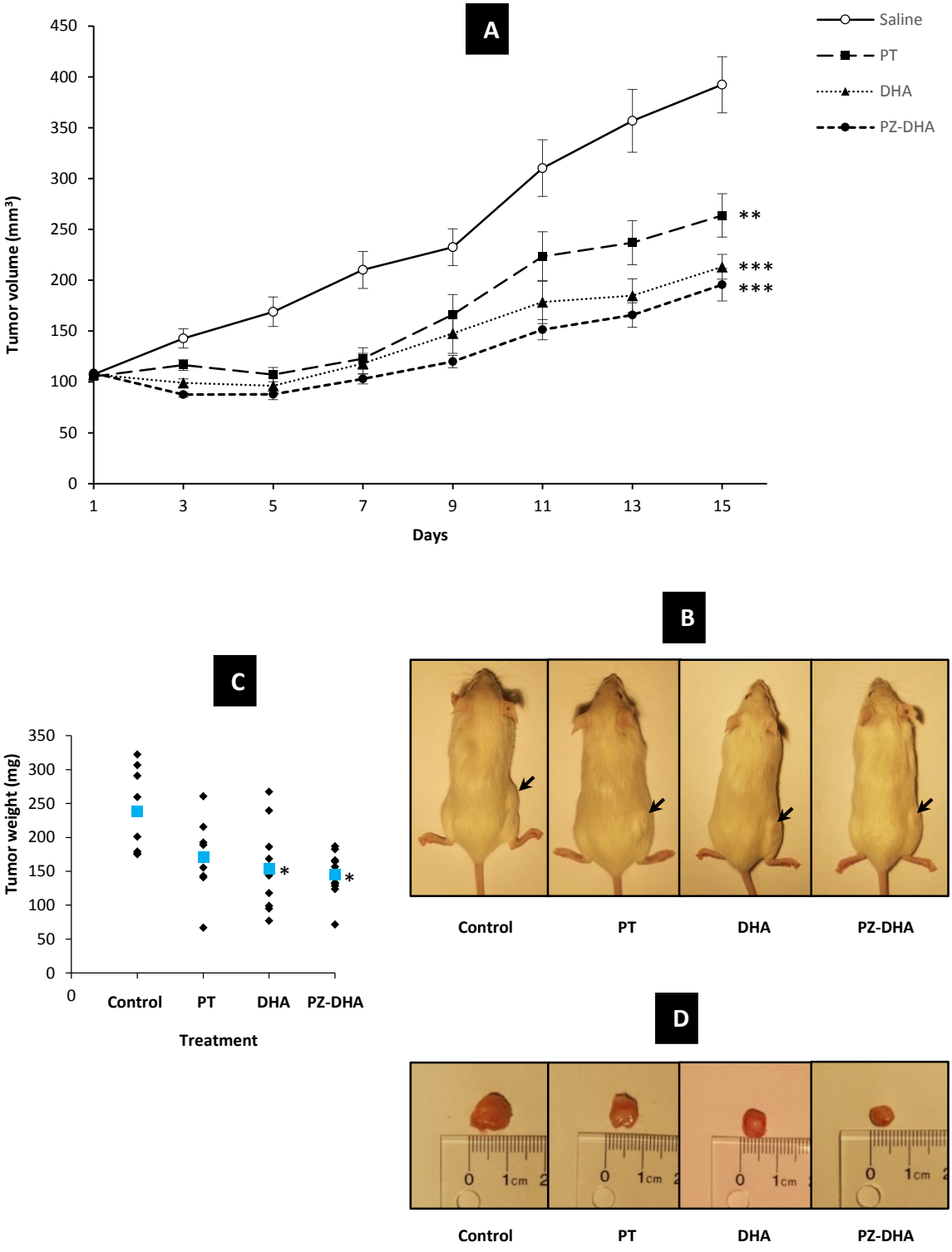
A
Saline
PT
DHA
PZ-DHA
Tumor volume (mm³)
Days
**
***
***
B
Control
PT
DHA
PZ-DHA
C
Tumor weight (mg)
Treatment
*
*
D
Control
PT
DHA
PZ-DHA

Figure 3.13: PT, DHA and PZ-DHA suppress tumor growth in MDA-MB-231 cells xenografted into NOD SCID mice

MDA-MB 231 breast cancer cells were injected into right hind flanks of NOD SCID mice and Saline+DMSO vehicle control, PT, DHA or PZ-DHA were injected intratumorally on days 1, 3, 5, 7 and 9. **A)** Caliper measurements of tumors were noted on days 1, 3, 5, 7, 9, 11, 13 and 15 and tumor volumes were determined. **B)** On day 15, the mice were euthenized and photographed. After euthanization excised tumors were **C)** weighed and **D)** photographed. Data shown are averaged results of 5 independent experiments. Values considered significant at *** $p < 0.001$, ** $p < 0.01$, * $p < 0.05$.

3.13 Haemotoxylin and Eosine Stain Indicates Clear Necrotic Zones in PT, DHA and PZ-DHA Treated MDA-MB-231 Tumor Sections Excised from NOD-SCID mice

As shown in Figure 3.14 all test compound-treated tumor sections indicated clear necrotic zones on haematoxylin and eosin staining. Haematoxylin stains nuclear contents and its counter stain eosin stains cellular matrix.

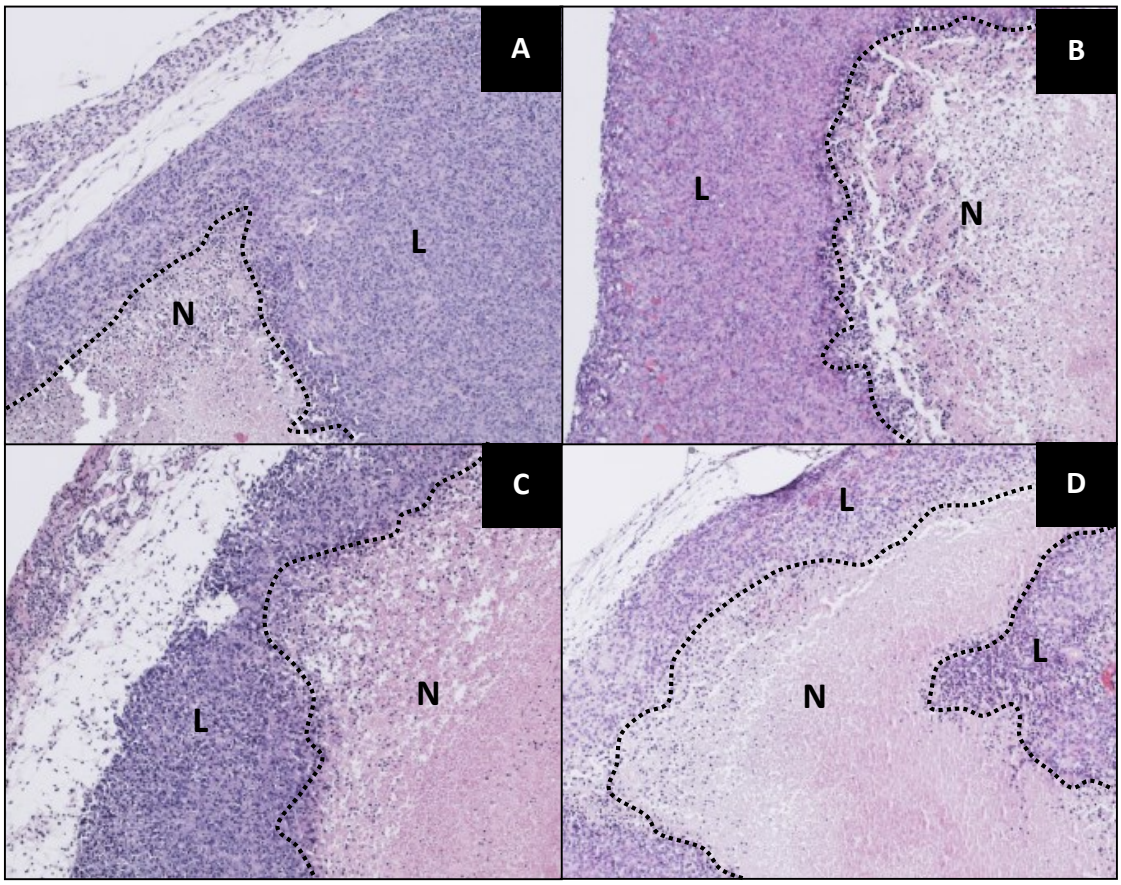

Figure 3.14: PT, DHA and PZ-DHA show tumor necrosis on haematoxylin and eosin staining

Excised tumors were fixed and cut into 5 µM thick sections and mounted on glass slides for staining. Specimens were dried and stained with haematoxylin and its counter stain eosine. Representative pictures of sections of tumors treated with **A)** Saline + DMSO vehicle control **B)** PT **C)** DHA and **D)** PZ-DHA are shown. Sections were photographed under the bright field microscope [AxioPlan 11MOT AxioCam HRc, Carl Zeiss Canada Ltd] at × 400 magnification. L: Live cells; N: Necrotic cells.

CHAPTER 4 : DISCUSSION

4.1 PZ-DHA-Induced MDA-MB-231-Targeted Cytotoxic Effect is both Time- and Dose-Dependent

The cytotoxic effects of PT, PZ, DHA and PZ-DHA were measured in terms of the reduction of metabolic activity and cytosolic phosphatase activity using MDA-MB-231 cells (measured using MTS and acid phosphatase assays respectively) and HMEpiCs (measured using MTS assay) in both time- and dose-dependent manner. Both MTT (Mosmann, 1983) and MTS (Cory et al., 1991) assays are based on the principle of measuring metabolic activity of living cells. Hence, the assays identify living cells, but not dead cells. The MTS assay carries a major limitation, leading to false positive results as this method is unable to distinguish between cell cycle inhibition and cellular death (Smith et al., 2011). Fatty acids and formazan could also compete for the binding site of bovine serum albumin (BSA) (Huang et al., 2004). The acid phosphatase assay was conducted in addition to MTS assay. Acid phosphatase assay may overcome the principle limitation of MTS assay (instability of the substrate which degrades spontaneously to generate high background) and MTT assay (difficulty of the organic extraction step on quantifying formazan) (Yang et al., 1996). On the other hand, the acid phosphatase assay also carries the limitation of phosphatase activity being inhibited by some chemicals in cell culture systems. For example, PT and PZ are reported to exert inhibitory effects on kidney phosphatase (Kalckar, 1936) and seman acid phosphatase (Beling and Diczfalusy, 1958). A series of flavonols and isoflavone glycosides are hydrolysed at the small intestine by the brush border enzyme, lactase phlorizin hydrolase (LPH) (Day et al., 2000). The β-

glucosidase activity of LPH hydrolyses PZ to PT and glucose in the microvillus membrane of small intestinal brush border (Malathi and Crane, 1969). Therefore, the efficacy of PZ-DHA, killing breast cancer cells was compared to PT and PZ both in *in vitro* and *in vivo* studies. The antiproliferative efficacy of flavonoids such as apigenin (Fang et al., 2005; Chiang et al., 2006; Long et al., 2008), luteolin (Triantafyllou et al., 2008; Markaverich et al., 2011; Rao et al., 2012), quercetin (Triantafyllou et al., 2007; Wu et al., 2011; Mocanu et al., 2013) as well as flavonoid derivatives (Sudan and Rupasinghe, 2014; Ying et al., 2008; Zhang et al., 2014b) have been studied widely in *in vitro* and *in vivo* experimental models. PT showed a consistent reduction in metabolic activity over the experimental period (3-24 hr) in a dose-dependent manner in the MTS assay, and no reduction in phosphatase activity in acid phosphatase assay *in vitro*. A possible explanation could be that the NADPH-dependent oxidoreductases and dehydrogenases involved in MTS reduction are more sensitive to PT than that of cytosolic acid phosphatase. PZ is known to possess anti-estrogen effects in the presence of excessive estrogen, and to inhibit cell proliferation induced by estradiol in estrogen sensitive human breast cancer cells (e.g.: MCF-7) (Wang et al., 2010). In agreement with the research findings of Wang et al. (2010), PZ did not show significant suppressive effects on the proliferation of MDA-MB-231 cells measured using the MTS and acid phosphatase assays in this study. Both DHA and PZ-DHA-induced inhibition in metabolic activity and cytosolic acid phosphatase activity was time- and dose-dependent. However, PZ-DHA started to exhibit a significant reduction in metabolic activity and phosphatase activity at an early time point (within 3 hr) (Figure 3.3 and 3.4). Further, phosphatase activity inhibition by PZ-DHA was significantly different from that of its parent compounds (PZ and DHA) at low concentrations (Figure 3.3). In

comparison, the metabolic activity reduction measured in the MTS assay is generally lower than the phosphatase activity inhibition measured by acid phosphatase assay for both DHA and PZ-DHA. When compared to PT, PZ-DHA-induced reduction of metabolic activity was less evident. However, PZ-DHA showed similar effects on acid phosphatase assay while PT was having no effect on acid phosphatase assay. This striking difference of results between MTS and acid phosphatase assays were not observed with any of the other test compounds except for PT. Facilitation of substrate diffusion into the cell interior, by Triton X-100 induced permeabilization of cell membrane, could be playing a significant role in measuring the cytosolic phosphatase enzyme activity. However, because of the associated high tendency of the MTS to reduce at the level of cell surface, MTS assay gives less information about the cellular uptake of drug molecules.

4.2 PZ-DHA-Induced MDA-MB-231 Cell Death does not Require ROS Production

Certain (poly) phenolic compounds react with HCO_3^- containing cell culture medium and produce H_2O_2. These chemicals exert antiproliferative properties are due to the artifacts of H_2O_2-induced oxidative stress. At micromolar range, EGCG, a polyphenolic catechin induces ROS production in ovarian (Chan et al., 2006) and Jurkat (Nakagawa et al., 2004) cells. Reversal of the cytotoxic effects of EGCG on ovarian cancer cells (SKOV3, CAOV3, OVCAR3, OVCAR10, A2780, CP70, C30, and C200) by the H_2O_2 scavenger sodium pyruvate suggests the involvement of H_2O_2 in EGCG-induced cell death (Chan et al., 2006). Hydroxytyrosol (3,4-dihydroxyphenylethanol (3,4-DHPEA)), a phenolic compound from olive oil, induces extracellular H_2O_2 production by human promyelocytic leukemia cells (HL60) in RPMI medium (Fabiani et al., 2009). The Amplex red assay in a

cell-free system and Annexin-V-FLUOS/PI staining of PT-, PZ-, DHA- and PZ-DHA-treated cells were carried out to investigate the possible involvement of ROS production. The Amplex red assay was performed in colourless (phenol red-free) DMEM and EGCG was used as the positive control. The test compound-induced H_2O_2 production was further quantified on a standard curve generated using a log-fold diluted-H_2O_2 concentration series. EGCG-induced extracellular H_2O_2 production was significantly higher when compared to the vehicle control in the Amplex red assay. None of the test compounds showed significant H_2O_2 production (Figure 3.7) in the absence of MDA-MB-231 cells suggesting that H_2O_2-induced oxidative stress is not the mechanism of PT- DHA- and PZ-DHA-induced cell death of MDA-MB-231 cells. Annexin-V-FLUOS/PI assay of test compounds-treated cells was slightly modified to incorporate an additional step to incubate cells either in the presence or absence of NAC. NAC, an antioxidant, is capable of minimizing the oxidative stress and down regulating the effects associated with the oxidative stress (Kerksick and Willoughby, 2005). Therefore, NAC is widely used to inhibit ROS-induced apoptosis (Halasi et al., 2013). Its cytoprotective properties against ROS-induced cytotoxicity *in vitro* have been studied extensively (Halasi et al., 2013; Oh and Lim, 2006; Zhang et al., 2011). NAC is an artificial precursor of intracellular cysteine and glutathione (Sun, 2010) as well. Glutathione, a non-protein thiol serves as a substrate for number of ROS scavenging enzymes (Circu and Aw, 2012). In the current study, NAC was used at 10 mM concentration to detect the involvement of ROS in cell death caused by the test compounds. None of the test compounds showed significant H_2O_2 production as measured by Amplex red assay and these negative results were confirmed in Annexin-V-FLUOS/PI staining of cells incubated with test compounds in the presence of NAC

(Figure 3.8-A). The Annexin-V-FLUOS/PI staining of PT-, PZ- and DHA- and PZ-DHA-treated MDA-MB-231 cells were performed after incubating cells either in the presence or absence of NAC. Consistent with Amplex red assay results, NAC failed to protect MDA-MB-231 cells from the cytotoxic effects and cell death caused by test compounds suggesting that ROS generation is not likely involved in the PT-, DHA- and PZ-DHA-mediated cell death.

4.3 PZ-DHA-Induced MDA-MB-231 Cell Death is Caspase Activation Dependent

The reduction of cellular enzyme activities of MDA-MB-231 cells treated with PT, DHA and PZ-DHA observed in MTS and acid phosphatase assays were confirmed to be a result of cell death as shown in 7-AAD staining. In 7-AAD staining, MDA-MB-231 cells were incubated with test compounds for 6 or 12 hr and stained with 7-AAD, a DNA intercalating dye, and dead cells were detected on the flow cytometer. Caspase activation and DNA fragmentation are hallmarks of apoptosis. Flavonoids-induced activation of caspase enzymes have been shown on human leukemia (U937: (Monasterio et al., 2004); HL-60: (Wang et al., 1999)), human breast cancer cells (MCF-7: (Wang et al., 2010)) and human hepatoma cells (HepG2: (Granado-Serrano et al., 2006)). The effect of PZ-DHA on the activation of caspase family enzymes and DNA fragmentation was detected in caspase 3/7 luminescence assay and TUNEL staining respectively. Caspase 3/7 activation was tested using DOX, DOC and STS as positive controls at 6 and 12 hr post treatment. Both DHA and PZ-DHA but not PT and PZ activated caspase 3/7 in MDA-MB-231 cells as compared to the control (Figure 3.9) and DHA-induced caspase 3/7 expression was significantly high ($p<0.05$) as that of PZ-DHA as well. However, PZ-DHA (Figure 3.10-D) treated MDA-MB-231 cells showed extensive TUNEL staining of fragmented DNA but not in DHA

(Figure 3.10-C) treated cells. PT and PZ did not show fragmented DNA (within 12 hr post treatment) on TUNEL assay. DHA-induced caspase activation is started at an early stage of post treatment but possibly, further incubation is necessary for the detection of fragmented DNA in DHA-treated cells since extensive DNA fragmentation is a late event of apoptosis (Collins et al., 1997). However, PZ-DHA induced caspase activation and DNA fragmentation were detected at comparatively same stage of post treatment suggesting PZ-DHA-induced effects initiate within a short period as compared to the parent compounds.

4.4 PZ-DHA does not cause Cell Cycle Arrest

Arrest at cell cycle check points (G_1, G_2 and M) is a well-recognized target of cancer chemotherapy. Flavonoids (Haddad et al., 2006), such as quercetin (Choi et al., 1999; Vidya et al., 2010), genistein (Zhao et al., 2009) and flavonoid extracts of *Nelumbo nucifera* L. (Yang et al., 2011) have shown antiproliferative properties by arresting cell cycle of various cell types including breast cancer cells. The effectiveness of PZ-DHA in the suppression of cell cycle was evaluated using 40 μM concentration and no significant cell cycle arrest was observed when compared to the medium control and vehicle (DMSO) control. However, significant caspase 3/7 activation was noted within 12 hr post-treatment of PZ-DHA and TUNEL staining for DNA fragmentation carried out at the same time point confirmed PZ-DHA-induced apoptosis. These findings were not reflected in the results of cell cycle analysis. A possibility could be the suppression of all phases of cell cycle to the same extent, or the antiproliferative property induced by PZ-DHA is not associated with cell cycle arrest. This uncertainty needs to be confirmed with Western blot analysis of cell cycle proteins (Clyclin A, B, D and C), Cdk 1, 2 and 4 and anaphase-promoting complex (APC) to detect their activation.

4.5 PZ-DHA Suppresses MDA-MB-231 Xenograft Growth in NOD-SCID Mice

In *in vivo* studies conducted to test the tumor suppressor properties of antiproliferative agents, tumor growth has been induced in several different ways and these methods are targeted at the activation of indigenous tumor initiation mechanisms such as DNA damage, activating oncogenic pathways and induction of inflammation. Commonly used methods to induce tumor growth in rodent models for experimental purposes include topical application of (7,12-dimethyl benz[a]anthracene (DMBA) and 12-O-tetradecanoyl phorbol-13-acetate (TPA)) (Chung et al., 2007; Wheeler et al., 2003), oral (urethane) (Berenblum and Haran-Ghera, 1957), intraperitoneal (Azoxymethane (AOX) dextran sodium sulfate (DSS)) (Tanaka et al., 2003) and subcutaneous Azoxymethane (AOX) (Pereira et al., 1996) and 1,2-dimethylhydrazine (DMH)) (Tsunoda et al., 1998) administration of carcinogens, radiation (Cheo et al., 2000; Mantena et al., 2005; Shuryak et al., 2009) and xenografting (Fan et al., 1993; Hilchie et al., 2011; Lundy et al., 1986; Singh et al., 2003; Verschraegen et al., 2003). *In vitro* cytotoxic properties of flavonoids on cell culture systems are investigated extensively but are proven on suitable animal models less frequently. Flavonoids (Kamei et al., 1996) such as EGCG (Shankar et al., 2013), rutin (Alonso-Castro et al., 2013), liquiritigenin (Liu et al., 2012), myricetin (Jung et al., 2010) and apigenin (Wang et al., 2011) inhibit the tumor growth *in vivo* in various mice models. In the current study, tumor growth was induced by xenografting MDA-MB-231 human breast cancer cells into NOD-SCID female mice. Considering the fact that PZ did not show significant cytotoxic properties *in vitro*, it was excluded from the *in vivo* experiments. After five intratumoral injections of saline, PT, DHA or PZ-DHA, PT showed a significant tumor growth inhibition at the 1% significance level ($p<0.01$) analyzed using

one-way ANOVA (Figure 3.13-A). Both DHA- and PZ-DHA-induced suppression of MDA-MB-231 xenografts was significant at 0.01% significant level ($p<0.001$) (Figure 3.13-A). Intratumoral injections of test compounds into MDA-MB-231 xenograft bearing mice were started when tumor volume reached 100 mm^3. Tumor volume was reduced after the first injection of PZ-DHA (87.45 mm^3) and DHA (99.15 mm^3). Tumors were controlled below/at initial tumor volume up to four injections of PZ-DHA and three injection of DHA and then started to increase gradually up to 195.59 mm^3 (PZ-DHA) and 213.19 mm^3 (DHA). PT-treated tumors were maintained at its initial tumor volume after two injections and then tumors continued to grow up to 263.69 mm^3 in volume. Interestingly, PZ-DHA induced a significant growth suppression ($p<0.001$) of xenografts throughout the experimental period. However, the average volume of PZ-DHA treated tumors recorded at the end of the study period was significantly ($p<0.05$) less compared to PT-treated tumors but not to DHA-treated tumors. The drug concentration within the tumor was maintained at 200 μM and it was the highest concentration used for *in vitro* studies. This concentration did not cause significant differences in the cytotoxic properties induced by DHA and PZ-DHA as measured using MTS assay and acid phosphatase assays. Therefore, this could be a potential explanation for the non-significant tumor growth inhibition of PZ-DHA when compared to DHA. None of the test compounds showed adverse side effects in mice during the experimental period. Specially, it is interesting to note that the novel phloridzin ester did not cause adverse effects on intratumoral administration, while showing remarkable inhibition in the MDA-MB-231 xenograft growth. Further, both DHA and PZ-DHA, but not PT, treatment reduced the tumor weights significantly ($p<0.05$) but not PT. Distinct necrotic zones were identified in all the three treatment groups when the tumor sections

were subjected to haematoxylin and eosin staining suggesting that PT, DHA and PZ-DHA have effective antiproliferative properties *in vivo*.

CHAPTER 5 : CONCLUSION

5.1 Summary of the research

Despite of the development of advanced methods to detect breast cancer at an early stage and the introduction of new efficacious drugs to treat breast cancer, still this disease remains the top most health burden among women. This underlies the necessity of continuing further investigations to discover novel drugs with the aim of reducing the breast cancer mortality rate. The major limitation of current chemotherapy is the lack of selectivity, i.e., the considerable amount of adverse side effects on normal healthy cells (Chidambaram et al., 2011; Marin et al., 2009; Zimmermann et al., 2014). Therefore, there is an increasing demand for anticancer agents derived from food since they are expected to have reduced adverse side effects on normal healthy cells due to their natural origin. However, some phytochemicals, such as flavonoids are associated with a poor bioavailability due to diminished cellular uptake. To facilitate the cellular uptake and there by biological activity, PZ-DHA, a novel long chain fatty acid derivative of phloridzin was synthesized in our laboratory by a regioselective acylation reaction catalyzed by *Candida antarctica* lipase B in our lab. In the present study the efficacy of PZ-DHA in killing TNBC cells was studied using MDA-MB-231 cells. PZ-DHA showed significant cytotoxic properties when compared to its parent compounds, PZ and DHA measured using the MTS and acid phosphatase assays. Further, its cytotoxic properties did not depend on the generation of ROS as measured in *in vitro* cell culture systems. Instead caspase family enzyme activation and the presence of oligonucleosomal DNA fragments in the TUNEL staining showed that cell death occurred mainly *via* apoptosis and necrosis. PZ-DHA-induced MDA-MB-231 cell growth inhibition was selective with less inhibitory effects on

HMEpiCs. However, PZ-DHA failed to arrest the cell cycle indicating that the death of MDA-MB-231 cells caused by PZ-DHA is not associated with the cell cycle arrest. *In vitro* antiproliferative properties were needed to be conformed on a suitable animal model to understand the efficacy and safety in a physiological environment. As an effective approach to initiate the preliminary *in vivo* studies to demonstrate PZ-DHA-induced tumor suppressor activities, NOD-SCID mice xenografted with MDA-MB-231 human breast cancer cells and intratumoral injections of PZ-DHA were selected. Interestingly, a remarkable suppression in the growth of MDA-MB-231 xenografts was observed after the first intratumoral administration of PZ-DHA and the tumor volume was maintained under control when compared to the vehicle control treated mice. Further, PZ-DHA did not induce any distress or adverse side effects on mice during the study period and necrotic tumor sections were observed after haematoxylin and eosin staining. Taken together, considering the *in vitro* and *in vivo* findings of this research it can be concluded that PZ-DHA shows a promise to continue further studies to develop it into a potential anticancer drug candidate to treat triple negative breast cancer effectively and safely.

5.2 Future Recommendations

The current study was targeted at the evaluation of preliminary antiproliferative and cytotoxic effects of a novel phloridzin derivative in *in vitro* using MDA-MB-231 cells and *in vivo* using NOD-SCID female mice xenografted with MDA-MB-231 cells. The MTS assay and acid phosphatase assay demonstrated promising cytotoxic effects, further needed to be confirmed on assays such as clonogenic assay (to determine the IC_{50}) and oregon green assay (to confirm the effect on proliferation). It was found that, the PZ-DHA induced cell death of MDA-MB-231 cells is ROS production-independent. Involvement of PZ-

DHA-induced caspase activation in the death of in the death of MDA-MB-231 cells need to be confirmed by blocking caspase activity using suitable caspase inhibitor or a cell line lacking caspase expression. However, PZ-DHA did not arrest cell cycle at any phase and this is remained to be confirmed using Western blot analysis of cyclins and Cdks. Since tumor suppressor properties of intratumorally administered PZ-DHA has been confirmed in a mouse model with no adverse side effects, further evaluations need to be started. Further studies should include investigation of the involvement of PZ-DHA in the inhibition of *in vitro* (using cell cultures) and *in vivo* metastasis to lung tissue (using a mouse model xenografted with mouse mammary carcinoma cells to mammary fat pad). Future research to investigate the ability of PZ-DHA to suppress angiogenesis would bring an added-advantage in developing PZ-DHA as a potential drug candidate to treat breast cancer. In order to proceed with human clinical trials of PZ-DHA to treat breast cancer, the tumor suppressor properties already demonstrated on intratumoral administration of PZ-DHA should be re-validated by intraperitoneal and oral gavage mouse model since intratumoral route is not applicable or acceptable in a real clinical setup. However, when proceeding with oral administration of PZ-DHA, it would be challenging to predict the stability of PZ-DHA through the intestinal tract due to the susceptibility of hydrolysis of ester linkage. The bioavailability of PZ-DHA would be affected by lipase induced hydrolysis of ester linkage and conjugation due to the phase II enzymes in liver. Therefore, it is worthwhile to conduct bioavailability studies in future research. As a part of bioavailability studies, the availability, in terms of PZ-DHA concentration in blood should be measured in a time dependent manner to determine the $t_{1/2}$, elimination half-life of PZ-DHA. Since PZ-DHA was tested only on one triple negative breast cancer cell line it

should also be tested on other estrogen negative cell lines such as MDA-MB-468 and 435, and estrogen-positive breast cancer cells (MCF-7) to understand the antiproliferative effects of PZ-DHA in a broad sense. Although, PZ-DHA was tested on HMEpiCs, further analysis should be conducted to understand the safety of PZ-DHA on normal healthy cells such as human fibroblasts and mouse mammary epithelial cells. Since PZ, the parent compound used to synthesize PZ-DHA has shown inhibitory properties on cellular glucose uptake, the efficacy of PZ-DHA in suppressing the cellular glucose uptake would also be important to investigate. Finally, since PZ-DHA is a flavonoid derivative it could suppress the cell survival pathways such as HIF-1α/AKT, PI-3K/AKT/mTOR and RAF/MAPK which are known to be inhibited by flavonoids. (Adhami et al., 2012; Ansó et al., 2010; Muthian and Bright, 2004; Senggunprai et al., 2014; Triantafyllou et al., 2007; Zhang et al., 2014a) Therefore, Western blot analysis to measure the inhibition/activation of expression of these proteins will also be important.

REFERENCES

Adhami, V.M., Syed, D.N., Khan, N., and Mukhtar, H. (2012). Dietary flavonoid fisetin: a novel dual inhibitor of PI3K/Akt and mTOR for prostate cancer management. Biochem. Pharmacol. *84*, 1277–1281.

Agnantis, N.J., Fatouros, M., Arampatzis, I., Briasoulis, E., Ignatiadou, E. V, Paraskevaidis, E., and Roukos, D. (2004). Carcinogenesis of Breast Cancer: Advances and Applications. Gastric Breast Cancer *3*, 13–22.

Aksamitiene E. , Achanta S., A.K. and H.J.B.. (2012). Synergistic anti-tumor effect by a combination treatment with the dietary flavonoid luteolin and the chemotherapy drugs Tasigna or Adrucil in human pancreatic cancer cells. FASEB J. *26*, 999.

Albini, A., Dell'Eva, R., Vené, R., Ferrari, N., Buhler, D.R., Noonan, D.M., and Fassina, G. (2006). Mechanisms of the antiangiogenic activity by the hop flavonoid xanthohumol: NF-kappaB and Akt as targets. FASEB J. *20*, 527–529.

Al-Ejeh, F., Simpson, P.T., Sanus, J.M., Klein, K., Kalimutho, M., Shi, W., Miranda, M., Kutasovic, J., Raghavendra, A., Madore, J., et al. (2014). Meta-analysis of the global gene expression profile of triple-negative breast cancer identifies genes for the prognostication and treatment of aggressive breast cancer. Oncogenesis *3*, 1–12.

Alonso-Castro A. J., A.J.A., and Domínguez F., Alejandro, G.C. (2013). Rutin exerts antitumor effects on nude mice bearing SW480 tumor. Arch. Med. Res. *44*, 346–351.

American Cancer Society (2012). Breast Cancer Detailed Guide TOC. http://www.cancer.org/cancer/breastcancer/detailedguide/

Andrew Morton, L.C. and L.D.B. (2013). A flavonoid-rich apple extract inhibits growth of HCT116 human colon cancer cells -- Morton et al. 27 (1): 1079.38 -- The FASEB Journal.

Angst, E., Park, J.L., Moro, A., Lu, Q., Li, G., King, J., Chen, M., Reber, H.A., Go, V.L.W., Eibl, G., et al. (2014). NIH Public Access. *42*, 223–229.

Ansó, E., Zuazo, A., Irigoyen, M., Urdaci, M.C., Rouzaut, A., and Martínez-Irujo, J.J. (2010). Flavonoids inhibit hypoxia-induced vascular endothelial growth factor expression by a HIF-1 independent mechanism. Biochem. Pharmacol. *79*, 1600–1609.

Ardhaoui, M., Falcimaigne, A., Engasser, J.-M., Moussou, P., Pauly, G., and Ghoul, M. (2004a). Acylation of natural flavonoids using lipase of candida antarctica as biocatalyst. J. Mol. Catal. B Enzym. *29*, 63–67.

Ardhaoui, M., Falcimaigne, a, Ognier, S., Engasser, J.M., Moussou, P., Pauly, G., and Ghoul, M. (2004b). Effect of acyl donor chain length and substitutions pattern on the enzymatic acylation of flavonoids. J. Biotechnol. *110*, 265–271.

ATCC MDA-MB-231 ATCC ® HTB-26™ Homo sapiens mammary gland/breast. http://www.atcc.org/products/all/HTB-26.aspx.

Baba, A.I. (2009). APOPTOSIS AND NECROSIS. *XLII*, 3–5.

Barreca, D., Bellocco, E., Laganà, G., Ginestra, G., and Bisignano, C. (2014). Biochemical and antimicrobial activity of phloretin and its glycosilated derivatives present in apple and kumquat. Food Chem. *160*, 292–297.

Bates, S.E., Davidson, N.E., Valverius, E.M., Freter, C.E., Dickson, R.B., Tam, J.P., Kudlow, J.E., Lippman, M.E., and Salomon, D.S. (1988). Expression of transforming growth factor alpha and its messenger ribonucleic acid in human breast cancer: its regulation by estrogen and its possible functional significance. Mol. Endocrinol. *2*, 543–555.

Bates, S.E., Valverius, E.M., Ennis, B.W., Bronzert, D.A., Sheridan, J.P., Stampfer, M.R., Mendelsohn, J., Lippman, M.E., and Dickson, R.B. (1990). Expression of the transforming growth factor-alpha/epidermal growth factor receptor pathway in normal human breast epithelial cells. Endocrinology *126*, 596–607.

Beling C. G. and Diczfalusy E. (1958). The Inhibition of Seminal Acid Phosphatase by Macromolecular Compounds. Biochem. J. *71*, 229–233.

Berenblum, I., and Haran-Ghera, N. (1957). A quantitative study of the systemic initiating action of urethane (ethyl carbamate) in mouse skin carcinogenesis. Br. J. Cancer *11*, 77–84.

Berridge, M. V, Herst, P.M., and Tan, A.S. (2005). Tetrazolium dyes as tools in cell biology: new insights into their cellular reduction. Biotechnol. Annu. Rev. *11*, 127–152.

Bhanot, A., Sharma, R., and Noolvi, M.N. (2011). Natural sources as potential anti-cancer agents : A review. Int. J. Phytomed. *3*, 9–26.

Bhat, T.A., Nambiar, D., Tailor, D., Pal, A., Agarwal, R., and Singh, R.P. (2013). Acacetin inhibits in vitro and in vivo angiogenesis and downregulates Stat signaling and VEGF expression. Cancer Prev. Res. (Phila). *6*, 1128–1139.

Bishayee, K., Ghosh, S., Mukherjee, a, Sadhukhan, R., Mondal, J., and Khuda-Bukhsh, a R. (2013). Quercetin induces cytochrome-c release and ROS accumulation to promote apoptosis and arrest the cell cycle in G2/M, in cervical carcinoma: signal cascade and drug-DNA interaction. Cell Prolif. *46*, 153–163.

Boardman, L.A., Thibodeau, S.N., Schaid, D.J., Lindor, N.M., McDonnell, S.K., Burgart, L.J., Ahlquist, D.A., Podratz, K.C., Pittelkow, M., and Hartmann, L.C. (1998). Increased risk for cancer in patients with the Peutz-Jeghers syndrome. Ann. Intern. Med. *128*, 896–899.

Breast Cancer Foundation (2013). Breast Cancer in Canada. http://www.cbcf.org/central/AboutBreastCancerMain/AboutBreastCancer/Pages/BreastCancerinCanada.aspx.

Cailleau, R., Olivé, M., and Cruciger, Q.V.J. (1978). Long-term human breast carcinoma cell lines of metastatic origin: Preliminary characterization. In Vitro *14*, 911–915.

Canadian Cancer Statistics (2014). Cancer statistics at a glance - Canadian Cancer Society.

Cancer Australia (2012). Breast cancer | Cancer Australia. http://www.cbcf.org/Pages/default.aspx.

Cancer Research UK (2014). Cancer incidence for common cancers. http://www.cancerresearchuk.org/cancer-info/cancerstats/incidence/uk-cancer-incidence-statistics.

Chan, M.M., Soprano, K.J., Weinstein, K., and Fong, D. (2006). Epigallocatechin-3-Gallate Delivers Hydrogen Peroxide to Induce Death of Ovarian Cancer Cells and Enhances Their Cisplatin Susceptibility. *396*, 389–396.

Chang, Y.-F., Chi, C.-W., and Wang, J.-J. (2006). Reactive oxygen species production is involved in quercetin-induced apoptosis in human hepatoma cells. Nutr. Cancer *55*, 201–209.

Chebil, L., Humeau, C., Falcimaigne, A., Engasser, J.-M., and Ghoul, M. (2006). Enzymatic acylation of flavonoids. Process Biochem. *41*, 2237–2251.

Cheo, D.L., Meira, L.B., Burns, D.K., Reis, A.M., Issac, T., and Friedberg, E.C. (2000). Ultraviolet B radiation-induced skin cancer in mice defective in the Xpc, Trp53, and Apex (HAP1) genes: genotype-specific effects on cancer predisposition and pathology of tumors. Cancer Res. *60*, 1580–1584.

Chian, S., Thapa, R., Chi, Z., Wang, X.J., and Tang, X. (2014). Luteolin inhibits the Nrf2 signaling pathway and tumor growth in vivo. Biochem. Biophys. Res. Commun. *447*, 602–608.

Chiang, L.-C., Ng, L.T., Lin, I.-C., Kuo, P.-L., and Lin, C.-C. (2006). Anti-proliferative effect of apigenin and its apoptotic induction in human Hep G2 cells. Cancer Lett. *237*, 207–214.

Chidambaram, M., Manavalan, R., and Kathiresan, K. (2011). Nanotherapeutics to overcome conventional cancer chemotherapy limitations. J. Pharm. Pharm. Sci. *14*, 67–77.

Choi, S.U., Ryu, S.Y., Yoon, S.K., Jung, N.P., Park, S.H., Kim, K.H., Choi, E.J., and Lee, C.O. (1999). Effects of flavonoids on the growth and cell cycle of cancer cells. Anticancer Res. *19*, 5229–5233.

Chung, W.Y., Park, J.H., Kim, M.J., Kim, H.O., Hwang, J.K., Lee, S.K., and Park, K.K. (2007). Xanthorrhizol inhibits 12-O-tetradecanoylphorbol-13-acetate-induced acute inflammation and two-stage mouse skin carcinogenesis by blocking the expression of ornithine decarboxylase, cyclooxygenase-2 and inducible nitric oxide synthase through mitogen-acti. Carcinogenesis *28*, 1224–1231.

Ciardiello, F., Kim, N., McGeady, M.L., Liscia, D.S., Saeki, T., Bianco, C., and Salomon, D.S. (1991). Expression of transforming growth factor alpha (TGF alpha) in breast cancer. Ann. Oncol. *2*, 169–182.

Circu, M.L., and Aw, T.Y. (2012). Glutathione and modulation of cell apoptosis. Biochim. Biophys. Acta *1823*, 1767–1777.

Collins, J. a., Schandl, C. a., Young, K.K., Vesely, J., and Willingham, M.C. (1997). Major DNA Fragmentation Is a Late Event in Apoptosis. J. Histochem. Cytochem. *45*, 923–934.

Connolly, J.M., Gilhooly, E.M., and Rose, D.P. (1999). Effects of reduced dietary linoleic acid intake, alone or combined with an algal source of docosahexaenoic acid, on MDA-MB-231 breast cancer cell growth and apoptosis in nude mice. Nutr. Cancer *35*, 44–49.

Connor, W.E., and Connor, S.L. (2007). The importance of fish and docosahexaenoic acid in Alzheimer disease. Am J Clin Nutr *85*, 929–930.

Cory, A.H., Owen, T.C., Barltrop, J.A., and Cory, J.G. (1991). Use of an aqueous soluble tetrazolium/formazan assay for cell growth assays in culture. Cancer Commun. *3*, 207–212.

Cragg, G.M., and Newman, D.J. (2005). Plants as a source of anti-cancer agents. J. Ethnopharmacol. *100*, 72–79.

Cunnane, S.C., Plourde, M., Pifferi, F., Bégin, M., Féart, C., and Barberger-Gateau, P. (2009). Fish, docosahexaenoic acid and Alzheimer's disease. Prog. Lipid Res. *48*, 239–256.

Dai, Z.-J., Lu, W.-F., Gao, J., Kang, H.-F., Ma, Y.-G., Zhang, S.-Q., Diao, Y., Lin, S., Wang, X.-J., and Wu, W.-Y. (2013). Anti-angiogenic effect of the total flavonoids in Scutellaria barbata D. Don. BMC Complement. Altern. Med. *13*, 150.

Day, A.J., Cañada, F.J., Díaz, J.C., Kroon, P.A., Mclauchlan, R., Faulds, C.B., Plumb, G.W., Morgan, M.R., and Williamson, G. (2000). Dietary flavonoid and isoflavone glycosides are hydrolysed by the lactase site of lactase phlorizin hydrolase. FEBS Lett. *468*, 166–170.

Denecker, G., Dooms, H., Van Loo, G., Vercammen, D., Grooten, J., Fiers, W., Declercq, W., and Vandenabeele, P. (2000). Phosphatidyl serine exposure during apoptosis precedes release of cytochrome c and decrease in mitochondrial transmembrane potential. FEBS Lett. *465*, 47–52.

Ding, W., Vaught, J.L., Yamauchi, H., and Lind, S.E. (2004). Differential sensitivity of cancer cells to docosahexaenoic acid − induced cytotoxicity : The potential importance of down-regulation of superoxide dismutase 1 expression Differential sensitivity of cancer cells to docosahexaenoic acid – induced cytotoxic. 1109–1117.

Dolle, J.M., Daling, J.R., White, E., Brinton, L.A., Doody, D.R., Porter, P.L., and Malone, K.E. (2009). Risk factors for triple-negative breast cancer in women under the age of 45 years. Cancer Epidemiol. Biomarkers Prev. *18*, 1157–1166.

Ehrenkranz, J.R.L., Lewis, N.G., Kahn, C.R., and Roth, J. (2005). Phlorizin: a review. Diabetes. Metab. Res. Rev. *21*, 31–38.

Elmore, S. (2007). Apoptosis: a review of programmed cell death. Toxicol. Pathol. *35*, 495–516.

Eroles, P., Bosch, A., Pérez-Fidalgo, J.A., and Lluch, A. (2012). Molecular biology in breast cancer: intrinsic subtypes and signaling pathways. Cancer Treat. Rev. *38*, 698–707.

Fabiani, R., Fuccelli, R., Pieravanti, F., De Bartolomeo, A., and Morozzi, G. (2009). Production of hydrogen peroxide is responsible for the induction of apoptosis by hydroxytyrosol on HL60 cells. Mol. Nutr. Food Res. *53*, 887–896.

Fadok, V. a, Bratton, D.L., Frasch, S.C., Warner, M.L., and Henson, P.M. (1998). The role of phosphatidylserine in recognition of apoptotic cells by phagocytes. Cell Death Differ. *5*, 551–562.

Fan, Z., Baselga, J., Masui, H., and Mendelsohn, J. (1993). Antitumor effect of anti-epidermal growth factor receptor monoclonal antibodies plus cis-diamminedichloroplatinum on well established A431 cell xenografts. Cancer Res. *53*, 4637–4642.

Fang, J., Xia, C., Cao, Z., Zheng, J.Z., Reed, E., and Jiang, B.-H. (2005). Apigenin inhibits VEGF and HIF-1 expression via PI3K/AKT/p70S6K1 and HDM2/p53 pathways. FASEB J. *19*, 342–353.

Fang, J., Zhou, Q., Shi, X., and Jiang, B. (2007a). Luteolin inhibits insulin-like growth factor 1 receptor signaling in prostate cancer cells. Carcinogenesis *28*, 713–723.

Fang, J., Zhou, Q., Liu, L.-Z., Xia, C., Hu, X., Shi, X., and Jiang, B.-H. (2007b). Apigenin inhibits tumor angiogenesis through decreasing HIF-1alpha and VEGF expression. Carcinogenesis *28*, 858–864.

Ferguson, P.J., Kurowska, E., Freeman, D.J., Chambers, A.F., Koropatnick, D.J., and Al, F.E.T. (2004). Nutrition and Cancer A Flavonoid Fraction from Cranberry Extract Inhibits Proliferation of Human. 1529–1535.

Fernando Wasundara and Rupasinghe H. P. Vasantha (2013). Anticancer Properties of Phytochemicals Present in Medicinal Plants of North America. In Using Old Solutions to New Problems - Natural Drug Discovery in the 21st Century, M. Kulka, ed. (InTech), pp. 159–180.

Fu, B., Xue, J., Li, Z., Shi, X., Jiang, B.-H., and Fang, J. (2007). Chrysin inhibits expression of hypoxia-inducible factor-1alpha through reducing hypoxia-inducible factor-1alpha stability and inhibiting its protein synthesis. Mol. Cancer Ther. *6*, 220–226.

Gibellini, L., Pinti, M., Nasi, M., De Biasi, S., Roat, E., Bertoncelli, L., and Cossarizza, A. (2010). Interfering with ROS Metabolism in Cancer Cells: The Potential Role of Quercetin. Cancers (Basel). *2*, 1288–1311.

Giordano, S.H. (2005). A review of the diagnosis and management of male breast cancer. Oncologist *10*, 471–479.

Globocan (2012). Fact Sheets by Cancer. http://globocan.iarc.fr/Pages/fact_sheets_cancer.aspx.

Goldhirsch, a, Wood, W.C., Coates, a S., Gelber, R.D., Thürlimann, B., and Senn, H.-J. (2011). Strategies for subtypes--dealing with the diversity of breast cancer: highlights of the St. Gallen International Expert Consensus on the Primary Therapy of Early Breast Cancer 2011. Ann. Oncol. *22*, 1736–1747.

Granado-Serrano, A.B., Martin, M.A., Bravo, L., Goya, L., and Ramos, S. (2006). Quercetin Induces Apoptosis via Caspase Activation, Regulation of Bcl-2, and Inhibition of PI-3-Kinase/Akt and ERK Pathways in a Human Hepatoma Cell Line (HepG2). J. Nutr. *136*, 2715–2721.

Guthrie, N. (2000). Effect of cranberry juice and products on human breast cancer cell growth. FASEB J *14*, 531.13.

Haddad, A.Q., Venkateswaran, V., Viswanathan, L., Teahan, S.J., Fleshner, N.E., and Klotz, L.H. (2006). Novel antiproliferative flavonoids induce cell cycle arrest in human prostate cancer cell lines. Prostate Cancer Prostatic Dis. *9*, 68–76.

Halasi, M., Wang, M., Chavan, T.S., Gaponenko, V., Hay, N., and Gartel, A.L. (2013). ROS inhibitor N-acetyl-L-cysteine antagonizes the activity of proteasome inhibitors. Biochem. J. *454*, 201–208.

Hammer, C., Fanning, A., and Crowe, J. (2008). Overview of breast cancer staging and surgical treatment options. Cleve. Clin. J. Med. *75*, S10–S10.

Hang, H., and Fox, M.H. (2004). Analysis of the mammalian cell cycle by flow cytometry. Methods Mol. Biol. *241*, 23–35.

Hashimoto, M., Hossain, S., Shimada, T., Sugioka, K., Yamasaki, H., Fujii, Y., Ishibashi, Y., Oka, J.-I., and Shido, O. (2002). Docosahexaenoic acid provides protection from impairment of learning ability in Alzheimer's disease model rats. J. Neurochem. *81*, 1084–1091.

He, L., Zhang, E., Shi, J., Li, X., Zhou, K., Zhang, Q., Le, A.D., and Tang, X. (2013). (-)-Epigallocatechin-3-gallate inhibits human papillomavirus (HPV)-16 oncoprotein-induced angiogenesis in non-small cell lung cancer cells by targeting HIF-1α. Cancer Chemother. Pharmacol. *71*, 713–725.

Hilchie, A.L., Doucette, C.D., Pinto, D.M., Patrzykat, A., Douglas, S., and Hoskin, D.W. (2011). Pleurocidin-family cationic antimicrobial peptides are cytolytic for breast carcinoma cells and prevent growth of tumor xenografts. Breast Cancer Res. *13*, R102.

Horrocks, L.A., and Yeo, Y.K. (1999). Health benefits of docosahexaenoic acid (DHA). Pharmacol. Res. *40*, 211–225.

Hoskins, C., Wang, L., Cheng, W.P., and Cuschieri, A. (2012). Dilemmas in the reliable estimation of the in-vitro cell viability in magnetic nanoparticle engineering: which tests and what protocols? Nanoscale Res. Lett. *7*, 77.

Huang, K.T., Chen, Y.H., and Walker, A.M. (2004). Inaccuracies in MTS assays: major distorting effects of medium, serum albumin, and fatty acids. Biotechniques *37*, 406, 408, 410–412.

Hwang, K.Y., Oh, Y.T., Yoon, H., Lee, J., Kim, H., Choe, W., and Kang, I. (2008). Baicalein suppresses hypoxia-induced HIF-1alpha protein accumulation and activation through inhibition of reactive oxygen species and PI 3-kinase/Akt pathway in BV2 murine microglial cells. Neurosci. Lett. *444*, 264–269.

Imyanitov, E.N., and Hanson, K.P. (2004). Mechanisms of breast cancer. Drug Discov. Today Dis. Mech. *1*, 235–245.

Ju, W., Wang, X., Shi, H., Chen, W., Belinsky, S.A., and Lin, Y. (2007). A critical role of luteolin-induced reactive oxygen species in blockage of tumor necrosis factor-activated nuclear factor-kappaB pathway and sensitization of apoptosis in lung cancer cells. Mol. Pharmacol. *71*, 1381–1388.

Jung, S.K., Lee, K.W., Byun, S., Lee, E.J., Kim, J.-E., Bode, A.M., Dong, Z., and Lee, H.J. (2010). Myricetin inhibits UVB-induced angiogenesis by regulating PI-3 kinase in vivo. Carcinogenesis *31*, 911–917.

Kalckar, H. (1936). Inhibitory Effect of Phloridzin and Phloretin on Kidney Phosphatase : Abstract : Nature. Nature *138*, 289.

Kale, A., Gawande, S., and Kotwal, S. (2008). Cancer Phytotherapeutics : Role for Flavonoids at the Cellular Level. Phytother. Res. *22*, 567–577.

Kamei, H., Koide, T., Kojimam, T., Hasegawa, M., Terabe, K., Umeda, T., and Hashimoto, Y. (1996). Flavonoid-Mediated Tumor Growth Suppression Demonstrated by in vivo Study. Cancer Biother. Radiopharm. *11*, 193–196.

Kandaswami, C., Kanadaswami, C., Lee, L.-T., Lee, P.-P.H., Hwang, J.-J., Ke, F.-C., Huang, Y.-T., and Lee, M.-T. (2005). The antitumor activities of flavonoids. In Vivo *19*, 895–909.

Kang, K.S., Wang, P., Yamabe, N., Fukui, M., Jay, T., and Zhu, B.T. (2010). Docosahexaenoic acid induces apoptosis in MCF-7 cells in vitro and in vivo via reactive oxygen species formation and caspase 8 activation. PLoS One *5*, e10296.

Kato, T., Kolenic, N., and Pardini, R.S. (2007). Docosahexaenoic acid (DHA), a primary tumor suppressive omega-3 fatty acid, inhibits growth of colorectal cancer independent of p53 mutational status. Nutr. Cancer *58*, 178–187.

Katzung, B.G. (2006). Basic and Clinical Pharmacology (McGraw Hill).

Kenis, H., van Genderen, H., Bennaghmouch, A., Rinia, H. a, Frederik, P., Narula, J., Hofstra, L., and Reutelingsperger, C.P.M. (2004). Cell surface-expressed phosphatidylserine and annexin A5 open a novel portal of cell entry. J. Biol. Chem. *279*, 52623–52629.

Kerksick, C., and Willoughby, D. (2005). The antioxidant role of glutathione and N-acetyl-cysteine supplements and exercise-induced oxidative stress. J. Int. Soc. Sports Nutr. *2*, 38–44.

Kerr, J.F., Wyllie, A.H., and Currie, A.R. (1972). Apoptosis: a basic biological phenomenon with wide-ranging implications in tissue kinetics. Br. J. Cancer *26*, 239–257.

Khan, N. a, Nishimura, K., Aires, V., Yamashita, T., Oaxaca-Castillo, D., Kashiwagi, K., and Igarashi, K. (2006). Docosahexaenoic acid inhibits cancer cell growth via p27Kip1, CDK2, ERK1/ERK2, and retinoblastoma phosphorylation. J. Lipid Res. *47*, 2306–2313.

Kim, J.-H., Lee, E.-O., Lee, H.-J., Ku, J.-S., Lee, M.-H., Yang, D.-C., and Kim, S.-H. (2007). Caspase Activation and Extracellular Signal-Regulated Kinase/Akt Inhibition Were Involved in Luteolin-Induced Apoptosis in Lewis Lung Carcinoma Cells. Ann. N. Y. Acad. Sci. *1095*, 598–611.

Kobori, M., Shinmoto, H., Tsushida, T., and Shinohara, K. (1997). Phloretin-induced apoptosis in B16 melanoma 4A5 cells by inhibition of glucose transmembrane transport. Cancer Lett. *119*, 207–212.

Krysko, D. V, Vanden Berghe, T., Parthoens, E., D'Herde, K., and Vandenabeele, P. (2008). Methods for distinguishing apoptotic from necrotic cells and measuring their clearance. Methods Enzymol. *442*, 307–341.

Labat-Moleur, F., Guillermet, C., Lorimier, P., Robert, C., Lantuejoul, S., Brambilla, E., and Negoescu, a. (1998). TUNEL Apoptotic Cell Detection in Tissue Sections: Critical Evaluation and Improvement. J. Histochem. Cytochem. *46*, 327–334.

Lau, C.B.S., Ho, C.Y., Kim, C.F., Leung, K.N., Fung, K.P., Tse, T.F., Chan, H.H.L., and Chow, M.S.S. (2004). Cytotoxic activities of Coriolus versicolor (Yunzhi) extract on human leukemia and lymphoma cells by induction of apoptosis. Life Sci. *75*, 797–808.

Lee, C.Y., Sit, W., Fan, S., Man, K., Jor, I.W., Wong, L.E.O.L., Wan, M.L., Tan-un, K.C., and Wan, J.M. (2010). The cell cycle effects of docosahexaenoic acid on human metastatic hepatocellular carcinoma proliferation. Int. J. Oncol. *36*, 991–998.

Lee, S.-H., Meng, X.W., Flatten, K.S., Loegering, D. a, and Kaufmann, S.H. (2013). Phosphatidylserine exposure during apoptosis reflects bidirectional trafficking between plasma membrane and cytoplasm. Cell Death Differ. *20*, 64–76.

Lei, H., Sjöberg-Margolin, S., Salahshor, S., Werelius, B., Jandáková, E., Hemminki, K., Lindblom, A., and Vorechovský, I. (2002). CDH1 mutations are present in both ductal and lobular breast cancer, but promoter allelic variants show no detectable breast cancer risk. Int. J. Cancer *98*, 199–204.

Li, S., Priceman, S.J., Xin, H., Zhang, W., Deng, J., Liu, Y., Huang, J., Zhu, W., Chen, M., Hu, W., et al. (2013). Icaritin inhibits JAK/STAT3 signaling and growth of renal cell carcinoma. PLoS One *8*, e81657.

Liu, L.-Z., Jing, Y., Jiang, L.L., Jiang, X.-E., Jiang, Y., Rojanasakul, Y., and Jiang, B.-H. (2011). Acacetin inhibits VEGF expression, tumor angiogenesis and growth through AKT/HIF-1α pathway. Biochem. Biophys. Res. Commun. *413*, 299–305.

Liu, Y., Xie, S., Wang, Y., Luo, K., Wang, Y., and Cai, Y. (2012). Liquiritigenin inhibits tumor growth and vascularization in a mouse model of HeLa cells. Molecules *17*, 7206–7216.

Lockshin, R.A. (1969). Programmed cell death. Activation of lysis by a mechanism involving the synthesis of protein. J. Insect Physiol. *15*, 1505–1516.

Lockshin, R.A., and Williams, C.M. (1964). Programmed cell death—II. Endocrine potentiation of the breakdown of the intersegmental muscles of silkmoths. J. Insect Physiol. *10*, 643–649.

Lockshin, R.A., and Williams, C.M. (1965). Programmed cell death—I. Cytology of degeneration in the intersegmental muscles of the Pernyi silkmoth. J. Insect Physiol. *11*, 123–133.

Long, X., Fan, M., Bigsby, R.M., and Nephew, K.P. (2008). Apigenin inhibits antiestrogen-resistant breast cancer cell growth through estrogen receptor-alpha-dependent and estrogen receptor-alpha-independent mechanisms. Mol. Cancer Ther. *7*, 2096–2108.

Lundy, J., Mornex, F., Keenan, A.M., Greiner, J.W., and Colcher, D. (1986). Radioimmunodetection of human colon carcinoma xenografts in visceral organs of congenitally athymic mice. Cancer *57*, 503–509.

MacDonald, R.E., and Bishop, C.J. (1952). Phloretin: An Antibacterial Substance obtained from Apple Leaves. Can. J. Bot. *30*, 486–489.

Malathi, P., and Crane, R.K. (1969). Phlorizin hydrolase: A β-glucosidase of hamster intestinal brush border membrane. Biochim. Biophys. Acta - Biomembr. *173*, 245–256.

Malkin, D., Li, F.P., Strong, L.C., Fraumeni, J.F., Nelson, C.E., Kim, D.H., Kassel, J., Gryka, M.A., Bischoff, F.Z., and Tainsky, M.A. (1990). Germ line p53 mutations in a familial syndrome of breast cancer, sarcomas, and other neoplasms. Science *250*, 1233–1238.

Mantena, S.K., Meeran, S.M., Elmets, C.A., and Katiyar, S.K. (2005). Orally administered green tea polyphenols prevent ultraviolet radiation-induced skin cancer in mice through activation of cytotoxic T cells and inhibition of angiogenesis in tumors. J. Nutr. *135*, 2871–2877.

Marin, J.J.G., Romero, M.R., Blazquez, A.G., Herraez, E., Keck, E., and Briz, O. (2009). Importance and limitations of chemotherapy among the available treatments for gastrointestinal tumours. Anticancer. Agents Med. Chem. *9*, 162–184.

Markaverich, B.M., Shoulars, K., and Rodriguez, M.A. (2011). Luteolin Regulation of Estrogen Signaling and Cell Cycle Pathway Genes in MCF-7 Human Breast Cancer Cells. Int. J. Biomed. Sci. *7*, 101–111.

De Martel, C., Ferlay, J., Franceschi, S., Vignat, J., Bray, F., Forman, D., and Plummer, M. (2012). Global burden of cancers attributable to infections in 2008: a review and synthetic analysis. Lancet Oncol. *13*, 607–615.

Martin, A.-M. (2000). Genetic and Hormonal Risk Factors in Breast Cancer. J. Natl. Cancer Inst. *92*, 1126–1135.

McCann, J.C., and Ames, B.N. (2005). Is docosahexaenoic acid, an n-3 long-chain polyunsaturated fatty acid, required for development of normal brain function? An overview of evidence from cognitive and behavioral tests in humans and animals. Am. J. Clin. Nutr. *82*, 281–295.

McLennan, P., Howe, P., Abeywardena, M., Muggli, R., Raederstorff, D., Mano, M., Rayner, T., and Head, R. (1996). The cardiovascular protective role of docosahexaenoic acid. Eur. J. Pharmacol. *300*, 83–89.

Mcpherson, K., Steel, C.M., and Dixon, J.M. (2000). Breast cancer — epidemiology , risk factors , and genetics Risk factors for breast cancer. Br. Med. J. *321*, 624-8.

Mellou, F., Lazari, D., Skaltsa, H., Tselepis, a D., Kolisis, F.N., and Stamatis, H. (2005). Biocatalytic preparation of acylated derivatives of flavonoid glycosides enhances their antioxidant and antimicrobial activity. J. Biotechnol. *116*, 295–304.

Mellou, F., Loutrari, H., Stamatis, H., Roussos, C., and Kolisis, F.N. (2006). Enzymatic esterification of flavonoids with unsaturated fatty acids: Effect of the novel esters on vascular endothelial growth factor release from K562 cells. Process Biochem. *41*, 2029–2034.

Merken, H.M., and Beecher, G.R. (2000). Measurement of food flavonoids by high-performance liquid chromatography: A review. J. Agric. Food Chem. *48*, 577–599.

Milne, R.L., and Antoniou, A.C. (2011). Genetic modifiers of cancer risk for BRCA1 and BRCA2 mutation carriers. Ann. Oncol. *22 Suppl 1*, i11–7.

Mirzoeva, S., Kim, N.D., Chiu, K., Franzen, C.A., Bergan, R.C., and Pelling, J.C. (2008). Inhibition of HIF-1 alpha and VEGF expression by the chemopreventive bioflavonoid apigenin is accompanied by Akt inhibition in human prostate carcinoma PC3-M cells. Mol. Carcinog. *47*, 686–700.

Mocanu, M-M., Surcel M.,, Ursaciuc, C., and Katona, E., Ganea, C. (2013). Antiproliferative effect of quercetin in mammary and epidermoid cancer cells. Rom. Biotechnol. Lett. *18*, 8796–8803.

Monasterio, A., Urdaci, M.C., Pinchuk, I. V, López-Moratalla, N., and Martínez-Irujo, J.J. (2004). Flavonoids induce apoptosis in human leukemia U937 cells through caspase- and caspase-calpain-dependent pathways. Nutr. Cancer *50*, 90–100.

Mori, T.A., Bao, D.Q., Burke, V., Puddey, I.B., and Beilin, L.J. (1999). Docosahexaenoic acid but not eicosapentaenoic acid lowers ambulatory blood pressure and heart rate in humans. Hypertension *34*, 253–260.

Morris, M.C., Evans, D. a, Bienias, J.L., Tangney, C.C., Bennett, D. a, Wilson, R.S., Aggarwal, N., and Schneider, J. (2003). Consumption of fish and n-3 fatty acids and risk of incident Alzheimer disease. Arch. Neurol. *60*, 940–946.

Morse, N.L. (2012). Benefits of docosahexaenoic acid, folic acid, vitamin D and iodine on foetal and infant brain development and function following maternal supplementation during pregnancy and lactation. Nutrients *4*, 799–840.

Mosmann, T. (1983). Rapid colorimetric assay for cellular growth and survival: application to proliferation and cytotoxicity assays. J. Immunol. Methods *65*, 55–63.

Muthian, G., and Bright, J.J. (2004). Quercetin, a flavonoid phytoestrogen, ameliorates experimental allergic encephalomyelitis by blocking IL-12 signaling through JAK-STAT pathway in T lymphocyte. J. Clin. Immunol. *24*, 542–552.

Nagata, S. (2000). Apoptotic DNA fragmentation. Exp. Cell Res. *256*, 12–18.

Nakagawa, H., Hasumi, K., Woo, J.-T., Nagai, K., and Wachi, M. (2004). Generation of hydrogen peroxide primarily contributes to the induction of Fe(II)-dependent apoptosis in Jurkat cells by (-)-epigallocatechin gallate. Carcinogenesis *25*, 1567–1574.

Nakamoto, K., Nishinaka, T., Mankura, M., Fujita-Hamabe, W., and Tokuyama, S. (2010). Antinociceptive effects of docosahexaenoic acid against various pain stimuli in mice. Biol. Pharm. Bull. *33*, 1070–1072.

Nathanson, K.L., Wooster, R., Weber, B.L., and Nathanson, K.N. (2001). Breast cancer genetics: what we know and what we need. Nat. Med. *7*, 552–556.

Nelen, M.R., Padberg, G.W., Peeters, E.A., Lin, A.Y., van den Helm, B., Frants, R.R., Coulon, V., Goldstein, A.M., van Reen, M.M., Easton, D.F., et al. (1996). Localization of the gene for Cowden disease to chromosome 10q22-23. Nat. Genet. *13*, 114–116.

Nelson, J.A., and Falk, R.E. (1993a). The efficacy of phloridzin and phloretin on tumor cell growth. Anticancer Res. *13*, 2287–2292.

Nelson, J.A., and Falk, R.E. (1993b). Phloridzin and phloretin inhibition of 2-deoxy-D-glucose uptake by tumor cells in vitro and in vivo. Anticancer Res. *13*, 2293–2299.

Nicholson, D.W., and Thornberry, N.A. (1997). Caspases: killer proteases. Trends Biochem. Sci. *22*, 299–306.

Nicoletti, I., Migliorati, G., Pagliacci, M.C., Grignani, F., and Riccardi, C. (1991). A rapid and simple method for measuring thymocyte apoptosis by propidium iodide staining and flow cytometry. J. Immunol. Methods *139*, 271–279.

Nielsen, I.L.F., Chee, W.S.S., Poulsen, L., Offord-cavin, E., Rasmussen, S.E., Frederiksen, H., Enslen, M., Barron, D., Horcajada, M., and Williamson, G. (2006). Nutrient Physiology , Metabolism , and Nutrient-Nutrient Interactions Bioavailability Is Improved by Enzymatic Modification of the Citrus. 404–408.

Nirmala, M.J., Samundeeswari, A., and Sankar, P.D. (2011). Natural plant resources in anti-cancer therapy-A review. Res. Plant Biol. *1*, 1–14.

Odiatou, E.M., Skaltsounis, A.L., and Constantinou, A.I. (2013). Identification of the factors responsible for the in vitro pro-oxidant and cytotoxic activities of the olive polyphenols oleuropein and hydroxytyrosol. Cancer Lett. *330*, 113–121.

Oh, S.-H., and Lim, S.-C. (2006). A rapid and transient ROS generation by cadmium triggers apoptosis via caspase-dependent pathway in HepG2 cells and this is inhibited through N-acetylcysteine-mediated catalase upregulation. Toxicol. Appl. Pharmacol. *212*, 212–223.

De Oliveira, E.B., Humeau, C., Chebil, L., Maia, E.R., Dehez, F., Maigret, B., Ghoul, M., and Engasser, J.-M. (2009). A molecular modelling study to rationalize the regioselectivity in acylation of flavonoid glycosides catalyzed by Candida antarctica lipase B. J. Mol. Catal. B Enzym. *59*, 96–105.

Ono, M., Takeshima, M., Higuchi, T., Chen, C., and Nakano, S. (2014). Mechanistic study for non-oxidative anticancer activity of epigallocatechin-3-gallate in MCF-7 human breast cancer cells (644.6). FASEB J *28*, 644.6–.

Ovcaricek, T., Frkovic, S.G., Matos, E., Mozina, B., and Borstnar, S. (2011). Triple negative breast cancer - prognostic factors and survival. Radiol. Oncol. *45*, 46–52.

Patel, D., Shukla, S., and Gupta, S. (2007). Apigenin and cancer chemoprevention: progress, potential and promise (review). Int. J. Oncol. *30*, 233–245.

Pereira, M.A., Grubbs, C.J., Barnes, L.H., Li, H., Olson, G.R., Eto, I., Juliana, M., Whitaker, L.M., Kelloff, G.J., Steele, V.E., et al. (1996). Effects of the phytochemicals, curcumin and quercetin, upon azoxymethane-induced colon cancer and 7, 12-dimethylbenz[a]anthracene-induced mammary cancer in rats. Carcinogenesis *17*, 1305–1311.

Philpott, N.J., Turner, a J., Scopes, J., Westby, M., Marsh, J.C., Gordon-Smith, E.C., Dalgleish, a G., and Gibson, F.M. (1996). The use of 7-amino actinomycin D in identifying apoptosis: simplicity of use and broad spectrum of application compared with other techniques. Blood *87*, 2244–2251.

Polyak, K. (2011). Review series introduction Heterogeneity in breast cancer. *121*.

Porter, a G., and Jänicke, R.U. (1999). Emerging roles of caspase-3 in apoptosis. Cell Death Differ. *6*, 99–104.

Prasain, J.K., Jones, K., Moore, R., Barnes, S., Leahy, M., Juliana, M.M., and Grubbs, C.J. (2009). Effect of cranberry juice concentrate on chemically-induced urinary bladder cancers urinary bladder cancers. Oncol. Rep. *19*, 1565–70.

Pratheeshkumar, P., Son, Y.-O., Budhraja, A., Wang, X., Ding, S., Wang, L., Hitron, A., Lee, J.-C., Kim, D., Divya, S.P., et al. (2012a). Luteolin inhibits human prostate tumor growth by suppressing vascular endothelial growth factor receptor 2-mediated angiogenesis. PLoS One *7*, e52279.

Pratheeshkumar, P., Budhraja, A., Son, Y.-O., Wang, X., Zhang, Z., Ding, S., Wang, L., Hitron, A., Lee, J.-C., Xu, M., et al. (2012b). Quercetin inhibits angiogenesis mediated human prostate tumor growth by targeting VEGFR- 2 regulated AKT/mTOR/P70S6K signaling pathways. PLoS One *7*, e47516.

Rabinovitch, P. (1994). Introduction to cell cycle analysis (Phoenix Flow Systems, Inc. USA).

Raisova, M., Hossini, a M., Eberle, J., Riebeling, C., Wieder, T., Sturm, I., Daniel, P.T., Orfanos, C.E., and Geilen, C.C. (2001). The Bax/Bcl-2 ratio determines the susceptibility of human melanoma cells to CD95/Fas-mediated apoptosis. J. Invest. Dermatol. *117*, 333–340.

Rao, P.S., Satelli, A., Moridani, M., Jenkins, M., and Rao, U.S. (2012). Luteolin induces apoptosis in multidrug resistant cancer cells without affecting the drug transporter function: involvement of cell line-specific apoptotic mechanisms. Int. J. Cancer *130*, 2703–2714.

Ren, W., Qiao, Z., Wang, H., Zhu, L., and Zhang, L. (2003). Flavonoids: promising anticancer agents. Med. Res. Rev. *23*, 519–534.

Reszka, K.J., Wagner, B. a, Burns, C.P., and Britigan, B.E. (2005). Effects of peroxidase substrates on the Amplex red/peroxidase assay: antioxidant properties of anthracyclines. Anal. Biochem. *342*, 327–337.

Rezk, B.M., Haenen, G.R.M.M., van der Vijgh, W.J.F., and Bast, A. (2002). The antioxidant activity of phloretin: the disclosure of a new antioxidant pharmacophore in flavonoids. Biochem. Biophys. Res. Commun. *295*, 9–13.

Riccardi, C., and Nicoletti, I. (2006). Analysis of apoptosis by propidium iodide staining and flow cytometry. Nat. Protoc. *1*, 1458–1461.

Rose, D.P., and Connolly, J.M. (1993). Effects of dietary omega-3 fatty acids on human breast cancer growth and metastases in nude mice. J. Natl. Cancer Inst. *85*, 1743–1747.

Rose, D.P., Connolly, J.M., Rayburn, J., and Coleman, M. (1995). Influence of diets containing eicosapentaenoic or docosahexaenoic acid on growth and metastasis of breast cancer cells in nude mice. J. Natl. Cancer Inst. *87*, 587–592.

Rupasinghe H.P.V., T.S. and N.S. (2012). Polyphenols: Chemistry, Dietary Sources and Health Benefits. In Polyphenols: Chemistry, Dietary Sources and Health Benefits, X.Y. and L.L. J. Sun, K. N. Prasad, A. Ismail, B. Yang, ed. (Nova Science Publishers, Inc. Hauppauge, NY, USA), pp. 333–368.

Salem, J.H., Humeau, C., Chevalot, I., Harscoat-Schiavo, C., Vanderesse, R., Blanchard, F., and Fick, M. (2010). Effect of acyl donor chain length on isoquercitrin acylation and biological activities of corresponding esters. Process Biochem. *45*, 382–389.

Schley, P.D., Jijon, H.B., Robinson, L.E., and Field, C.J. (2005). Mechanisms of omega-3 fatty acid-induced growth inhibition in MDA-MB-231 human breast cancer cells. Breast Cancer Res. Treat. *92*, 187–195.

Schmid, I., Krall, W.J., Uittenbogaart, C.H., Braun, J., and Giorgi, J. V (1992). Dead cell discrimination with 7-amino-actinomycin D in combination with dual color immunofluorescence in single laser flow cytometry. Cytometry *13*, 204–208.

Schumacher, V., Vogel, T., Leube, B., Driemel, C., Goecke, T., Möslein, G., and Royer-Pokora, B. (2005). STK11 genotyping and cancer risk in Peutz-Jeghers syndrome. J. Med. Genet. *42*, 428–435.

Senggunprai, L., Kukongviriyapan, V., Prawan, A., and Kukongviriyapan, U. (2014). Quercetin and EGCG Exhibit Chemopreventive Effects in Cholangiocarcinoma Cells via Suppression of JAK/STAT Signaling Pathway. Phytother. Res. *28*, 841–848.

Serini, S., Trombino, S., Oliva, F., Piccioni, E., Monego, G., Resci, F., Boninsegna, A., Picci, N., Ranelletti, F.O., and Calviello, G. (2008). Docosahexaenoic acid induces apoptosis in lung cancer cells by increasing MKP-1 and down-regulating p-ERK1/2 and p-p38 expression. Apoptosis *13*, 1172–1183.

Shankar, S., Marsh, L., and Srivastava, R.K. (2013). EGCG inhibits growth of human pancreatic tumors orthotopically implanted in Balb C nude mice through modulation of FKHRL1/FOXO3a and neuropilin. Mol. Cell. Biochem. *372*, 83–94.

Shen, Q., Li, X., Li, W., and Zhao, X. (2011). Enhanced intestinal absorption of daidzein by borneol/menthol eutectic mixture and microemulsion. AAPS PharmSciTech *12*, 1044–1049.

Shikov, A., and Pozharitskaya, O. (2008). Self-microemulsifying drug delivery system as nanosystems for bioavailability enhancement of flavonoids in vitro. Eur. J. ….

Shim, H., Park, J., Paik, H., Nah, S., Kim, D.S.H.L., and Han, Y.S. (2007). Molecules and Acacetin-induced Apoptosis of Human Breast Cancer MCF-7 Cells Involves Caspase Cascade , Mitochondria-mediated Death Signaling and SAPK / JNK1 / 2-c-Jun Activation. *24*, 95–104.

Shoeb, M. (2006). Minireview: Anticancer agents from medicinal plants. *2002*, 35–41.

Shukla, S., and Gupta, S. (2008). Apigenin-induced prostate cancer cell death is initiated by reactive oxygen species and p53 activation. Free Radic. Biol. Med. *44*, 1833–1845.

Shuryak, I., Hahnfeldt, P., Hlatky, L., Sachs, R.K., and Brenner, D.J. (2009). A new view of radiation-induced cancer: integrating short- and long-term processes. Part II: second cancer risk estimation. Radiat. Environ. Biophys. *48*, 275–286.

Singh, R.P., Sharma, G., Dhanalakshmi, S., Agarwal, C., and Agarwal, R. (2003). Suppression of advanced human prostate tumor growth in athymic mice by silibinin feeding is associated with reduced cell proliferation, increased apoptosis, and inhibition of angiogenesis. Cancer Epidemiol. Biomarkers Prev. *12*, 933–939.

Smith, S.M., Wunder, M.B., Norris, D. a, and Shellman, Y.G. (2011). A simple protocol for using a LDH-based cytotoxicity assay to assess the effects of death and growth inhibition at the same time. PLoS One *6*, e26908.

Stangl, V., Lorenz, M., Ludwig, A., Grimbo, N., Guether, C., Sanad, W., Ziemer, S., Martus, P., Baumann, G., and Stangl, K. (2005). Biochemical and Molecular Actions of Nutrients The Flavonoid Phloretin Suppresses Stimulated Expression of Endothelial Adhesion Molecules and Reduces Activation of Human Platelets. J. Nutri. *135*,172–178.

Stankovic, T., Kidd, A.M., Sutcliffe, A., McGuire, G.M., Robinson, P., Weber, P., Bedenham, T., Bradwell, A.R., Easton, D.F., Lennox, G.G., et al. (1998). ATM mutations and phenotypes in ataxia-telangiectasia families in the British Isles: expression of mutant ATM and the risk of leukemia, lymphoma, and breast cancer. Am. J. Hum. Genet. *62*, 334–345.

Stevenson, D.E., Wibisono, R., Jensen, D.J., Stanley, R. a., and Cooney, J.M. (2006). Direct acylation of flavonoid glycosides with phenolic acids catalysed by Candida antarctica lipase B (Novozym 435®). Enzyme Microb. Technol. *39*, 1236–1241.

Sudan, S., and Rupasinghe, H.P.V. (2014). Quercetin-3-O-glucoside induces human DNA topoisomerase II inhibition, cell cycle arrest and apoptosis in hepatocellular carcinoma cells. Anticancer Res. *34*, 1691–1699.

Sun, S.-Y. (2010). N-acetylcysteine, reactive oxygen species and beyond. Cancer Biol. Ther. *9*, 109–110.

Sun, F., Zheng, X.Y., Ye, J., Wu, T.T., Wang, J.L., and Chen, W. (2012). Potential anticancer activity of myricetin in human T24 bladder cancer cells both in vitro and in vivo. Nutr. Cancer *64*, 599–606.

Sun, S.-N., Jia, W.-D., Chen, H., Ma, J.-L., Ge, Y.-S., Yu, J.-H., and Li, J.-S. (2013). Docosahexaenoic acid (DHA) induces apoptosis in human hepatocellular carcinoma cells. Int. J. Clin. Exp. Pathol. *6*, 281–289.

Surh, Y. (1999). Molecular mechanisms of chemopreventive effects of selected dietary and medicinal phenolic substances. Mutat. Res. *428*, 305–327.

Sweeney, C., Blair, C.K., Anderson, K.E., Lazovich, D., and Folsom, A.R. (2004). Risk factors for breast cancer in elderly women. Am. J. Epidemiol. *160*, 868–875.

Talanian, R. V, Quinlan, C., Trautz, S., Hackett, M.C., Mankovich, J. a, Banach, D., Ghayur, T., Brady, K.D., and Wong, W.W. (1997). Substrate specificities of caspase family proteases. J. Biol. Chem. *272*, 9677–9682.

Tanaka, T., Kohno, H., Suzuki, R., Yamada, Y., Sugie, S., and Mori, H. (2003). A novel inflammation-related mouse colon carcinogenesis model induced by azoxymethane and dextran sodium sulfate. Cancer Sci. *94*, 965–973.

Touil, Y.S., Seguin, J., Scherman, D., and Chabot, G.G. (2011). Improved antiangiogenic and antitumour activity of the combination of the natural flavonoid fisetin and cyclophosphamide in Lewis lung carcinoma-bearing mice. Cancer Chemother. Pharmacol. *68*, 445–455.

Triantafyllou, A., Liakos, P., Tsakalof, A., Chachami, G., Paraskeva, E., Molyvdas, P.-A., Georgatsou, E., Simos, G., and Bonanou, S. (2007). The flavonoid quercetin induces hypoxia-inducible factor-1alpha (HIF-1alpha) and inhibits cell proliferation by depleting intracellular iron. Free Radic. Res. *41*, 342–356.

Triantafyllou, A., Mylonis, I., Simos, G., Bonanou, S., and Tsakalof, A. (2008). Flavonoids induce HIF-1alpha but impair its nuclear accumulation and activity. Free Radic. Biol. Med. *44*, 657–670.

Tsunoda, A., Shibusawa, M., Tsunoda, Y., Yokoyama, N., Nakao, K., Kusano, M., Nomura, N., Nagayama, S., and Takechi, T. (1998). Antitumor effect of S-1 on DMH induced colon cancer in rats. Anticancer Res. *18*, 1137–1141.

Vermes, I., Haanen, C., Steffens-Nakken, H., and Reutelingsperger, C. (1995). A novel assay for apoptosis. Flow cytometric detection of phosphatidylserine expression on early apoptotic cells using fluorescein labelled Annexin V. J. Immunol. Methods *184*, 39–51.

Verschraegen, C.F., Hu, W., Du, Y., Mendoza, J., Early, J., Deavers, M., Freedman, R.S., Bast, R.C., Kudelka, A.P., Kavanagh, J.J., et al. (2003). Establishment and characterization of cancer cell cultures and xenografts derived from primary or metastatic Mullerian cancers. Clin. Cancer Res. *9*, 845–852.

Vidya Priyadarsini, R., Senthil Murugan, R., Maitreyi, S., Ramalingam, K., Karunagaran, D., and Nagini, S. (2010). The flavonoid quercetin induces cell cycle arrest and mitochondria-mediated apoptosis in human cervical cancer (HeLa) cells through p53 induction and NF-κB inhibition. Eur. J. Pharmacol. *649*, 84–91.

Viskupicova, J., Ondrejovic, M., and Maliar, T. (2010). Enzyme-Mediated Preparation of Flavonoid Esters and Their Applications.

Vitale, M., Zamai, L., Mazzotti, G., Cataldi, A., Falcieri, E., Biomediche, S., Anatomia, S., Cnr, N.P., and Umana, M. (1993).] R2. 223–229.

Voduc, K.D., Cheang, M.C.U., Tyldesley, S., Gelmon, K., Nielsen, T.O., and Kennecke, H. (2010). Breast cancer subtypes and the risk of local and regional relapse. J. Clin. Oncol. *28*, 1684–1691.

Vu, H.A., Beppu, Y., Chi, H.T., Sasaki, K., Yamamoto, H., Xinh, P.T., Tanii, T., Hara, Y., Watanabe, T., Sato, Y., et al. (2010). Green tea epigallocatechin gallate exhibits anticancer effect in human pancreatic carcinoma cells via the inhibition of both focal adhesion kinase and insulin-like growth factor-I receptor. J. Biomed. Biotechnol. *2010*, 290516.

Walle, T., Uni, V., and Carolina, S. (2007). reviews Methylation of Dietary Flavones Greatly Improves Their Hepatic Metabolic Stability and Intestinal Absorption. 166–170.

Wang, Y.-C., and Bachrach, U. (2002). The specific anti-cancer activity of green tea (-)-epigallocatechin-3-gallate (EGCG). Amino Acids *22*, 131–143.

Wang, I.-K., Lin-Shiau, S.-Y., and Lin, J.-K. (1999). Induction of apoptosis by apigenin and related flavonoids through cytochrome c release and activation of caspase-9 and caspase-3 in leukaemia HL-60 cells. Eur. J. Cancer *35*, 1517–1525.

Wang, J., Chung, M.H., Xue, B., Ma, H., Ma, C., and Hattori, M. (2010). Estrogenic and antiestrogenic activities of phloridzin. Biol. Pharm. Bull. *33*, 592–597.

Wang, Q.R., Yao, X.Q., Wen, G., Fan, Q., Li, Y.-J., Fu, X.Q., Li, C.K., and Sun, X.G. (2011). Apigenin suppresses the growth of colorectal cancer xenografts via phosphorylation and up-regulated FADD expression. Oncol. Lett. *2*, 43–47.

Warner, E., Plewes, D.B., Shumak, R.S., Catzavelos, G.C., Di Prospero, L.S., Yaffe, M.J., Goel, V., Ramsay, E., Chart, P.L., Cole, D.E., et al. (2001). Comparison of breast magnetic resonance imaging, mammography, and ultrasound for surveillance of women at high risk for hereditary breast cancer. J. Clin. Oncol. *19*, 3524–3531.

Weischer, M., Bojesen, S.E., Tybjaerg-Hansen, A., Axelsson, C.K., and Nordestgaard, B.G. (2007). Increased risk of breast cancer associated with CHEK2*1100delC. J. Clin. Oncol. *25*, 57–63.

Wen, W., Lu, J., Zhang, K., and Chen, S. (2008). Grape seed extract inhibits angiogenesis via suppression of the vascular endothelial growth factor receptor signaling pathway. Cancer Prev. Res. (Phila). *1*, 554–561.

Wheeler, D.L., Ness, K.J., Oberley, T.D., and Verma, A.K. (2003). Protein Kinase Cε Is Linked to 12-O-tetradecanoylphorbol-13-acetate-induced Tumor Necrosis Factor-α Ectodomain Shedding and the Development of Metastatic Squamous Cell Carcinoma in Protein Kinase Cε Transgenic Mice. Cancer Res. *63*, 6547–6555.

WHO (2013). WHO | Breast cancer: prevention and control http://www.who.int/cancer/detection/breastcancer/en/.

Williams, G.M. (2001). Mechanisms of chemical carcinogenesis and application to human cancer risk assessment. Toxicology *166*, 3–10.

Wu, L.-C., Lu, I.-W., Chung, C.-F., Wu, H.-Y., and Liu, Y.-T. (2011). Antiproliferative mechanisms of quercetin in rat activated hepatic stellate cells. Food Funct. *2*, 204–212.

Xu, Y., Xin, Y., Diao, Y., Lu, C., Fu, J., Luo, L., and Yin, Z. (2011). Synergistic effects of apigenin and paclitaxel on apoptosis of cancer cells. PLoS One *6*, e29169.

Xue, M., Wang, Q., Zhao, J., Dong, L., Ge, Y., Hou, L., Liu, Y., and Zheng, Z. (2014). Docosahexaenoic acid inhibited the Wnt/β-catenin pathway and suppressed breast cancer cells in vitro and in vivo. J. Nutr. Biochem. *25*, 104–110.

Yang, M.-Y., Chang, Y.-C., Chan, K.-C., Lee, Y.-J., and Wang, C.-J. (2011a). Flavonoid-enriched extracts from Nelumbo nucifera leaves inhibits proliferation of breast cancer in vitro and in vivo. Eur. J. Integr. Med. *3*, e153–e163.

Yang, M.-Y., Chang, Y.-C., Chan, K.-C., Lee, Y.-J., and Wang, C.-J. (2011b). Flavonoid-enriched extracts from Nelumbo nucifera leaves inhibits proliferation of breast cancer in vitro and in vivo. Eur. J. Integr. Med. *3*, e153–e163.

Yang, T.T., Sinai, P., and Kain, S.R. (1996). An acid phosphatase assay for quantifying the growth of adherent and nonadherent cells. Anal. Biochem. *241*, 103–108.

Yao, H., Xu, W., Shi, X., and Zhang, Z. (2011). Dietary flavonoids as cancer prevention agents. J. Environ. Sci. Health. C. Environ. Carcinog. Ecotoxicol. Rev. *29*, 1–31.

Ying, M., Tu, C., Ying, H., Hu, Y., He, Q., and Yang, B. (2008). MSFTZ , a Flavanone Derivative , Induces Human Hepatoma Cell Apoptosis via a Reactive Oxygen Species- and Caspase-Dependent Mitochondrial Pathway. J Pharmacol. Exp. Ther. *325*, 758–765.

Zhang, F., Lau, S.S., and Monks, T.J. (2011). The cytoprotective effect of N-acetyl-L-cysteine against ROS-induced cytotoxicity is independent of its ability to enhance glutathione synthesis. Toxicol. Sci. *120*, 87–97.

Zhang, L., Pu, Z., Wang, J., Zhang, Z., Hu, D., and Wang, J. (2014a). Baicalin inhibits hypoxia-induced pulmonary artery smooth muscle cell proliferation via the AKT/HIF-1α/p27-associated pathway. Int. J. Mol. Sci. *15*, 8153–8168.

Zhang, M., Liu, C., Zhang, Z., Yang, S., Zhang, B., Yin, L., Swarts, S., Vidyasagar, S., Zhang, L., and Okunieff, P. (2014b). A new flavonoid regulates angiogenesis and reactive oxygen species production. Adv. Exp. Med. Biol. *812*, 149–155.

Zhang, W., Tang, B., Huang, Q., and Hua, Z. (2013). Galangin inhibits tumor growth and metastasis of B16F10 melanoma. J. Cell. Biochem. *114*, 152–161.

Zhao, R., Xiang, N., Domann, F.E., and Zhong, W. (2009). Effects of selenite and genistein on G2/M cell cycle arrest and apoptosis in human prostate cancer cells. Nutr. Cancer *61*, 397–407.

Zhao, W., Sun, J., Xiang, H., Zeng, Y., Li, X., Xiao, H., Chen, D., and Ma, R. (2011). Synthesis and biological evaluation of new flavonoid fatty acid esters with anti-adipogenic and enhancing glucose consumption activities. Bioorg. Med. Chem. *19*, 3192–3203.

Zheng, Y., Scow, J.S., Duenes, J. a, and Sarr, M.G. (2012). Mechanisms of glucose uptake in intestinal cell lines: role of GLUT2. Surgery *151*, 13–25.

Ziaullah, Bhullar, K.S., Warnakulasuriya, S.N., and Rupasinghe, H.P.V. (2013). Biocatalytic synthesis, structural elucidation, antioxidant capacity and tyrosinase inhibition activity of long chain fatty acid acylated derivatives of phloridzin and isoquercitrin. Bioorg. Med. Chem. *21*, 684–692.

Zimmermann, S., Dziadziuszko, R., and Peters, S. (2014). Indications and limitations of chemotherapy and targeted agents in non-small cell lung cancer brain metastases. Cancer Treat. Rev. *40*, 716–722.

Zuo, A., Yanying, Y., Li, J., Binbin, X., Xiongying, Y., Yan, Q., and Shuwen, C. (2011). Study on the relation of structure and antioxidant activity of isorhamnetin, quercetin, phloretin, silybin and phloretin isonicotinyl hydrazone. Free Rad. Antiox. *1*, 39–47.